# Dynamics of Daytime Seasonal Variability of Land Surface Temperature and Its Driving Factors: A Case of Dire Dawa City.

Name of candidate: Dursitu Abdella

A Thesis Submitted to the Department of Geomatics Engineering
College of Civil Engineering and Architecture

Presented in Partial Fulfillment of the Requirements for the degree of
Master's in Geo-Informatics

Office of Graduate Students
Adama Science and Technology University

Oct 2024
Adama, Ethiopia

# Dynamics of Daytime Seasonal Variability of Land Surface Temperature and Its Driving Factors: A Case of Dire Dawa City

Dursitu Abdella

Advisor: Dejene Tesema (PhD)

A Thesis Submitted to the Department of Geomatics Engineering College of Civil Engineering and Architecture

Presented in Partial Fulfillment of the Requirements for the degree of Master's in Geo-Informatics

Office of Graduate Students Adama Science and Technology University

.

Oct 2024

Adama, Ethiopia

## DECLARATION

I, Dursitu Abdella hereby declare that this thesis entitled "Dynamics of Daytime Seasonal Variability of Land Surface Temperature and Its Driving Factors: A Case of Dire Dawa City." is my own work and has not been submitted to any university for similar purpose. The references used in this thesis are duly recognized by proper citations.

| | | |
|---|---|---|
| Dursitu Abdella | _______________ | _______________ |
| Name of student | Signature | Date |

## RECOMMENDATION OF ADVISORS

I, the major advisor/supervisor of this research thesis, hereby certify that I have closely advised/supervised the student while developing this thesis and read the draft thesis entitled "Dynamics of Daytime Seasonal Variability of Land Surface Temperature and Its Driving Factors: A Case of Dire Dawa City." prepared under my guidance by Dursitu Abdella. Therefore, I recommend the submission of the thesis to the department for further review and evaluation.

| | | |
|---|---|---|
| Dejene Tesema (PhD) | _______________________ | ______________ |
| Major Advisor/Supervisor | Signature | Date |

## APPROVAL SHEET

I/we hereby certify that the recommendation and suggestion given by the thesis review committee are appropriately incorporated into the final thesis proposal entitled "Dynamics of Daytime Seasonal Variability of Land Surface Temperature and Its Driving Factors: A Case of Dire Dawa City." by Dursitu Abdella.

| | | |
|---|---|---|
| Dejene Tesema (PhD) | ______________________ | ______________ |
| Major Advisor/Supervisor | Signature | Date |

## APPROVAL OF BOARD OF REVIEWERS

We, the undersigned, members of the Board of Reviewers of the thesis open defense by Dursitu Abdella have read and evaluated the thesis l entitled "Dynamics of Daytime Seasonal Variability of Land Surface Temperature and Its Driving Factors: A Case of Dire Dawa City.." and assessed the understanding of the candidate about the proposed research. This is, therefore, to certify that the thesis is accepted for partial fulfillment of the requirement of the degree of Master of Science in Geoinformatics.

| | | |
|---|---|---|
| ______________________________ | __________________ | _______________ |
| Chairperson | Signature | Date |
| _Gizachew Kabite (PhD)___________ | __________________ | _12/11/2024_____ |
| External Examiner | Signature | Date |
| ______________________________ | __________________ | _______________ |
| Internal Examiner | Signature | Date |

Finally approval and acceptance of the thesis is contingent upon submission of its final copy to the Office of Postgraduate Studies (OPGS) through the Department Graduate Council (DGC) and School Graduate Committee (SGC).

| | | |
|---|---|---|
| ______________________________ | ______________________ | ____________________ |
| Department Head | Signature | Date |
| ______________________________ | ______________________ | ____________________ |
| School Dean | Signature | Date |
| ______________________________ | ______________________ | ____________________ |
| Office of Postgraduate Studies, Dean | Signature | Date |

# ACKNOWLEDGMENT

I would like to express my heartfelt gratitude to all those who supported me throughout the journey of completing this thesis. First and foremost, I thank Allah, whose guidance and blessings have been a constant source of strength and inspiration throughout this endeavor.

I extend my sincere appreciation to my advisor, Dr. Dejene Tessema, whose guidance, expertise, and encouragement were invaluable. Your insights and constructive feedback helped shape my research and improve my writing significantly.

I am also grateful to the faculty and staff of Adama Science and Technology University, School of Civil Engineering and Architecture, and the Department of Geomatics Engineering for their support and resources, which greatly facilitated my research. Special thanks to my fellow students and friends for their camaraderie, motivation, and shared experiences during this challenging process.

Lastly, I wish to thank my family for their unwavering love and encouragement. Your belief in me kept me motivated and focused throughout this journey.

Thank you all for your invaluable support.

**Table of Contents**

## LIST OF ACRONYMS

| | |
|---|---|
| BT | Brightness Temperature |
| DEM | Digital Elevation Model |
| CSA | Central Statistical Agency |
| NDVI | Normalized Difference Vegetation Index |
| NDBI | Normalized Difference Built-up Index |
| ENVI | Environment for Visualizing Images |
| HVI | Heat Vulnerability Index |
| LSE | Land surface emissivity |
| LST | Land Surface Temperature |
| LULC | Land Use Land Cover |
| MLST | Mean Land Surface Temperature |
| MWA | Mono-window algorithm |
| OLI | Operational Land Imager |
| PCA | Principal Component Analysis |
| SC | Single-channel |
| SUHI | Surface Urban Heat Island |
| SWA | Split window algorithm |
| TM | Thematic Mapper |
| TOA | Top of Atmosphere |
| UHI | Urban Heat Island |
| USGS | United States Geological Survey |
| UHV | Urban Heat Vulnerability |

## LIST OF FIGURE

## LIST OF TABLE

**ABSTRACT**

*Rapid urbanization in Dire Dawa City, Ethiopia, has led to significant increases in LST, affecting both socioeconomic and environmental conditions. This study investigates the dynamics of seasonal and temporal variations in daytime LST from 2002 to 2024, addressing LST fluctuations during wet and dry seasons. By analyzing the influence of LULC changes; this research identifies key factors driving LST variability. Employing a mixed-methods approach, the study assesses seasonal patterns and temporal trends in LST, correlating them with, land cover changes, and Land cover indices. LST data derived from thermal bands using an emissivity-corrected Landsat imagery by using Single-Channel Method for Landsat 7 and Split-Window Method for Landsat 8 images. Analyses using the NDVI and the NDBI quantified the extent of vegetation and built-up areas. In contrast, rural areas stayed cooler this season due to higher soil moisture in both bare and vegetated lands, which enhanced evapotranspiration and provided a natural cooling effect. Overall, throughout these years, Kiremt consistently represented the coolest temperatures, whereas Tseday typically recorded the warmest conditions, highlighting a trend of increasing temperatures across all seasons in Dire Dawa City for all LULC. The mean LST experienced fluctuations, beginning at 24.1°C in 2002, increasing to 25.75°C in 2012, and then rising again to 27.25°C in 2017. By 2024, the average LST reached 29.7°C, reflecting an overall warming trend during the Study. These changes demonstrate how sensitive LST is to seasonal variations and urbanization. These results illustrate the complex relationship between different land cover types and LST, which fluctuates with the seasons based on how land cover responds to climatic conditions. The study underscores the urgent need for integrated urban planning and sustainable development that balances growth with environmental preservation, especially in managing urban thermal environments. These insights are vital for planners, stakeholders, and policymakers in crafting strategies to address the negative impacts of rising Land Surface temperatures.*



*Keywords: Land surface temperature, Land use and land cover, Seasonal variation; Dire Dawa City; Ethiopia*

# 1 CHAPTER 1: INTRODUCTION

## 1.1 Background of the study

Human-induced modifications to the Earth's environment have been ongoing for thousands of years, driven by a range of activities(Haylemariyam, 2018). These environmental changes are increasingly intensified by factors such as high population density, migration, and various socio-economic activities. These modifications can be observed on multiple spatial scales, from local to global levels (Guha, 2021). For instance, large-scale human activities, including agriculture and the expansion of settlements, continuously contribute to the reduction of the Earth's vegetative cover (Belete, 2017). Cities, as centers of human activity and survival, face growing challenges with urban development and population expansion. This growth necessitates effective urban management and planning to address a range of issues, including the significant impacts on urban climate (Chen et al., 2021).

The urban population has grown exponentially since the mid-20th century, with projections indicating that it will increase by 66% by 2050, according to United Nations estimates (United Nations, Department of Economic and Social Affairs, Population Division, 2015). This rapid urbanization results in direct environmental impacts. Research consistently shows that urbanization significantly affects urban climate, particularly in developing countries (Dong & Wurm, 2022; Shirgholami & Masoodian, 2022).

In Africa, urbanization is projected to grow at an annual rate of 1.1% from 2010 to 2015, with an anticipated urbanization rate of 56% by that period. For Ethiopia, a country in Africa, urban population rates were 19% in 2014 and are projected to reach 38% by 2050. According to a 2014 UN report, Ethiopia's urban growth rate from 2010 to 2015 was 2.3% (Desa, U.N., 2014). The city of Diredawa in Ethiopia has recently been undergoing significant urbanization, driven by economic development, increased migration, and improvements in infrastructure.

As urbanization progresses, there is growing concern about local warming effects induced by these changes. Understanding the underlying mechanisms between urban thermal environments and the driving factors of landscape transformation is crucial (Liu et al., 2019). Urbanization often involves converting natural land use and cover to build environments, leading to a decline in natural vegetation and an increase in paved surfaces (Zhang et al., 2017). This transformation underscores the importance of monitoring Land Surface Temperature (LST) to evaluate the environmental impacts of urbanization.

LST is a critical parameter that reflects the temperature of the Earth's surface, including terrain, vegetation, and man-made structures. It plays a vital role in various scientific disciplines such as meteorology, climatology, environmental science, and remote sensing. The data on LST, obtained through advanced technologies like satellite-based remote sensing and ground-based sensors, provides detailed insights into spatial and temporal variations in temperature. This information is essential for understanding phenomena like urban heat islands, drought conditions, and changes in land cover (Backlund et al., 2008).

Global warming, characterized by an average increase in land and sea surface temperatures, is primarily driven by increased greenhouse gases from human activities. This rise in temperatures affects critical environmental components such as glaciers, ice sheets, permafrost, and vegetation (Alahmad et al., 2020). Monitoring LST helps scientists track these changes and their implications for public health, energy consumption, and overall urban livability.

LST variability is a key factor in developing methodologies for various environmental studies, including climate change, vegetation phenology, and ecological research (Sholihah & Shibata, 2019). The land-use and land-cover (LULC) changes due to urbanization impact LST, and the temporal aspect of monitoring are crucial. Seasonal variations in LST, influenced by changes in sun elevation and azimuth, are important for accurate landscape studies (Guha & Govil, 2020).

## 1.2 Statement of the problem

Rapid and unplanned urban growth is a major factor driving increases in land surface temperature (LST) in urban areas (Xiao, 2022). Dire Dawa City has experienced accelerated urbanization and land use changes in recent decades. The expansion of urban areas, changes in vegetation cover, and alterations in land use patterns contribute to the modification of the local surface energy balance. Understanding the impact of these changes on daytime LST is crucial for predicting climate trends and implementing effective urban planning measures. Rising LST can adversely affect both socioeconomic and environmental conditions (Dissanayake, 2019). Higher LST can disrupt the surface energy balance (Dissanayake et al., 2019) and is associated with various health and environmental issues. Extreme temperature changes can impact human health, spread vector-borne diseases, and disrupt ecosystems, especially in regions with extreme temperatures like dire dawa.

In Dire Dawa City, urbanization has led to rising LST due to land cover changes from population growth and new developments (Haylemariyam, 2018). Issues like land degradation, insufficient land use policies, and inadequate green infrastructure contribute to increasing temperatures (Amanuel, 2020). Dire Dawa, characterized by a warm, dry climate with low precipitation (Kidanewald, 2018), is experiencing significant urbanization and environmental change. Understanding how land use and land cover (LULC) variations affect LST at different scales is crucial for urban sustainability.

Previous studies have primarily concentrated on Land Surface Temperature (LST) during the dry season, as evidenced by the research conducted by (Haylemariyam, 2018),(Kidanewald, 2018), and (Amanuel, 2020). However, these investigations have not sufficiently addressed the variations in LST during the wet season or across different temporal scales, thereby creating significant gaps in our understanding of LST dynamics also these studies only focused on the urban part of the City. Dire Dawa presents a compelling case for examining these phenomena due to its unique climatic variations and the environmental changes resulting from both natural processes and human activities. The interplay of urbanization and rural land use in this region offers a valuable context for studying urban heat islands and the associated temperature disparities between urban and rural areas. Such research is crucial for informing urban planning and environmental management strategies in the face of ongoing climate change.

Recent consecutive year's warnings from the Dire Dawa Health Bureau about increasing temperatures highlight the need for more research on LST in the city (Dire Dawa Administration Health Bureau). Despite growing interest in LST and its impact on urban health and sustainability (Chen et al., 2021), there is a lack of specific studies for Dire Dawa. This study will address seasonal and temporal LST variations in Dire Dawa, offering insights into local climate dynamics and providing valuable information for urban planning and climate resilience.

In summary, investigating daytime seasonal LST variability in Dire Dawa is crucial for understanding climate change impacts, urban development, and public health. This research aims to fill existing knowledge gaps and support efforts towards sustainable urban development and will be useful for local authorities and policymakers in promoting sustainable urban development.

## 1.3 Objectives of the study

### 1.3.1 General objective

- The general objective of this study is to analyze the dynamics seasonal and temporal variations in daytime land surface temperature (LST) in Dire Dawa City from 2002 to 2024.

### 1.3.2 Specific objective

- To analyze the seasonal variability of LST in Dire Dawa City during daytime from 2002 to 2024.
- To analyze the Spatio-temporal variation of Land surface Temperature from 2002 to 2024.

- To Identify and assess the main driving factors influencing seasonal variation of Land Surface Temperature in Dire Dawa City.

## 1.4 Research questions

- Which season of year experiences the highest and lowest mean LST during 2002 to 2024?
- What patterns or trends can be identified in the temporal evolution of LST during this period?
- What are the primary driving factors influencing the seasonal variation of Land Surface Temperature (LST) in Dire Dawa City, and how can these factors be assessed and identified over the study period?
- What are the relationships between changes in driving factor and variations in land surface temperature in Dire Dawa City?

## 1.5 Significance of the study

The significance of studying the "Dynamics of Daytime Seasonal Variability of Land Surface Temperature and Its Driving Factors: A Case of Dire Dawa City" lies in several critical areas. Understanding the seasonal variability of Land Surface Temperature (LST) is essential for assessing the impact of climate change on urban environments. Dire Dawa, with its unique climatic conditions and rapid urbanization, provides an important case study for investigating how LST fluctuates between different seasons, particularly in relation to human activities and natural processes.

The study can also contribute to the understanding of urban heat islands, which are areas within cities that experience higher temperatures than their rural surroundings. By analyzing LST variations in Dire Dawa, researchers can identify the factors contributing to these temperature discrepancies, such as land-use changes, vegetation cover, and urban infrastructure. This knowledge is vital for urban planning and the development of strategies to mitigate the adverse effects of increased temperatures on public health and energy consumption.

The findings from this research can inform local and regional policymakers about the environmental impacts of urbanization, allowing for the formulation of targeted interventions that promote sustainable urban development. Furthermore, understanding the driving factors behind LST variability can aid in predicting future temperature trends, thereby enhancing resilience to climate-related challenges.

This study will fill existing gaps in the literature by providing a comprehensive analysis of both daytime seasonal variability and the specific conditions in Dire Dawa, contributing to broader discussions in climate science, urban ecology, and environmental management. By focusing on this case, the research can serve as a model for similar studies in other regions facing comparable environmental changes.

### 1.6 Scope of the study

The geographic scope of the study "Dynamics of Daytime Seasonal Variability of Land Surface Temperature and Its Driving Factors: A Case of Dire Dawa City" centers on Dire Dawa, a city located in eastern Ethiopia. This region is characterized by its semi-arid climate, which features distinct wet and dry seasons, providing a unique backdrop for examining Land Surface Temperature (LST) dynamics. The research explores LST variations between urban areas of Dire Dawa and its surrounding rural landscapes, emphasizing the temperature differences induced by urbanization. By analyzing various land cover types, the study aims to capture the spatial variability of LST across the city and its periphery, thus providing insights into how different surfaces interact with climatic conditions.

The contextual scope of the study encompasses the examination of daytime seasonal fluctuations in Land Surface Temperature (LST) and the driving factors influencing these variations specifically focus on understanding how LST changes between the wet and dry seasons, with particular attention to the impacts of urbanization, land cover changes, and human activities. Additionally, the study aims to explore broader themes such as climate change and urban heat islands, assessing their implications for public health, energy consumption, and urban planning. The findings are intended to inform local and regional policymakers about the environmental effects of urbanization, thereby promoting sustainable development strategies. Moreover, the research will contribute to the global discourse on urbanization and environmental change, offering valuable insights applicable to similar contexts in other regions.

## 1.7 Knowledge Gap

While there is a growing body of literature on LST variability, significant knowledge gaps persist, particularly concerning the seasonal dynamics of LST in rapidly urbanizing areas like Dire Dawa City. However, these studies often focus on dry seasons, leaving a gap in knowledge regarding seasonal variations in LST due to urbanization in Dire Dawa City. Most existing studies have primarily focused on either global patterns or have been conducted in well-studied urban environments, neglecting the unique climatic and geographical conditions of emerging cities. Furthermore, there is a lack of comprehensive studies that integrate socio-economic factors with environmental data to understand how human activities influence LST variability over different seasons. Addressing these gaps will provide valuable insights that can inform local policies and strategies for sustainable urban development and climate resilience in Dire Dawa City.

# 2 CHAPTER 2: LITERATURE REVIEW

This literature review provides a comprehensive overview pertinent to the study titled "Dynamics of Daytime Seasonal Variability of Land Surface Temperature and Its Driving Factors: A Case of Dire Dawa City." It establishes a solid foundation by integrating findings from global, regional, and local research, emphasizing the role of both natural and human-induced factors in influencing LST variations. These insights are instrumental for developing informed strategies to enhance climate-resilient urban development in Dire Dawa City.

## 2.1 Introduction to Land Surface Temperature

Land Surface Temperature (LST) is defined as the temperature of the Earth's surface, which encompasses soil, water bodies, and vegetation. It is a critical parameter in various scientific disciplines, including meteorology, climatology, ecology, and urban studies, as it directly influences the energy balance of the Earth, weather patterns, and ecological processes (Sullivan et al., 2020).

LST reflects the energy absorbed from solar radiation and is affected by surface properties, vegetation cover, soil moisture, and anthropogenic activities (Riahi et al., 2018). Understanding LST is essential for assessing land-atmosphere interactions, predicting climate change impacts, and managing natural resources. Additionally, LST plays a significant role in urban environments; elevated LST can exacerbate heat waves and contribute to the urban heat island (UHI) effect, wherein urban areas experience higher temperatures than their rural counterparts due to human activities and land-use changes (Oke, 1982). Monitoring LST is crucial for urban planning, public health, and environmental management, as it helps identify areas vulnerable to overheating and informs strategies to enhance urban resilience (Zhang et al., 2020).

LST is primarily measured using remote sensing technologies, which offer the capability to cover extensive areas and provide continuous data. Satellite sensors, such as the Moderate Resolution Imaging Spectroradiometer (MODIS) and Landsat series, utilize thermal infrared wavelengths to estimate LST (Li et al., 2021). These measurements enable researchers to analyze spatial and temporal variations in LST across diverse landscapes and climatic conditions. Ground-based measurements, including infrared thermometers and temperature sensors, are also essential for validating satellite data, providing accurate readings of surface temperatures at specific locations (Weng, 2001).

The applications of LST studies are broad and varied. In climate science, LST data is utilized to model and predict temperature changes over time, facilitating the assessment of climate change impacts (Hulme et al., 2019). In ecology, understanding LST variations aids in assessing habitat suitability for various species and the effects of climate on biodiversity (Peñuelas et al., 2013). Furthermore, LST is increasingly recognized as a key factor in urban studies; research indicates that urbanization significantly alters LST, affecting energy consumption, air quality, and public health (Davis et al., 2018). As a result, monitoring LST is essential for sustainable urban planning and developing strategies aimed at mitigating the effects of urban heat.

Land Surface Temperature is a vital parameter that reflects the thermal state of the Earth's surface. Its measurement and analysis provide critical insights into climatic, ecological, and urban processes. As urbanization accelerates globally, understanding LST dynamics will become increasingly important for informing climate adaptation and sustainable development strategies.

## 2.2 Seasonal Variability of Land Surface Temperature (LST)

Seasonal variability of Land Surface Temperature (LST) is a critical aspect of understanding how temperature dynamics fluctuate in response to changing climatic conditions throughout the year. LST is influenced by various factors, including solar radiation, surface moisture, vegetation cover, and land use, which all exhibit significant seasonal changes (Chen et al., 2019). The interaction between these factors can lead to distinct patterns in LST during the wet and dry seasons, necessitating an in-depth examination of how these variations manifest in different geographic contexts.

Research has shown that during the dry season, LST tends to increase due to higher solar radiation and reduced surface moisture (Zhou et al., 2018). The lack of vegetation cover in urban areas exacerbates this effect, leading to higher temperatures compared to rural regions. Conversely, during the wet season, increased precipitation and vegetation growth can contribute to lower LST values as the soil moisture content rises and the cooling effects of evapotranspiration become more pronounced (Wang et al., 2020). These seasonal dynamics are particularly relevant in regions experiencing rapid urbanization, where the conversion of natural land cover to impervious surfaces significantly alters local temperature patterns.

Several studies have utilized remote sensing data to analyze seasonal variations in LST across various landscapes. For example, (Liu et al., 2017) employed MODIS satellite data to assess LST fluctuations in urban and rural settings, revealing that urban areas consistently exhibit higher LST, especially during the dry season. This underscores the importance of considering both seasonal and spatial dimensions when studying LST dynamics.

The implications of seasonal LST variability are significant for various applications, including climate modeling, urban planning, and ecological assessments. Understanding how LST changes with the seasons can help predict the effects of climate change on local environments and inform strategies for mitigating heat-related issues, particularly in urban areas (Huang et al., 2019). Additionally, recognizing the seasonal patterns in LST can enhance our understanding of habitat suitability for various species, as temperature fluctuations can affect ecosystem dynamics and biodiversity (Peñuelas et al., 2013).

The seasonal variability of Land Surface Temperature is a vital aspect of climate science and urban ecology. By examining how LST fluctuates throughout the year, researchers can gain insights into the driving factors behind these changes and their implications for environmental management and urban planning.

## 2.3 Urban Heat Islands (UHIs)

Urban Heat Islands (UHIs) are defined as urban areas that experience significantly higher temperatures than their rural surroundings due to human activities and alterations in land cover. This phenomenon is primarily attributed to the extensive use of impervious surfaces, such as asphalt and concrete, which absorb and retain heat more effectively than natural landscapes (Oke, 1982). The UHI effect is particularly pronounced during the day and at night, leading to increased energy consumption, elevated air pollution levels, and negative impacts on public health (Santamouris, 2015).

The formation of UHIs is influenced by several factors, including urban geometry, vegetation cover, and the thermal properties of construction materials. Urban environments typically have a higher density of buildings, which can obstruct airflow and trap heat, exacerbating temperature differences between urban and rural areas (Taha, 1997). Additionally, a lack of vegetation in urban settings limits the cooling effects of evapotranspiration, further contributing to elevated temperatures (Wang et al., 2020).

Numerous studies have documented the extent and impact of UHIs across various cities worldwide. For example, research by (Ruddell et al., 2019) highlighted that cities can experience temperature increases of up to 5°C or more compared to surrounding rural areas, especially during summer months. This temperature disparity poses risks to public health, as higher temperatures are linked to heat-related illnesses and increased mortality rates, particularly among vulnerable populations (Anderson et al., 2012).

The implications of UHIs extend beyond health concerns; they also affect energy consumption and environmental quality. Higher temperatures lead to increased demand for air conditioning, which can strain energy resources and contribute to elevated greenhouse gas emissions (Huang et al., 2011). Moreover, elevated surface temperatures can exacerbate air quality issues, as warmer conditions facilitate the formation of ground-level ozone and other pollutants (Sarrat et al., 2006).

Addressing the UHI effect requires effective urban planning and management strategies. Implementing green infrastructure, such as parks, green roofs, and urban forests, can help mitigate the impact of UHIs by increasing vegetation cover and enhancing evapotranspiration (Bowler et al., 2010). Additionally, using reflective materials in construction and improving urban design can further reduce heat absorption and promote cooler urban environments.

Urban Heat Islands are a significant urban phenomenon characterized by elevated temperatures in cities compared to their rural counterparts. Understanding the mechanisms behind UHIs and their implications is essential for developing strategies to mitigate their effects and promote healthier urban environments.

## 2.4 Impacts of Urban Heat Islands

The impacts of Urban Heat Islands (UHIs) are broad and significant, influencing energy consumption, air quality, and public health. One of the primary consequences of UHIs is increased energy use, particularly for cooling purposes. Research by (Santamouris et al., 2017) quantifies this effect, revealing that cities with pronounced UHI effects experience substantially higher energy demands for air conditioning and cooling systems. This increased energy consumption not only raises utility costs but also contributes to greater greenhouse gas emissions, exacerbating the urban heat problem (Santamouris et al., 2017).

In addition to higher energy use, UHIs are linked to worsened air quality. Elevated temperatures associated with UHIs can intensify the formation of ground-level ozone, a harmful air pollutant. (Davis et al., 2018) found that the heat generated by UHIs accelerates the chemical reactions that produce ozone, thereby increasing its concentration in urban areas. This elevated ozone level poses serious health risks, including respiratory problems and aggravated conditions such as asthma and bronchitis (Davis et al., 2018).

Furthermore, UHIs contribute to a rise in heat-related illnesses. Increased temperatures associated with UHIs can lead to a higher incidence of conditions such as heat stroke, dehydration, and heat exhaustion. (Koppe et al., 2004), highlight that these health issues disproportionately affect vulnerable populations, including the elderly, children, and individuals with pre-existing health conditions. Prolonged exposure to elevated temperatures can exacerbate these health problems, leading to an increased burden on healthcare systems (Koppe et al., 2004).

Overall, the multifaceted impacts of UHIs underscore the urgent need for effective mitigation strategies to address their effects on energy use, air quality, and public health. This includes implementing urban planning measures that reduce heat absorption and improve overall urban resilience.

### 2.5 Driving Factors of Land Surface Temperature (LST) Variability

The variability of Land Surface Temperature (LST) is influenced by a complex interplay of natural and anthropogenic factors. Understanding these driving factors is essential for accurately assessing LST dynamics and their implications for climate, ecology, and urban planning.

Land Use and Land Cover Changes significantly impact LST due to alterations in surface materials and vegetation. Urbanization, which involves replacing natural landscapes with impervious surfaces like asphalt and concrete, leads to increased heat absorption and reduced cooling through evapotranspiration (Zhou et al., 2018). As a result, urban areas often experience higher LST compared to their rural counterparts, particularly in densely built environments (Oke, 1982). Studies have shown that changes in land cover, such as deforestation or the conversion of agricultural land to urban settings, can dramatically influence local temperature patterns (Zhang et al., 2020).

Vegetation Cover, Vegetation plays a crucial role in regulating LST through processes such as shading and evapotranspiration. Areas with abundant vegetation generally exhibit lower LST due to the cooling effects of transpiration and reduced solar radiation absorption (Fang et al., 2017). Conversely, areas with limited vegetation, such as urban heat islands, tend to have elevated LST. Research indicates that maintaining and increasing vegetation cover in urban environments can mitigate heat impacts and improve overall thermal comfort (Bowler et al., 2010).

Soil moisture is another critical factor influencing LST. Higher soil moisture levels enhance evaporative cooling, thereby reducing surface temperatures (Riahi et al., 2018). During dry periods, reduced soil moisture can lead to elevated LST as the land surface absorbs more heat without the moderating effects of evaporation. The interplay between precipitation patterns and LST highlights the importance of monitoring soil moisture, particularly in regions susceptible to drought (Wang et al., 2020).

Topographical features, such as elevation, slope, and aspect, significantly influence LST variability. Areas with different elevations can experience varying temperatures due to differences in solar exposure and wind patterns (Miller et al., 2021). Additionally, local climatic conditions, including temperature, humidity, and wind speed, play a vital role in shaping LST dynamics. For instance, regions with consistent high temperatures and low humidity are likely to exhibit higher LST throughout the year (Chen et al., 2019).

Human activities, such as industrial processes, transportation, and energy consumption, contribute to the release of anthropogenic heat, which can elevate LST in urban areas (Grimmond et al., 2010). This additional heat input can intensify the UHI effect and lead to significant temperature disparities between urban and rural areas. Understanding the sources and impacts of anthropogenic heat is essential for developing effective urban management strategies.

The variability of Land Surface Temperature is driven by a multitude of factors, including land use changes, vegetation cover, soil moisture, topography, and anthropogenic heat release. Recognizing the interplay of these elements is crucial for comprehensively understanding LST dynamics and their implications for climate adaptation, urban planning, and environmental management

## 2.6 Urbanization

Urbanization represents a complex and multifaceted process through which rural landscapes transition into urban environments, characterized by a marked increase in the urban population. This transformation encompasses not only the physical expansion of cities but also economic development and shifts in social and cultural practices. According to the United Nations (2018), urbanization is primarily driven by economic opportunities and the development of infrastructure. The World Bank (2021) identifies it as a cornerstone of modernization and economic growth, emphasizing its integral role in shaping contemporary societies.

Currently, urbanization has emerged as a defining global trend, with over 56% of the world's population residing in urban areas, a figure projected to escalate to 68% by 2050 (United Nations, 2022). This demographic shift is particularly pronounced in developing regions such as Sub-Saharan Africa and Asia, where cities in countries like India and Nigeria are experiencing unprecedented growth (UN-Habitat, 2021). Conversely, urbanization rates in developed nations have stabilized, yet challenges remain, including the management of urban sprawl and the deterioration of aging infrastructure (OECD, 2023).

In developing nations, the rapid pace of urbanization poses dual challenges: the swift influx of populations into urban centers and the inadequacy of existing infrastructure. This often results in the proliferation of informal settlements and increased pollution levels, directly contributing to the rise in urban land surface temperatures (World Bank, 2023). Addressing these critical issues necessitates the implementation of sustainable urban planning practices and the establishment of resilient infrastructure, as highlighted by the International Institute for Environment and Development (2024).

Moreover, urban areas are significant contributors to greenhouse gas emissions, underscoring the urgency for adopting greener practices to mitigate climate change impacts (IPCC, 2023). Social inequality remains a pressing concern, with marginalized communities disproportionately affected by inadequate housing and limited access to essential services.

This reality accentuates the need for inclusive urban policies that prioritize the needs of all citizens (UN-Habitat, 2023).

While urbanization propels significant economic and social transformations, it simultaneously demands careful and strategic management to effectively address its environmental and social challenges. The relationship between urbanization and land surface temperature dynamics is a critical area of focus, particularly in rapidly expanding urban centers, where the implications of these transformations must be understood and managed holistically.

### 2.6.1 Urbanization in Ethiopia: Trends, Challenges, and Climate Implications

Urbanization in Ethiopia has been accelerating rapidly, mirroring broader trends observed across Sub-Saharan Africa. Recent statistics indicate that Ethiopia's urban population has surged, with the urbanization rate now approaching approximately 25% of the total population, up from around 20% a decade ago (World Bank, 2022). This growth is largely driven by rural-to-urban migration and the expansion of major cities like Addis Ababa, which has experienced significant increases in both population and infrastructure development.

However, this rapid urbanization presents several environmental challenges, particularly concerning climate and land surface temperature (LST). As urban areas expand, they often replace natural landscapes with heat-retaining surfaces, contributing to the Urban Heat Island (UHI) effect. This phenomenon leads to higher temperatures in urban areas compared to their rural counterparts, exacerbating heat-related health issues and increasing energy demands for cooling.

A report by the Ethiopian Development Research Institute (2023) outlines several pressing issues arising from this urban growth, including inadequate housing, strained public services, and severe traffic congestion. These problems are intensified by the continuous influx of people into urban areas and the consequent environmental degradation. The surge in urbanization has also led to the proliferation of informal settlements, where residents often lack access to essential services like clean water and sanitation (UN-Habitat, 2023). These conditions are further complicated by rising land surface temperatures, which can hinder urban resilience and amplify vulnerabilities to climate change.

To address these intertwined challenges, comprehensive urban planning and substantial investment in climate-resilient infrastructure are essential. Strategies that incorporate green spaces and sustainable building practices can mitigate the UHI effect and enhance urban livability. Effective management of urbanization is crucial to ensure sustainable development and improve living conditions in Ethiopian cities while also addressing the critical issue of rising land surface temperatures. Policymakers must prioritize resilient and inclusive urban development practices to combat the dual threats of urbanization and climate change, safeguarding the future of Ethiopian urban centers.

## 2.7 Impact of Urbanization on Land Surface Temperature (LST)

Urbanization significantly alters Land Surface Temperature (LST), leading to notable temperature increases in urban areas compared to their rural counterparts. This phenomenon, often referred to as the Urban Heat Island (UHI) effect, arises from a combination of land cover changes, human activities, and the unique thermal properties of urban materials.

The transition from natural landscapes to urban environments involves the replacement of vegetation with impervious surfaces such as asphalt, concrete, and buildings. These materials have high heat capacities and low albedo, meaning they absorb and retain more solar radiation than natural surfaces (Oke, 1982). As a result, urban areas tend to experience higher LST, particularly during the day and at night, when heat retention is most pronounced (Zhou et al., 2018). Studies have shown that urbanization can lead to LST increases of up to 5°C or more relative to surrounding rural areas (Ruddell et al., 2019).

Urbanization often leads to a significant reduction in vegetation cover, which plays a crucial role in moderating LST through shading and evapotranspiration. Vegetation helps cool the air and surface temperatures by releasing moisture into the atmosphere (Fang et al., 2017). In contrast, areas with limited or no vegetation experience elevated temperatures due to increased heat absorption and reduced cooling effects. This loss of green spaces contributes to the UHI effect and exacerbates temperature disparities between urban and rural areas. Human activities associated with urbanization, such as transportation, industrial processes, and energy consumption, introduce additional heat into the urban environment. This anthropogenic heat release can intensify the UHI effect, leading to even higher LST in densely populated areas (Grimmond et al., 2010). During warmer months, the cumulative effects of heat generated by vehicles, air conditioning, and industrial operations can contribute significantly to urban temperature increases.

Urbanization changes natural hydrological processes, impacting soil moisture and surface temperatures. The replacement of permeable surfaces with impermeable ones reduces water infiltration and increases runoff, leading to decreased soil moisture (Wang et al., 2020). Lower soil moisture levels can result in higher LST, particularly during dry seasons, as less moisture is available for evaporation and cooling.

Impacts of urbanization on LST have significant implications for local climate, public health, and energy consumption. Higher urban temperatures are associated with increased heat-related illnesses, particularly among vulnerable populations (Anderson et al., 2012). Additionally, elevated LST can lead to increased energy demand for cooling, straining energy resources and contributing to higher greenhouse gas emissions (Huang et al., 2011).

Mitigating the impacts of urbanization on LST requires strategic urban planning that incorporates green infrastructure, such as parks, green roofs, and urban forests. These interventions can help restore vegetation cover, improve evapotranspiration, and reduce heat absorption, ultimately contributing to cooler urban environments.

Urbanization has a profound impact on Land Surface Temperature, primarily through land cover changes, reduced vegetation, anthropogenic heat release, and altered hydrological patterns. Understanding these dynamics is essential for developing effective strategies to mitigate the UHI effect and promote sustainable urban living.

## 2.8 Land Use and Land Cover Changes

Land cover refers to the physical material present on the surface of the Earth, such as vegetation, bare soil, or water bodies (Muro et al., 2018). Changes in land use and land cover (LULC) have a profound impact on Land Surface Temperature (LST), reflecting the complex interactions between human activities and the Earth's surface. In contrast, land use describes how humans utilize land for various purposes, including settlements, agriculture, and forestry (Mekasha, 2020). The transformation from one type of land cover to another—such as converting forests to urban areas or agricultural land—can significantly alter surface temperatures (Abel, 2018).

These changes in land cover and use are often initiated at the parcel level, where administrative decisions lead to the replacement of one land cover type with another (Bayable et al., 2022). For example, the urbanization process typically involves replacing natural vegetation with impervious surfaces like asphalt and concrete, which absorb and retain more heat compared to natural land cover types (Oke, 1982). Similarly, deforestation can increase LST by removing the cooling effects of forest canopy and exposing the soil to direct solar radiation (Grimmond et al., 1999).

Studies examining the effects of urbanization, deforestation, and agricultural practices on LST have highlighted how human-induced modifications to land cover and use contribute to increased surface temperatures. Research in this area provides valuable insights into how these changes impact the local and regional climate, informing strategies for mitigating the adverse effects of LULC changes on LST (Du et al., 2020) (Santamouris et al., 2017). Understanding these dynamics is crucial for developing effective land management and urban planning strategies that aim to balance development needs with environmental sustainability and climate resilience

## 2.9 Impacts of Land Use Land Cover change on Land Surface Temperature

The environmental changes, growth of the human population, and economic development are key causes of LULC change (Bayable , 2022). It is quite evident that land-use/land-cover (LULC) and landscape patterns have ecological implications at varying spatial scales, which in turn influence the distribution of habitat and material/energy fluxes in the landscape(Zhanga et al., 2013).LST is affected by the characteristics of the land surface such as vegetation cover and its type, land cover and surface imperviousness. Incessant urbanization has resulted in many fold increase in the urban area and it has caused significant changes in the land surface (Khandelwal et al., 2018). Many studies showed the relationship between LULC and LST, Some studied the seasonal variations of temperature and identified the impact of different LULC classes on LST varies.

### 2.10 Land cover spectral indices

A spectral index is a mathematical formula utilized in remote sensing and earth observation that combines multiple spectral bands from satellite imagery to derive valuable insights about surface properties and processes. By applying this formula to each pixel of an image, spectral indices generate data that is crucial for various modeling, prediction, and analysis tasks related to surface phenomena. These indices are essential tools in interpreting complex environmental and geological data, as they enhance our understanding of various surface processes through specific spectral combinations.

Spectral indices are derived from different combinations of satellite spectral bands, each tailored to highlight particular surface characteristics. For instance, vegetation indices such as the Normalized Difference Vegetation Index (NDVI) use combinations of red and near-infrared bands to assess vegetation health and density (Tucker, 1979). Similarly, indices like the Normalized Difference Water Index (NDWI) are used to monitor water bodies by exploiting differences in the reflectance of green and near-infrared bands (McFeeters, 1996).

The applications of these indices are diverse and have been extensively explored in previous research. In agriculture, spectral indices help in monitoring crop health, assessing soil moisture, and optimizing irrigation practices (Moran et al., 1994). In water resource management, indices are used to track changes in water bodies, assess water quality, and manage aquatic ecosystems (Gao, 1996). Urban development studies employ spectral indices to analyze land use changes, assess urban sprawl, and monitor heat island effects (Weng, 2001). Spectral indices play a critical role in various fields by providing valuable information that supports surface process modeling, prediction, and inference, thereby enhancing our ability to manage and understand environmental and ecological systems (Prasad et al., 2022).

### 2.10.1 Normalized difference vegetation index (NDVI)

The Normalized Difference Vegetation Index (NDVI) is a widely used, dimensionless metric that quantifies vegetation health by comparing the reflectance in visible and near-infrared wavelengths. This index is instrumental in estimating the density and coverage of green vegetation across a given area (Weier et al., 2000). NDVI values range from -1 to 1, which remains consistent regardless of whether the inputs are radiance, reflectance, or digital numbers (DN). Generally, NDVI values are close to zero for non-vegetated surfaces such as rocks, sand, or concrete. In contrast, bodies of water typically exhibit negative NDVI values, while vegetation, including crops, shrubs, grasses, and forests, typically shows positive NDVI values (Jones et al., 2011).

### 2.10.2 Normalized Difference Built-Up Index (NDWI)

Normalized Difference Built-up Index (NDBI), in remote sensing and urban analysis, (Zha et al, 2003) introduced the significant advancement designed to facilitate the extraction and analysis of urban built-up areas. The NDBI was developed to specifically target and monitor urban expansion and built-up regions using satellite imagery. This index is particularly effective for identifying urban areas due to its reliance on the reflective properties of near-infrared (NIR) and mid-infrared (MIR) wavelengths (bands 4 and 5, respectively, of the Landsat TM satellite).

This index capitalizes on the fact that built-up surfaces, such as roads and buildings, typically exhibit higher reflectance in the MIR compared to the NIR. By leveraging this characteristic, the NDBI effectively distinguishes built-up areas from non-built-up surfaces, such as vegetation or water bodies, which do not exhibit the same reflectance pattern (Zha et al., 2003). One of the advantages of NDBI is its operational simplicity and efficiency. The index processes data quickly and does not require the use of training samples, making it a valuable tool for automatic recognition of built-up areas in satellite imagery. This is particularly useful for analyzing Landsat TM data, which provides medium spatial and spectral resolution imagery that is ideal for monitoring urban growth and land use changes (Liu et al., 2012).

The NDBI values range from -1 to +1, where positive values generally indicate the presence of built-up areas. This straightforward calculation and its ability to handle large datasets make the NDBI a popular choice for urban studies and land cover classification (Weng, 2002). Its widespread adoption underscores its effectiveness in tracking urbanization trends and providing insights into spatial patterns of built-up areas.

## 2.11 Land surface temperature retrieval Algorithms

Scientific literature extensively explores the development and validation of algorithms for retrieving Land Surface Temperature (LST), focusing on improving measurement accuracy through the integration of data from diverse sensors and platforms. These algorithms play a crucial role in enhancing the precision of LST assessments across various temporal and spatial scales. Research in this field encompasses both short-term variations, such as diurnal and seasonal changes, and long-term trends and anomalies, with spatial analyses ranging from regional assessments to global investigations (Li et al., 2019).

The recent deployment of the Landsat 8 and 9 satellites has significantly advanced the monitoring of urban heat island (UHI) effects. Equipped with two thermal infrared bands, these satellites offer high-resolution data that supports various LST retrieval algorithms (Rongali et al., 2018). Among the algorithms used for LST extraction from Landsat data are the Mono-Window Algorithm (MWA), the Split-Window Algorithm (SWA), and the Single-Channel (SC) method. Each of these algorithms has distinct sensitivities and applications.

The Split-Window Algorithm (SWA), which utilizes two thermal bands, is known for its robustness against errors in input parameters, making it a preferred choice for many studies (Wang et al., 2019). In contrast, the Mono-Window Algorithm (MWA) and the Single-Channel (SC) method, while also effective, are more sensitive to errors in atmospheric water vapor content and land surface emissivity (LSE). These sensitivities can lead to greater uncertainties in LST retrieval when compared to SWA (Sharma et al., 2022). For instance, the accuracy of MWA and SC methods can be significantly impacted by variations in atmospheric conditions, highlighting the need for careful calibration and validation in diverse environments (Wang et al., 2019).

Overall, the choice of algorithm for LST retrieval depends on the specific requirements of the study, including the desired accuracy, spatial resolution, and the environmental conditions of the study area. Continued advancements in satellite technology and algorithm development are expected to further enhance the reliability and applicability of LST measurements in understanding and managing urban heat dynamics

### 2.11.1 The mono-window algorithm (MWA)

This algorithm was originally proposed by qin's mono-window algorithm. This algorithm requires three parameters: the effective mean atmospheric temperature ($T_a$), land surface emissivity ($\varepsilon$), and atmospheric transmittance ($\tau$) (Guha, 2021).

### 2.11.2 The split window algorithm (SWA)

This algorithm was originally proposed by (Guha, 2021). The principle is that two adjacent thermal infrared bands have different absorption characteristics; the attenuation information of the atmosphere on the thermal radiation can be obtained by the difference between the brightness temperatures of the two TIR bands (Wang et al., 2019). The SWA is widely used due to the fact that this algorithm has less dependence on atmospheric parameters and is simple to operate (Wang et al., 2019).

### 2.11.3 The single-channel (SC)

This method was proposed in 2003 and improved in 2009 by Jiménez-Muñoz and Sobrino (Xie et al., 2013). This algorithm requires only two input parameters, the LSE and the atmospheric water vapor content (Wang et al., 2019). Differing from the MWA, the SC method does not need the effective mean atmospheric temperature (Ta) parameter, and the atmospheric water vapor content is not required to be calculated to the atmospheric transmittance which reduces the error of the final retrieved LST due to the error of the effective mean atmospheric temperature (Ta).(Wang et al., 2019)

### 2.11.4 The inversion of the Planck function

The inversion of the Planck function is a critical process in remote sensing and radiative transfer studies, enabling the extraction of physical properties such as temperature from observed radiance. The Planck function describes the spectral radiance of a blackbody in thermal equilibrium at a given temperature, and its inversion involves solving for the temperature based on the measured radiance. This process is essential for accurate retrieval of land surface temperature (LST) and other thermal properties in remote sensing applications. Observed radiance is often converted into temperature through inversion of this function. This process involves determining the surface or atmospheric temperature from the measured radiance using the inverse relationship, which requires solving the Planck function.

The inversion of the Planck function is fundamental in retrieving LST from thermal infrared satellite data. For instance, the retrieval of LST from sensors on satellites such as Landsat involves converting measured radiance to temperature, which is critical for various applications, including climate monitoring, weather prediction, and environmental management (Price, 1984; Becker & Li, 1990). Accurate inversion allows for effective monitoring of surface temperature variations, which is essential for studying urban heat islands, vegetation health, and land surface dynamics. By converting observed radiance into temperature, this process supports various environmental and climatic studies.

### 2.11.5 Multi-angle method

The multi-angle method, also known as multi-angle remote sensing or multi-angle observation, is a sophisticated technique in remote sensing that involves capturing imagery of the Earth's surface from multiple viewing angles. This approach enhances the accuracy and detail of surface and atmospheric measurements by leveraging the perspective provided by different angles of observation. The method is crucial for a range of applications, including land surface temperature (LST) retrieval, vegetation monitoring, and atmospheric studies.

The multi-angle method involves collecting data from multiple vantage points or sensors at different angles relative to the surface. This technique allows for the observation of surface features and atmospheric phenomena from various perspectives, which can improve the retrieval of surface properties and correct for observational biases. By analyzing these multi-angle observations, researchers can better account for variations in surface reflectance, atmospheric scattering, and sensor viewing geometry (Tian et al., 2015). In the context of LST retrieval, the multi-angle method provides significant advantages. Traditional single-angle observations may suffer from inaccuracies due to atmospheric interference and surface anisotropy. By incorporating data from different angles, the multi-angle method can improve the estimation of LST by reducing errors related to atmospheric effects and enhancing the characterization of surface properties (Zhang et al., 2018). This method is particularly useful for correcting for the effects of varying solar and sensor angles, which can otherwise introduce significant biases in LST measurements.

### 2.11.6 Radiative Transfer Equation (RTE)

The Radiative Transfer Equation (RTE) is a fundamental tool in remote sensing and atmospheric sciences, used to describe the transfer of radiation through a medium. It provides a quantitative framework for understanding how electromagnetic radiation interacts with matter, which is essential for accurate retrieval of environmental parameters such as Land

Surface Temperature (LST).

The RTE expresses how the intensity of radiation changes as it travels through a medium, taking into account the absorption, emission, and scattering processes. The RTE is crucial for interpreting data from remote sensing instruments that measure radiance in various spectral bands. For instance, in the context of LST retrieval, the RTE helps in modeling how radiation emitted from the Earth's surface interacts with atmospheric components before reaching the sensor. Accurate LST retrieval requires correcting for atmospheric effects such as absorption and emission by water vapor and other gases, which are modeled using the RTE (Kaufman et al., 2002; Matus et al., 2008).

*Table 2-1: LST retrieval Methods, Assumptions, Advantages and Disadvantages*

| Methods | Pros | Cons |
|---|---|---|
| Mono-Window Algorithm (MWA) | - Simplicity in implementation<br>- Useful with limited spectral bands<br>- Good for moderate accuracy needs | - Sensitive to atmospheric water vapor errors<br>- Limited to fewer spectral bands<br>- Lower accuracy compared to advanced methods |
| Split-Window Algorithm (SWA) | - Improved accuracy by using two thermal bands<br>- Better atmospheric correction<br>- Widely used and validated | - Requires precise calibration and atmospheric data<br>- Complexity in processing<br>- Sensitive to atmospheric conditions |
| Single-Channel Method (SCM) | - Straightforward application<br>- Useful for single-band data<br>- Less computationally | - Limited accuracy due to atmospheric interference<br>- Sensitivity to input errors |

| | | |
|---|---|---|
| | intensive | - Not as robust for complex atmospheric conditions |
| Multi-Angle Method (MAM) | - Provides detailed surface and atmospheric characterization<br>- Reduces atmospheric biases<br>- Enhances surface property retrievals | - Complex data processing and integration<br>- High computational requirements<br>- Requires multi-angle observations and accurate calibration |
| Inversion of the Planck Function | - Directly relates observed radiance to temperature<br>- Fundamental for precise temperature retrieval<br>- Widely applicable in remote sensing | - Requires accurate radiative transfer modeling<br>- Sensitive to errors in atmospheric conditions and surface emissivity<br>- Complex calculations depending on the model used |
| Radiative Transfer Equation (RTE) | - Provides comprehensive modeling of radiative processes<br>- Can account for various atmospheric and surface conditions<br>- Accurate and flexible for diverse applications | - Computationally intensive<br>- Requires detailed atmospheric profiles and surface emissivity data<br>- Complex to implement and interpret |

Ultimately, the choice should align with the project's specific requirements, data availability, and desired accuracy level.

For General Use: Split-Window Algorithm (SWA**)** is often a good choice due to its balance between accuracy and complexity.

For Basic Needs: Mono-Window Algorithm (MWA) or Single-Channel Method (SCM**)** if simplicity and resource constraints are primary concerns.

## 2.12 Geographic Information System and Land Surface Temperature

Geographic Information Systems (GIS) are sophisticated frameworks that facilitate the comprehensive handling of spatial and geographic information, encompassing a range of functions including the capture, storage, manipulation, analysis, management, and presentation of data (Guo et al., 2019). Within the GIS paradigm, data is primarily classified into two categories: spatial data, which includes geographic coordinates that denote the specific locations of features on the Earth's surface, and non-spatial data, which provide contextual characteristics of these spatial features, typically formatted in tables. Belete (2017) emphasizes that GIS data operates within a multidimensional framework, incorporating three critical dimensions: spatial (geographic) data that maps physical locations, temporal data that reflects changes over time, and attribute data that describes various properties associated with the spatial elements. Beyond merely serving as a digital repository for geographical features—such as areas, points, and lines—GIS acts as a powerful analytical tool that enables the examination of spatial relationships and interactions among these features. This includes analyzing how the geometric properties and locations of different elements relate to one another, thus allowing for more profound insights into spatial patterns and dynamics (Tola & Engineering, 2018). By integrating these capabilities, GIS supports a wide range of applications across various fields, enhancing decision-making processes related to urban planning, environmental management, and resource allocation.

## 2.13 Remote sensing in land surface temperature study

Remote sensing is defined as the technique of gathering information about an object or area without direct physical contact (Rashash Ali & Mohammed, 2016). In contemporary applications, this term is increasingly associated with advanced technical methods for collecting data from airborne and spaceborne platforms. Satellite-based remote sensing is instrumental in providing crucial information across multiple domains, including atmospheric studies, climatology, meteorology, ecology, agronomy, and environmental protection (Verna, 2015). The essence of remote sensing involves measuring and recording the electromagnetic radiation that is either emitted or reflected from the Earth's surface (Sheik Mujabar, 2019). This radiation can provide insights into various environmental conditions and phenomena, making it a vital tool in environmental monitoring and assessment.

The field of remote sensing has gained significant attention for its ability to measure Land Surface Temperature (LST) using satellite technology.(Hu et al., 2019) Various instruments, notably the Moderate Resolution Imaging Spectroradiometer (MODIS) and the Advanced Spaceborne Thermal Emission and Reflection Radiometer (ASTER), are extensively employed for retrieving LST data.(Muro et al., 2018) These tools allow researchers to assess surface temperatures over large areas with high accuracy.

Recent advancements in remote sensing technology, particularly with high-resolution satellite sensors like MODIS and Landsat, have significantly enhanced the ability to monitor seasonal variations in LST across different spatial and temporal scales (Jiménez-Muñoz et al., 2014; Wan et al., 2004). These technological innovations offer valuable opportunities to conduct detailed analyses of the factors that influence daytime LST. For instance, by leveraging high-resolution imagery, researchers can examine the dynamics of LST at a fine spatial scale. This capability enables a more comprehensive understanding of how various factors such as land use, vegetation cover, urban heat islands, and climate change affect temperature variations in specific regions. In particular, applying these advanced remote sensing techniques to areas like Dire Dawa City allows for targeted investigations that can inform urban planning, environmental management, and climate adaptation strategies.

### 2.13.1 Supervised Image Classification

Supervised image classification is a classification technique in which the user chooses representative sample pixels from an image and instructs the image processing software to use these training sites as models for classifying the rest of the pixels in the image. It is commonly known that choosing an appropriate classifier is crucial for increasing classification accuracy (Lu et al., 2007) Several supervised classification classifiers and algorithms, including the parallelepiped, minimum distance, maximum likelihood, nonparametric classifiers, and machine learning techniques like the support vector machine, decision tree method, and artificial neural networks, have been developed over the past few decades.

#### 2.13.1.1 Parallelepiped classifiers algorithm

To determine if a particular pixel belongs to the designated class or not, a standard threshold is provided. The parallelepiped is based on the threshold of the standard deviation from the mean of each class (a class limit dimension). The pixels are categorized if the threshold range falls between the defined low and high. Unclassified areas are those that do not fall inside the given threshold range. This supervised classifier is fairly straightforward. Here, based on maximum and minimum pixel values, two image bands are employed to estimate the training area of the pixels in each band. Although the parallelepiped classification method is the most precise, it is not the most popular. Additionally, training pixels may overlap, leaving many pixels unlabeled. The candidate pixel's data values are contrasted with the upper and lower bounds. (Perumal et al., 2010)

#### 2.13.1.2 Minimum distance classifiers algorithm

It is based on the minimal distance decision rule, which determines the spectral separation between the mean vector for each sample and the measurement vector for the candidate pixel. The candidate pixel is then assigned to the class with the shortest spectral distance (Perumal et al., 2010). As a distinctive prototype, classes that are near one another are grouped. It is used to determine each class's mean vector and assign each pixel to the nearest group.

#### 2.13.1.3 Maximum Likelihood classifiers algorithm

The vector of a class with the highest probability is assigned among all the probabilities of vectors allotted to various classes. Based on the user-provided threshold value, the pixels are assigned to each class. The pixels are unclassified if the class probability value is less than the user-set threshold value (Ahmad et al., 2012). It is a parametric approach in decision making where the model parameters need to be estimated before they are applied for classification MLC is a process for determination of known class distribution as the maximum for a given statistic (Scott & Symons, 1971). This method has been used most widely and frequently in remote sensing where a pixel is assigned to the corresponding class with the maximum likelihood. If there has been m predefined classes, in that case the class posteriori probability is expressed.

This Classification use the training data by estimating the means and variances of the classes, which are then utilized to estimate probabilities while also taking into account the variety of brightness values in each class. This classifier is based on Bayesian probability theory. When accurate training data is made available, it is one of the most effective classification methods and algorithms. (Perumal et al., 2010)

The measurement vector with the highest likelihood of belonging to a certain class is given that classification. The MLC has an advantage over other known parametric classifiers in that it considers the variance-covariance within class distributions, and it outperforms them for normally distributed data (Erdas, 1999). However, the outcomes might not be adequate for data with a non-normal distribution (Otukei et al., 2010).

#### 2.13.1.4 Spectral Angle Mapper

An n-dimensional angle is used by the Spectral Angle Mapper, a physically based spectral classification, to match pixels to reference spectra. By calculating the angle between the spectra and treating them as vectors in a space with dimensionality equal to the number of bands, this technique calculates the degree of spectral similarity between two spectra. (Perumal et al., 2010)

#### 2.13.1.5 Decision Tree classifiers algorithm

A decision tree classifier is a non-parametric classifier, meaning that no previous statistical assumptions about the distribution of the data are necessary. However, the decision tree's fundamental structure consists of a root node, a number of internal nodes, and then a set of terminal nodes. Recursively, the input is dispersed along the decision tree in accordance with the established classification scheme. Each node needs to have a decision rule, which may be achieved using a splitting test (Otukei et al., 2010).

There is no complex design or training requirements for this method. Although computational efficiency is strong, it necessitates sophisticated calculations, and accuracy may entirely depend on feature design and selection.

#### 2.13.1.6 Support Vector Machines classifiers algorithm

This classification is applied for a complex dataset where the input numeric attributes are normalized and pre-processed before classifying. It is a non-parametric statistical learning method (Ustuner et al., 2015). Various kernel types such as, linear, polynomial, sigmoid, radial basis function can be set.SVM is a nonparametric approach, where the theoretic background is supervised machine learning.

This classification involves consideration of the training and testing sets from separate data. Each training set has separate target value and several attributes. Main function of the SVM is to predicts the target values of the given test data. The original goal of SVM, a nonparametric supervised machine learning technique, was to address binary classification issues [41(Implementation of Machine-Learning Classification in Remote Sensing: An Applied Review | Semantic Scholar, n.d.), (Huang et al., 2002)]. Based on the idea of structural risk minimization (SRM), it optimizes and isolates the hyper-plane and the data points closest to the hyper-spectral plane's angle mapper (SAM). It uses a hyper-spectral plane to divide data points into several classes. The vectors used in this technique guarantee that the margin's width will be maximized [(Bouaziz et al., 2017)]. Multiple continuous and categorical variables, as well as linear and non-linear samples with varying levels of class membership, can all be supported by SVM. Support vectors are the training samples or bordering samples that define the SVM's hyper-plane or margin (Shih et al., 2019).

2.13.1.7 Artificial Neural Network classifiers algorithm

In order to apply meaningful labels to images, algorithms using an artificial neural network method imitate the learning process used by humans. ANN mimics a select few mental processes (Mahmon et al., 2014) it consists of a series of layers, each of which contains a group of neurons, connected by weighted connections between the layers above and below. The network structure has a significant impact on the artificial neural network's accuracy and performance (Kaur et al., 2014) ANN networks are a self-adaptive and data driven approach. The processing speed is fast and can accommodate erratic input.

*Table 2-2: Classification Methods, assumptions, Advantages and Disadvantages of LULC*

| **Method** | **Advantage** | **Disadvantage** |
|---|---|---|
| Parallelepiped Classifier | - Simple to implement<br>- Fast processing<br>- Effective in well-separated classes<br>- Requires minimal computational resources | - Sensitive to noise and outliers<br>- Assumes that class distributions are parallel, which is often not the case<br>- Less accurate in complex or overlapping classes |
| Minimum Distance | - Simple and computationally efficient | - Assumes equal variance in all classes |

| | | |
|---|---|---|
| Classifier | - Effective for distinguishing well-separated classes<br>- Easy to understand and implement | - Not effective in cases of class overlap<br>- Sensitive to noise and variation in class distributions |
| Maximum Likelihood Classifier | - Provides probabilistic estimates of class membership<br>- Handles class variance well<br>- Generally more accurate in complex scenarios | - Requires accurate statistical parameters<br>- Computationally more intensive<br>- Assumes normal distribution of data, which may not always be true |
| Spectral Angle Mapper (S**AM)** | - Effective in identifying spectral similarities<br>- Robust to radiometric variations<br>- Useful for materials with distinct spectral signatures | - Less effective with mixed or overlapping spectra<br>- Not suitable for handling spatial or contextual information<br>- Computationally intensive for large datasets |
| Decision Tree Classifier | - Easy to understand and interpret<br>- Handles both numerical and categorical data<br>- Can model complex relationships with | - Prone to over fitting, especially with deep trees<br>- Sensitive to noisy data<br>- May require pruning to improve generalization |

| | | |
|---|---|---|
| | hierarchical rules | |
| Support Vector Machine (SVM) Classifier | - Effective in high-dimensional spaces<br>- Works well with both linear and non-linear boundaries<br>- Robust to over fitting with proper kernel selection | - Computationally expensive, especially for large datasets<br>- Requires careful tuning of parameters and kernel selection<br>- Less interpretable compared to some other methods |
| Artificial Neural Network (ANN) Classifier | - Capable of modeling complex, non-linear relationships<br>- Highly adaptable with the potential for high accuracy<br>- Handles large and complex datasets effectively | - Requires substantial computational resources<br>- Long training times<br>- Can be difficult to interpret and require careful tuning of network architecture and parameters |

Choosing the appropriate method will depend on the specific requirements of the classification task, including the nature of the data, the computational resources available, and the desired level of accuracy.

For Accuracy with Probabilistic Output**:** Maximum Likelihood Classifier: This probabilistic method estimates the probability of a pixel belonging to a class based on its statistical properties, making it robust to variations within classes. However, it requires accurate statistical data and can be computationally intensive.is a good choice if statistical parameters are well-understood.

## 2.14 Case Studies

Understanding the dynamics of Land Surface Temperature (LST) and its driving factors in Dire Dawa City requires examining comparable case studies in regions with similar climatic conditions. This section reviews relevant studies that highlight the interactions between urbanization, LST variability, and climate change in analogous environments.

- Addis Ababa, Ethiopia

Addis Ababa, the capital of Ethiopia, shares similar climatic characteristics with Dire Dawa, including a highland climate with pronounced seasonal variations. A study by (Abate et al. 2019) investigated the effects of urbanization on LST in Addis Ababa. The research found that rapid urban expansion has led to significant increases in LST, particularly during the dry season. The study emphasized the role of land cover changes, such as the conversion of green spaces into built environments, which significantly contributed to the Urban Heat Island (UHI) effect. This case study underscores the importance of sustainable urban planning to mitigate temperature increases and promote urban resilience.

- Guangzhou, China

Guangzhou's subtropical climate provides additional context for LST dynamics. A study by (Huang et al. 2021) investigated the relationship between urban expansion and LST in Guangzhou. The findings indicated that urbanization resulted in substantial increases in LST, especially in areas with high-density development. The authors emphasized the need for adaptive urban planning strategies that prioritize green spaces and climate-resilient infrastructure to combat rising temperatures and improve urban livability.

- Nairobi, Kenya

Nairobi presents another relevant case study, characterized by a similar altitude and climate. A study conducted by (Karanja et al. 2020) assessed LST variations in Nairobi and its relationship with urbanization. The researchers employed satellite remote sensing to analyze

LST patterns over a decade. Their findings revealed a marked increase in LST due to urban sprawl, with notable differences between urban and peri-urban areas. The study highlighted the critical need for urban green spaces to counteract rising temperatures and recommended integrating green infrastructure into urban planning to enhance climate resilience.

- Kigali, Rwanda

Kigali's climate and urban development trajectory make it an instructive case for understanding LST dynamics. A study by (Ngabonziza et al. 2021) explored LST changes in Kigali in relation to urbanization and vegetation cover. The research found that the loss of vegetative cover due to urban expansion led to higher surface temperatures, especially during the dry season. The authors suggested that urban greening initiatives, including reforestation and the creation of parks, could mitigate the UHI effect and improve local climate conditions. This case study emphasizes the importance of integrating ecological considerations into urban planning strategies.

- Accra, Ghana

Accra, with its tropical climate and rapid urbanization, provides another relevant context. A study by (Owusu et al. 2018) analyzed the impacts of urbanization on LST in Accra, using satellite data to identify spatial and temporal variations. The research indicated a significant rise in LST over the years, particularly in densely populated urban areas. The findings highlighted the correlation between increased impervious surfaces and higher LST, reinforcing the need for sustainable land-use policies. The study called for enhanced urban planning efforts that prioritize green spaces and sustainable infrastructure to mitigate climate impacts.

- Shanghai, China

In Shanghai, characterized by a humid subtropical climate, (Liu et al. 2020) examined the impact of urbanization on LST. The researchers found that the city's rapid expansion significantly elevated LST, particularly in summer months. Their analysis highlighted the importance of integrating green infrastructure, such as urban parks and green roofs, to mitigate the adverse effects of UHI. The authors also recommended promoting public transportation and non-motorized transport to reduce heat generated by vehicular traffic.

- Dakar, Senegal

Dakar, characterized by a semi-arid climate, provides additional insights into LST dynamics. A study by (Ndiaye et al. 2020) examined the impacts of urbanization on LST in Dakar, revealing significant temperature increases associated with land-use changes. The researchers highlighted the need for climate-responsive urban planning that considers local climatic conditions and incorporates adaptive measures to reduce LST, such as the development of shaded areas and green corridors.

- Brasília, Brazil

In Brasília, which features a tropical savanna climate, a study by (Tavares et al. 2020) analyzed the relationship between urbanization and LST. The researchers found that rapid urban expansion significantly increased LST, especially during the dry season. The study highlighted the importance of integrating green spaces into urban planning to mitigate the Urban Heat Island (UHI) effect and suggested the implementation of policies aimed at preserving existing vegetation.

- Pune, India

Pune's semi-arid climate provides another relevant context for understanding LST dynamics. In a study by (Bhagat et al. 2019), researchers used remote sensing data to examine LST variations over time. Their findings indicated a marked increase in LST corresponding to urban sprawl, driven by the conversion of agricultural land into urban areas. The study recommended sustainable urban planning practices, including the enhancement of green cover to reduce temperature increases and improve urban livability.

- Lima, Peru

Lima's coastal desert climate offers insights into urbanization's impact on LST. A study by (Salazar et al. 2021) investigated LST variations in Lima, revealing significant increases in urban areas due to land-use changes. The research underscored the critical need for urban planning strategies that incorporate green infrastructure to mitigate rising temperatures and improve the city's resilience to climate change.

- Beijing, China

Beijing, with its continental monsoon climate, presents a significant case for LST analysis. A study by (Li et al. 2019) explored the relationship between urbanization and LST variations over a 30-year period. The research revealed that rapid urban development has led to pronounced increases in LST, particularly in densely populated areas. The study emphasized the role of land-use changes, such as the conversion of green spaces into built environments, in exacerbating the Urban Heat Island (UHI) effect. Recommendations included enhancing urban greenery and implementing policies for sustainable land-use planning.

- Sydney, Australia

Sydney's temperate climate presents a different perspective on LST dynamics. A study by Stewart and (Oke 2012) examined the UHI effect in Sydney, highlighting how urbanization led to higher LST, particularly during summer months. The authors emphasized the importance of urban design strategies that promote green roofs and urban forests to counteract UHI effects. Their findings suggest that such measures can significantly lower LST and enhance urban microclimates.

- Jakarta, Indonesia

Jakarta, characterized by a tropical climate, offers another important case study. A research study by (Setiawan et al. 2019) assessed LST variations in Jakarta, finding that rapid urbanization and land-cover changes were directly correlated with increased surface temperatures. The study recommended comprehensive urban planning that prioritizes green space integration and effective water management strategies to mitigate the adverse effects of rising temperatures.

- Johannesburg, South Africa

Johannesburg, with its subtropical highland climate, offers further insights into urban heat dynamics. A study by (Meijers et al. 2019) investigated LST changes and UHI effects in Johannesburg. The researchers found that urbanization significantly contributed to increased LST, particularly in areas with high-density development. Their findings suggested the implementation of green infrastructure initiatives, such as urban parks and tree canopies, to mitigate temperature increases and enhance urban resilience to climate change.

- Chengdu, China

Chengdu, with its humid subtropical climate, offers further insights into LST variations. Research by (Wang et al. 2020) analyzed the effects of urbanization on LST patterns in Chengdu. The study found that urban expansion and changes in land cover led to increased surface temperatures, particularly during the dry season. The authors recommended implementing green corridors and enhancing urban vegetation to reduce LST and improve air quality, contributing to healthier urban environments.

- Xi’an, China

In Xi'an, characterized by a semi-arid climate, a study by (Zhang et al. 2021) explored LST dynamics and the UHI effect. The researchers found that urbanization has significantly increased LST, particularly in built-up areas, while rural regions showed more stable temperatures. Their findings underscored the importance of preserving green spaces and integrating sustainable practices in urban planning to mitigate the impacts of rising temperatures.

These case studies in climates similar to that of Dire Dawa City illustrate the critical relationship between urbanization and LST dynamics. They underscore the common challenges faced by rapidly urbanizing regions, including increased temperatures and the UHI effect. The findings from these studies can inform strategies for managing LST variability and promoting sustainable urban development in Dire Dawa, contributing to broader efforts in climate adaptation and resilience.

## 2.15 Empirical Review

The dynamics of daytime seasonal variability of Land Surface Temperature (LST) have garnered increasing attention due to their implications for urban planning, climate adaptation, and environmental management. LST is influenced by various factors, including land use, vegetation cover, and climatic conditions. Understanding these dynamics is crucial for regions like Dire Dawa City, where rapid urbanization and environmental changes are occurring. This review aims to synthesize existing literature on LST variability, focusing on both global and local perspectives while identifying gaps in current knowledge.

### 2.15.1 Global Perspective

Globally, numerous studies have explored the factors influencing LST variability. Research has highlighted the significant role of land cover changes due to urbanization, agriculture, and deforestation in altering surface temperatures. For instance, (Zhang et al. 2018) found that urban expansion leads to higher LST due to the urban heat island effect, where built environments absorb and retain heat more effectively than natural landscapes. Furthermore, satellite-based remote sensing technologies, such as MODIS and Landsat, have been pivotal in monitoring LST across various climatic zones (Jiménez-Muñoz et al., 2014). Studies by (Wan et al. 2004) have documented seasonal variations in LST and emphasized the importance of climatic factors, such as solar radiation and precipitation, in shaping these patterns. However, while extensive research has been conducted in different regions, there remains a need for localized studies that take into account specific geographical and socio-economic contexts.

### 2.15.2 Local Perspective

Focusing on the local context of Dire Dawa City, recent studies have begun to address the unique factors influencing LST in this region. For example, (Mohammed et al. 2020) investigated the relationship between land use change and LST in Dire Dawa, finding that areas with increased urbanization correspond to elevated surface temperatures. Their findings suggest that the expansion of built-up areas leads to significant alterations in local microclimates. Additionally, the work of (Abdi et al. 2021) highlighted the influence of vegetation cover on LST, demonstrating that areas with dense vegetation experienced lower temperatures compared to urbanized regions. Despite these insights, localized studies remain limited, necessitating further investigation into the seasonal dynamics of LST and their driving factors specific to Dire Dawa City.

### 2.16 Gaps in the Literature

Despite the extensive research on Land Surface Temperature (LST) dynamics and its relationship with urbanization, significant gaps remain in the literature that hinder a comprehensive understanding of these phenomena. This section identifies key areas where further investigation is needed, particularly in the context of rapidly urbanizing regions like Dire Dawa City.

Many existing studies predominantly focus on LST variations during specific seasons, often neglecting comprehensive analyses across all seasonal cycles. For instance, while research has extensively documented dry season LST increases, there is a relative scarcity of studies examining wet season dynamics and their implications for urban environments (Haylemariyam, 2018) (Kidanewald, 2018) (Amanuel, 2020). This gap limits our understanding of how seasonal variations in LST interact with urbanization and climate change throughout the year.

Most LST studies have been conducted in developed urban areas, leaving a notable gap in research focused on developing countries, particularly in Africa. The unique socio-economic, cultural, and environmental contexts of cities like Dire Dawa may result in different LST dynamics compared to those observed in more developed regions (Guha, 2021). More localized studies are necessary to capture the nuances of urbanization's impact on LST in these contexts.

While several studies have identified key drivers of LST variability, there is still limited exploration of specific local factors that influence LST in particular urban settings. For example, the interplay between socio-economic activities, land-use changes, and climatic conditions in shaping LST patterns is often under-researched (Dong et al., 2022) and (Shirgholami et al., 2022). Identifying these localized drivers is essential for developing targeted urban planning strategies.

The existing literature often lacks integrative frameworks that combine LST analysis with broader urban planning and climate adaptation strategies. Most studies tend to operate in silos, focusing on LST without adequately addressing the implications for urban infrastructure, public health, and community resilience (Chen et al., 2021). An integrated approach that links LST dynamics with urban planning efforts is crucial for developing effective interventions.

Many studies analyze LST data over short time frames, which may not accurately reflect long-term trends and patterns. Longitudinal studies that assess LST changes over extended periods can provide deeper insights into the effects of urbanization and climate change (Backlund et al., 2008). Understanding these long-term trends is essential for predicting future scenarios and informing sustainable urban development.

While advancements in remote sensing technologies have improved data collection for LST studies, there is still potential for enhanced application of these technologies in urban settings. Few studies have utilized high-resolution satellite imagery or machine learning techniques to analyze LST variability, which could provide more detailed insights into spatial patterns (Sholihah & Shibata, 2019). Leveraging these technologies can enhance the precision and relevance of LST research.

Addressing these gaps in the literature is essential for advancing our understanding of LST dynamics and their implications for urban planning and climate adaptation. Future research should focus on comprehensive seasonal analyses, contextual studies in developing regions, exploration of localized driving factors, and the development of integrative frameworks.

# 3 CHAPTER 3: MATERIAL AND METHODOLOGY

## 3.1 Description of the study area

### 3.1.1 Location

Dire Dawa is a city in eastern Ethiopia, situated near the border of Somalia. It is a relatively large urban area within Ethiopia. It is situated in the eastern part of the country and it's known for its diverse landscape, including plains, hills, and mountains. It is one of the oldest countries and most important urban centers, serving as a major transportation hub and economic center in the east region. Dire Dawa was established in 1902 as a relatively lowland with elevation of 1200 m above sea level. The Dire Dawa city is located in the eastern part of Ethiopia between $9^0$28.1" N and $9^0$ 49'1" N Latitude and between $41^0$ 38'1" E and $42^0$ 19'1" E Longitude. Dire Dawa is accessible by plane, train and cars, and is about 515kms road distance to the east of Addis Ababa and 311kms to the west of Djibouti port. It shares boundaries with East Hararge zone of Oromia Regional State in it's the south and southeast, and Shinele zone of Somalia Regional State in the north, east and west.

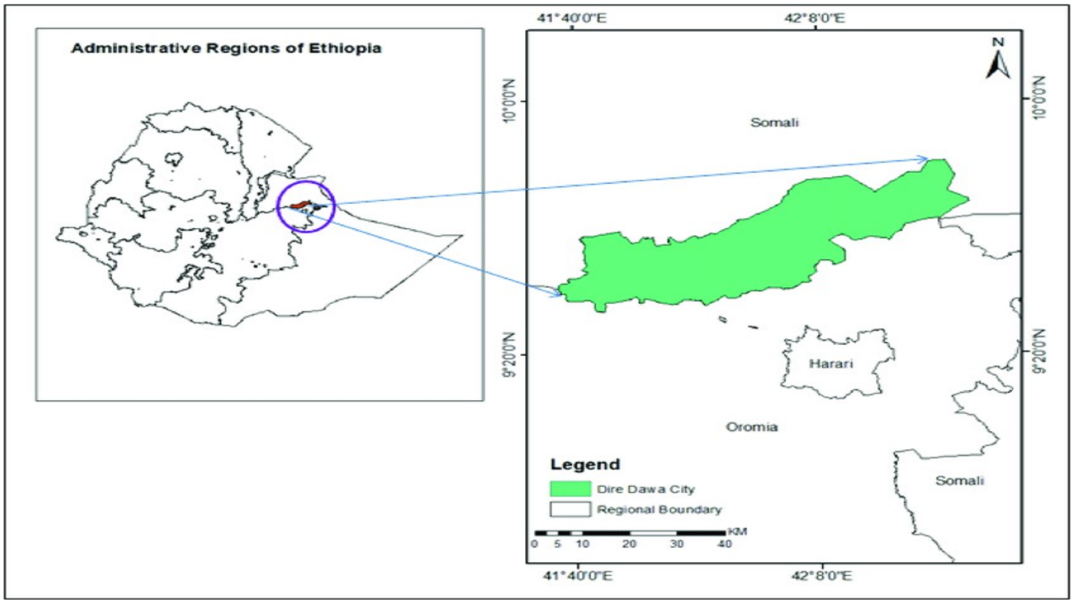


*Figure 3-1: location map Dire Dawa City Administration*

### 3.1.2 Land Size and Composition

The Dire Dawa Administration is a chartered city composed of 9 urban and 38 rural kebeles, encompassing a total land area of 1,300 square kilometers (or 130,000 hectares). Of this area, approximately 94.65% is classified as rural, while 5.34% pertains to urban regions (Abdi et al., 2020). The urban kebeles are significantly developed, featuring residential areas, commercial districts, industrial zones, and essential infrastructure. Additionally, areas adjacent to rural kebeles are often used for agriculture or livestock grazing. The region also boasts natural landscapes, including parks, forests, and hills (Hussein & Mulugeta, 2021).

### 3.1.3 Climate

Dire Dawa City exhibits a semi-arid climate characterized by warm temperatures and distinct seasonal variations, which are crucial for understanding the dynamics of daytime land surface temperature (LST) variability. The city's location in the Great Rift Valley and proximity to lowland areas significantly influence its climate. The mean annual temperature is approximately 25.91°C, with average maximum temperatures reaching 35°C and minimum temperatures around 22°C (Abdi et al., 2020).

The climatic conditions of Dire Dawa are heavily shaped by its topography and urbanization, resulting in a warm, dry climate with relatively low precipitation levels (Hussein & Mulugeta, 2021). The short wet season typically occurs from June to September, bringing moderate rainfall and slightly cooler temperatures, influenced by monsoon winds (Tadele et al., 2022). In contrast, the dry season, which lasts from October to May, is marked by minimal rainfall, higher temperatures, clear skies, and low humidity (Demisse et al., 2021). This semi-arid climate also predisposes Dire Dawa to dust and sandstorms, particularly during the dry season, which can adversely affect visibility and air quality. These climatic and environmental factors are integral to understanding the seasonal variability of LST in Dire Dawa and its driving influences, highlighting the interplay between urbanization, land use, and climatic conditions.

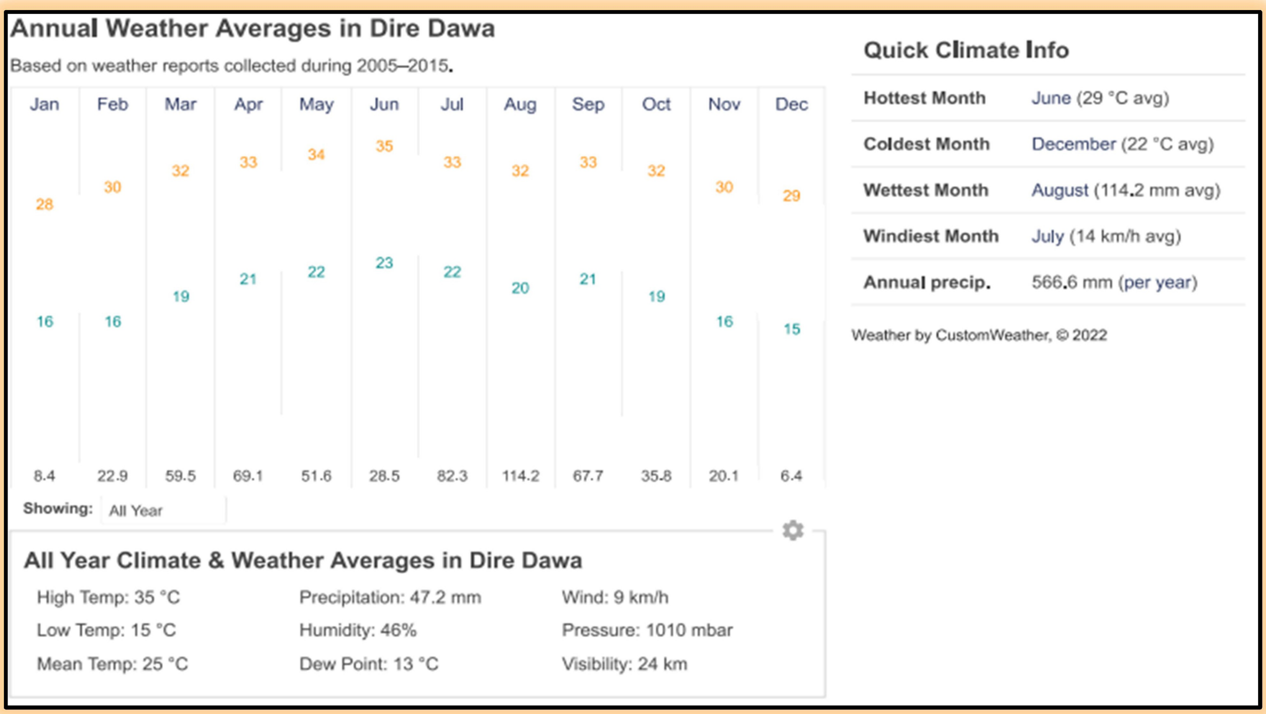


*Figure 3-2: Annual weather average of Dire Dawa*

*(Source: Climate & Weather Averages in Dire Dawa, Ethiopia (timeanddate.com))*

### 3.1.4 Demography

The population of Dire Dawa has grown over the years due to migration and urbanization. The city's population includes a mix of ethnic groups, creating a diverse and dynamic urban environment. Based on the 2022 Census conducted by the CSA of Ethiopia, Dire Dawa City Administration has a total population of 445,000 which is the second populated city in Ethiopia next to Addis Ababa (UN-Habitat, 2015; CSA, 2022).

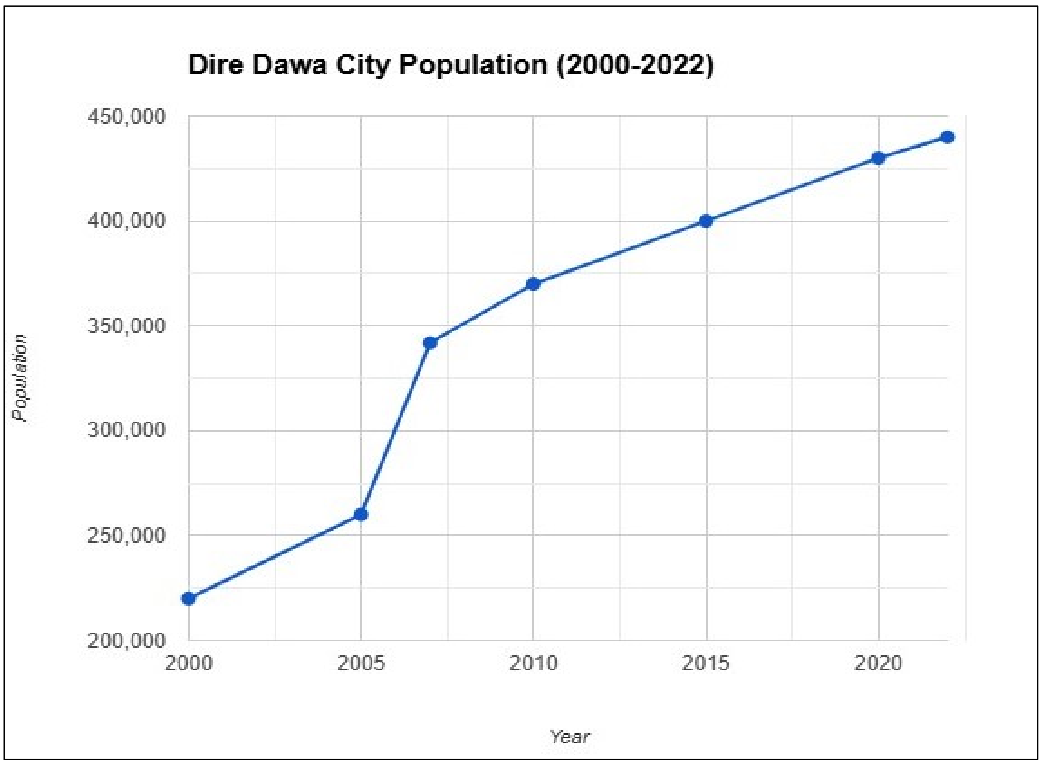


*Figure 3-3: The Population of Dire Dawa city over the past two decades*

### 3.1.5 Precipitation

Dire Dawa City has two rain seasons; that is, a light rainy season from March to April, and a heavy rainy season that extends from August to September. Climate change may bring alterations to the timing and intensity of rainfall. Dire Dawa's short wet season may experience changes in precipitation patterns, affecting water availability for agriculture and other purposes. The aggregate average annual rainfall that the region gets from these two seasons is about 566.6 mm. On the other hand, the region is believed to have an abundant underground water resource. (Source: NMA ).

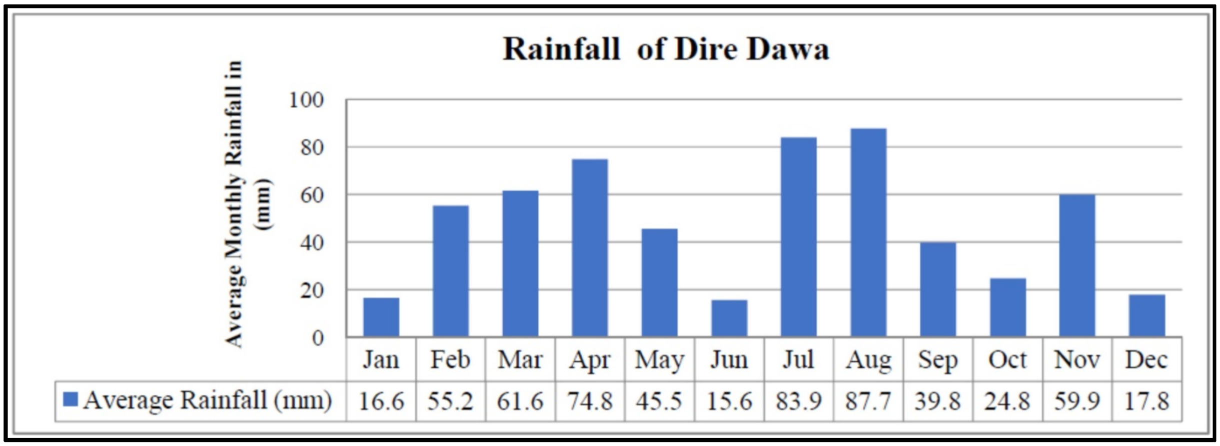


*Figure 3-4: Average Rainfall of Dire Dawa*

### 3.2 Data and Data source

The study area is covered by the Landsat satellite series, specifically within path 166 and row 54. To comprehensively analyze land surface temperature dynamics, all available images from this path and row are utilized for temporal analysis throughout the study period. This analysis included imagery collected during various seasons to capture the seasonal variability of land surface temperature.

For the dry seasons, cloud and haze-free images are generally more accessible, allowing for clearer analysis. However, during the wet seasons, challenges such as cloud cover arised. To mitigate these issues, we implemented image preprocessing techniques to enhance the quality of the wet-season imagery as much as possible. This preprocessing involved methods such as atmospheric correction, cloud masking, and image filtering to improve clarity and usability.

The dataset will comprise Landsat 7 ETM+ images for the years 2002 to 2012, as well as Landsat 8 OLI/TIRS and Landsat 9 OLI/TIRS images for the period from 2017 to 2024. By leveraging these diverse datasets, the study provides a comprehensive understanding of the dynamics of daytime seasonal variability of land surface temperature in Dire Dawa City. Detail descriptions of data's needed is given in the below.

*Table 3-1: Description of data and data source*

| No | Data type | Purpose | Resolution | Data source | Revisit time |
|---|---|---|---|---|---|
| 1 | Landsat 7 ETM+ | LST retrieval and LULC Mapping | 30*30m | http://earthexplorer.usgs.gov (USGS) | 16 days |
| 2 | Land Sat 8&9 OLI/TIRS | LST retrieval and LULC Mapping | 30*30m | http://earthexplorer.usgs.gov (USGS) | 16 days |
| 3 | Temperature | Validation of LST | _ | NMA | - |
| 4 | Population | | - | CSA | - |
| 5 | Administrative Boundary | | | Dire dawa City Administration | |
| 6 | Ground control point | Validation of Data | - | Google Image | |

| | | | | | |
|---|---|---|---|---|---|
| 7 | DEM | | 30*30 | http://earthexplorer.usgs.gov<br><br>(USGS) | 16 days |

## 3.3 Softwares

The Software's that are applicable for this study were identified by their problem solving capacity and relevance to the objective of the study and methodology. This included ArcGIS for retrieval of LST, NDVI and map preparation, ERDAS (Earth Resources Data Analysis System) Imagine 2015 for Remote Sensing application in order, Google earth will also be used to check and compare results with ground truth. In addition, ENVI software was used for, Gap filling, classification and to compare the results. For statistical analysis, graphical representation and reporting of a result the SPSS-software is used. : The lists of software utilized for the study are presented as follows in table shown below.

*Table 3-2: Softwares utilized in this study*

| Software packages | Purposes |
|---|---|
| ArcGIS | Database creation and LST extraction.<br><br>Integration and management of spatial information, Data analysis LST retrieval and map preparation |
| ENVI 5.3 | For Gap filling, classification, to compare and contrast the results |
| Google Earth Pro | For reference in accuracy assessment |
| ERDAS IMAGINE | To process satellite images including image enhancement,<br><br>Preprocessing |
| Microsoft Office | To create word documents |

| | |
|---|---|
| Mendeley Desktop | To insert citation and references used for the study. |
| SPSS | For statistical analysis, graphical representation and reporting |

## 3.4 Methods

Understanding the dynamics of daytime seasonal variability of land surface temperature (LST) and its driving factors in Dire Dawa City requires a comprehensive methodological approach. This research employed a combination of remote sensing techniques, statistical analysis, and spatial analysis to assess LST patterns and their influencing factors effectively. By integrating those methods, the study aims to elucidate the complex interplay between land surface temperature dynamics and the driving factors in Dire Dawa City, providing valuable insights for urban planning and environmental management in semi-arid regions.

### 3.4.1 Data Collection

To ensure a robust analysis, various types of data are collected:

Satellite Imagery: The project involved the acquisition of Landsat satellite imagery that spanned multiple years to effectively capture seasonal variations. Available satellite data, focusing on specific time frames that would provide a broad perspective on the changes in land cover and vegetation throughout the seasons were specifically identified. After identifying suitable datasets, we secured access to imagery that included various seasons as spring, summer, autumn, and winter. This allowed for a detailed analysis of how landscapes transformed over time, influenced by factors such as weather patterns, agricultural cycles, and urban development. The imagery was meticulously cataloged and organized by date, enabling to compare the visual differences and assess the impacts of seasonal changes on the environment.

Landsat satellite imagery obtained for the years 2002, 2012, 2017, and 2024 from the USGS

Earth Explorer. Selection of specific Landsat scenes based on cloud cover, temporal resolution, and relevance to the study period these years were selected due to significant changes in land use and cover, which are expected to impact LST.

Land Cover Data a key component of this study involved extracting land cover data from satellite imagery collected over multiple years. This extraction was essential for analyzing how changes in land cover influenced LST and its seasonal variations. High-resolution satellite images were utilized to generate land cover maps. By employing remote sensing techniques, we were able to classify the land cover accurately, capturing the spatial distribution and extent of each type. This process allowed for a nuanced understanding of how the landscape of Dire Dawa City evolved over time. Specific timeframes was selected to examine the land cover changes, ensuring that the maps reflected significant periods of urban development and environmental shifts.

### 3.4.2 Pre-processing of Satellite Imagery

The pre-processing phase involves several critical steps to enhance the quality of the satellite imagery:

#### 3.4.2.1 Radiometric Calibration

This was a crucial process in the analysis of satellite imagery, as it involved translating the digital numbers captured by satellite imaging systems into physical units. This calibration enabled to accurately interpret the data, converting it into usable information for further analysis. We focused on two main physical units: radiance, measured in watts per square meter per steradian per meter ($W/m^2/sr/m$), and apparent top-of-atmosphere reflectance. These units were essential for assessing the electromagnetic energy reflected from the Earth's surface. To achieve this, we calibrated the thermal bands of the satellite data, which involved converting the digital numbers obtained from the sensors into radiance values. This process required careful adjustment based on specific calibration coefficients provided by the satellite's manufacturer. The calibration coefficients were crucial for correcting any sensor-related anomalies or distortions that could affect the accuracy of the data. Without proper radiometric calibration, the data could yield misleading results, leading to inaccurate interpretations of land surface temperatures and other environmental conditions. By applying radiometric calibration techniques it is ensured that the thermal imagery accurately reflected the physical state of the landscape. This step converts digital numbers (DN) captured by the satellite into spectral radiance ($L\lambda$) using the following equation

$$L\lambda = M\lambda \times Qcal + AL$$

Where:

$L\lambda$=Spectral radiance

$M\lambda$=Radiance multiplicative scaling factor (from metadata)

$A_L$= Radiance additive scaling factor (from metadata)

Qcal= Quantized and calibrated pixel values in DN.

3.4.2.2 Atmospheric Correction

Atmospheric correction was a critical step in the processing of satellite imagery, as it aimed to reduce the effects of atmospheric interference that could distort the data. Various atmospheric conditions, such as water vapor, aerosols, and gases, could alter the electromagnetic signals received by the satellite sensors. Without correction, these atmospheric influences could lead to inaccurate interpretations of the land surface characteristics, particularly in analyses related to land surface temperature.

To address these challenges advanced algorithms, specifically the Fast Line-of-sight Atmospheric Analysis of Spectral Hypercube (FLAASH) was employed. This algorithm was designed to enhance the quality of the satellite images by correcting for atmospheric scattering and absorption. The necessary atmospheric parameters, including information on the local humidity, temperature, and aerosol levels, which were essential inputs for the FLAASH algorithm were used, clearer and more reliable imagery were achieved.

#### 3.4.2.3 Gap Filling

This was an essential method utilized to estimate missing values in the satellite imagery; particularly those caused by cloud cover or sensor. Landsat 7 ETM+ suffered a scan line corrector failure in May 2003, causing the imaged region to be duplicated and the scanning pattern to exhibit wedge-shaped scan-to-scan gaps that ranged from a single pixel at the center of the image to about 14 pixels along the east and west corners of each scene on average (Maxwell et al., 2007). These gaps in the data could significantly hinder the accuracy of analyses related to land surface temperature and seasonal variability as well as the land cover. This scan line error is corrected in ENVI using Landsat gap fill.

Throughout the gap-filling process, we assessed the quality of the interpolated values to ensure that they were realistic and aligned with the overall patterns observed in the data. And we were able to create a more complete and continuous dataset from the satellite imagery. We conducted a validation check by comparing the filled values against Google earth, confirming that the estimates were both plausible and scientifically sound. The filled gaps allowed drawing more accurate conclusions regarding land cover changes, temperature dynamics.

#### 3.4.2.4 Layer Stacking

This step is employed to enhance the analysis of satellite imagery, aimed to combine multiple bands of satellite data into a single image, allowing for a more comprehensive interpretation of the landscape in Dire Dawa City. We first ensured that all bands were properly aligned in terms of spatial dimensions. This alignment was critical, as any discrepancies could lead to inaccuracies in the combined image, affecting subsequent analyses. Once the bands were aligned, we proceeded to stack them into a single multi-spectral image. This process involved combining different wavelengths of light captured by the satellite, which included visible, near-infrared, and thermal bands. Each band contained unique information about the Earth's surface, such as vegetation health, land cover types, and temperature variations. After the layer stacking was completed, we conducted quality checks to ensure that the final composite image accurately represented the data. We analyzed the image for any artifacts or misalignments that could compromise the results. This attention to detail ensured that the stacked layers provided a reliable foundation for further analysis. The resultant multi-spectral image facilitated a more nuanced understanding of the environmental conditions.

#### 3.4.2.5 Projection and Sub setting

Projection and sub setting were important steps undertaken to ensure relevance of the Landsat images for their analysis of Dire Dawa City. Subset the data to isolate the area of interest Dire Dawa City. This involved extracting only the portions of the satellite imagery that encompassed the city limits, thereby allowing for a more concentrated analysis of land cover changes and their effects on land surface temperature within that specific area.

Datum**:** WGS 84_UTM_zone_37

Projection Type**:** Transverse Mercator

Units**:** Meters

Projected Coordinates**:** Easting (X), Northing (Y)

### 3.4.3 Land Use/Land Cover Extraction

Land use and land cover extraction was a critical component of the research project, employing advanced techniques to classify the various types of land use within Dire Dawa City. This classification was aimed to provide insights into how different land cover types affected the dynamics of daytime seasonal variability of land surface temperature. we utilized a combination of remote sensing techniques and machine learning algorithms to carry out the classification process. The multi-spectral nature of the imagery allowed for the identification of different land cover types based on their spectral signatures.

To enhance the accuracy of the classification, we applied supervised classification methods.

This involved selecting representative training samples for each land cover type. We carefully chose those samples based on their visual characteristics in the satellite images, ensuring that they covered the diversity of land cover present in Dire Dawa City.

Using these training samples, we employed algorithm Support Vector Machines algorithm to robust classification results. This algorithm processed the spectral data and classified each pixel in the imagery according to the predefined land cover categories.

Supervised Classification: Supervised classification was a pivotal method employed to accurately categorize various surface cover types within the satellite imagery of Dire Dawa City. This process began with identifying representative samples of the different surface cover types relevant to the study. These samples, known as training areas, were crucial for guiding the classification.

We leveraged our familiarity with the region and understanding of the actual surface cover types depicted in the images to select appropriate training regions. This step was essential, as it ensured that the training samples accurately reflected the diversity of land cover present in Dire Dawa City. Once the training areas were established, we effectively supervised the classification process by utilizing these samples to train the classification algorithm. The numerical data from all spectral bands corresponding to the pixels within the training areas was employed to create a spectral profile for each class. This profile represented the unique spectral characteristics of each surface cover type. These signatures encompassed the distinct patterns of reflectance for each land cover type across the various spectral bands.

Support Vector Machine (SVM) Classification: The SVM algorithm was particularly well-suited for this study due to its ability to handle variations in training sample size and its performance in urban areas characterized by mixed pixels; it excels at separating different classes of data, even when those classes are not linearly separable. This capability was crucial in an urban setting like Dire Dawa, where land cover types often intermingle, leading to complex spectral signatures that could complicate classification efforts.

Initially we prepared dataset by defining training areas, which consisted of samples representing various land cover types. These training areas were used to instruct the SVM algorithm on how to distinguish between different surface covers based on their spectral characteristics. The SVM algorithm was applied to create a hyper plane that effectively separated the different classes in a multi-dimensional feature space. This hyper plane defined the boundary between the various land cover types, allowing the algorithm to classify each pixel in the imagery based on its proximity to the nearest class boundary.

One of the significant advantages of SVM was its robustness against variations in the size of the training samples. The algorithm could still perform effectively even if some classes had fewer training examples than others. After the SVM model was trained, it processed the entire satellite image, classifying each pixel according to the learned patterns. The resulting classification maps illustrated the spatial distribution of different land cover types within Dire Dawa City, providing valuable insights into the land cover change throughout the years.

Accuracy Assessment: Accuracy assessment was aimed at determining the reliability of the information produced from remotely sensed data. The primary objective was to quantitatively evaluate how well the pixels in Dire Dawa City were classified into their appropriate feature classes, ensuring the robustness of the analysis.

To conduct this evaluation ENVI software was used, which provided the necessary tools for accuracy assessment. The overall accuracy was the most common measure reported, along with the Kappa coefficient (K), which quantified the level of agreement between the classified data and the reference data.

To minimize bias in sampling, implemented a stratified random sampling approach. They generated ground truth data from Area of Interest using high-resolution Google imagery as a reference. This method ensured a diverse representation of the different land cover types within the study area. After establishing the ground truth AOIs, we constructed a confusion matrix to compare the classified image against the reference data. This matrix provided a clear overview of the classification accuracy for each land cover type.

Producer's Accuracy was calculated to quantify the percentage of correctly identified pixels for each specific class, which helped to reveal any errors of omission. The formula used was:

$$Producer's\ Accuracy = (Ci/Ct) \times 100$$

Where Ct represented the total number of sample sites in the column for a specific class, and Ciwas the number of correctly identified sample locations in that column.

User's Accuracy was also assessed, focusing on the total number of correct sample units in a category divided by the total number of samples classified into that category. This measure indicated the commission error and was calculated using the formula:

$$User's\ Accuracy = (Ri/Rt) \times 100$$

Where Ri indicated the correctly classified samples in the row, and Rt was the total number of samples in that row.

Overall Accuracy was determined by dividing the total number of correctly classified sample units by the total number of samples in the error matrix. This statistic, being one of the most frequently reported accuracy evaluations, was calculated as follows:

$$Overall\ Accuracy = (Sd/n) \times 100$$

Where Sd was the sum of values along the diagonal of the confusion matrix, and n was the total number of samples.

Kappa statistic was calculated to measure the agreement between the remote sensing-derived classification map and the reference data, offering a more nuanced understanding of the classification accuracy. The Kappa statistic was computed using the formula:

$$Kappa = (N * \sum nii - \sum ni + n + i)/(N2 - \sum ni - n - i)$$

Where:

nii represented the number of observations in the diagonal of the error matrix, ni+ was the totals of observations in row i, n+i was the total of observations in column i, and N was the total number of observations in the matrix.

Through this comprehensive accuracy assessment, we were able to quantify the effectiveness of their land cover classification and ensure the reliability of the findings regarding the dynamics of land surface temperature in Dire Dawa City. The results of the accuracy assessment provided a solid foundation for interpreting the relationships between land cover changes and environmental factors in the urban setting.

### 3.4.4 Land Use/Land Cover Indices

Land use and land cover indices were essential components of the research, providing quantitative measures to analyze the different land cover types within Dire Dawa City. These indices allowed assessing various aspects of the urban environment, including vegetation health, landing surface temperature, and overall land use dynamics. By calculating these land use and land cover indices, gained valuable insights into the spatial distribution and health of vegetation, the extent of urbanization, and the thermal characteristics of the landscape. These indices served as powerful tools for analyzing the interactions between land cover changes and land surface temperature dynamics, ultimately contributing to a deeper understanding of the environmental changes occurring in Dire Dawa City.

The following indices will be calculated to analyze land cover:

- Normalized Difference Vegetation Index (NDVI):

The Normalized Difference Vegetation Index (NDVI) is a key remote sensing tool that measures the greenness and density of vegetation as captured in satellite images. It quantifies vegetation health by evaluating the difference in reflectance between two specific wavelengths: near-infrared (NIR) light, which is strongly reflected by healthy vegetation, and red light, which is primarily absorbed during photosynthesis.

*Calculation of NDVI*

The NDVI is calculated using the following formula:

$$NDVI = (NIR - Red)/(NIR + Red)$$

Where:

NIR = Near-infrared band reflectance

Red = Red band reflectance

*Interpretation of NDVI Values*

NDVI values range from -1 to +1, providing a gradient of vegetation density and health:

- High Values (0.7 to 0.9): Indicate dense, healthy vegetation, such as forests and well-maintained agricultural fields.
- Moderate Values (0.2 to 0.6): Suggest sparse or stressed vegetation, like grasslands or areas with some vegetation cover.
- Low Values (0 to 0.2): Represent bare soil, rocks, or areas with minimal vegetation.
- Negative Values: Typically indicate non-vegetated surfaces, such as water bodies, clouds, or urban infrastructure.
- Normalized Difference Built-up Index (NDBI):

The Normalized Difference Built-up Index (NDBI) is a valuable remote sensing tool designed to emphasize and quantify urban built-up areas using satellite imagery. By utilizing the near-infrared (NIR) and shortwave infrared (SWIR) bands, NDBI effectively distinguishes constructed environments from other land cover types.

*Calculation of NDBI*

NDBI is calculated using the following formula:

$$NDBI = (SWIR - NIR)/(SWIR + NIR)$$

Where:

SWIR: represents the reflectance in the shortwave infrared band, which is sensitive to built-up surfaces.

NIR: denotes the reflectance in the near-infrared band, which vegetation reflects strongly but built-up areas absorb.

*Interpretation of NDBI Values*

NDBI values typically range from -1 to +1, with higher values indicating a greater presence of built-up areas.

High Values (typically > 0.1): Indicate significant built-up areas, such as urban infrastructure, roads, and buildings.

Low Values (around 0): Suggest the presence of vegetation or water bodies.

Negative Values: Often correspond to non-built-up surfaces, such as bare soil or agricultural fields.

### 3.4.5 Retrieval of Land Surface Temperature (LST)

Retrieving Land Surface Temperature (LST) from satellite imagery involves a series of steps designed to accurately convert thermal data from the satellite's sensors into usable temperature readings. Below is a detailed guide on how to perform LST retrieval, specifically using Landsat data. By following these steps, we have effectively compute Land Surface Temperature from Landsat imagery, leveraging the capabilities of the thermal bands and appropriate algorithms to derive valuable insights into environmental conditions and urban dynamics over the years. This methodology allows for a comprehensive understanding of how land surface temperatures evolve in relation to changing land use and cover patterns. The retrieval of LST from satellite imagery involves several steps:

*For Landsat 8 and 9 (Using Split-Window Algorithm*)

1. Radiance Calculation:

Convert digital numbers (DN) from bands 10 and 11 to radiance using:

$$L\lambda = ML \times DN + AL$$

Where:

$M_L$=is the radiance multiplicative scaling factor and

$A_L$=is the radiance additive scaling factor.

2. Brightness Temperature Calculation:

Convert radiance to brightness temperature (BT) using:

$$BT = K2/ln\,(K1/L\lambda + 1)$$

Where:

K1 and K2 are the thermal conversion constants for the respective bands.

3. Split-Window Algorithm:

Apply the split-window algorithm to calculate LST:

$$LST = BT - \ (BT10 - BT11)\ \times\ (1 - e - \tau)/\,\epsilon$$

Where:

τ is the atmospheric transmittance and ϵ is the emissivity of the surface.

For Landsat 7 (Using Single-Channel Method)

1. Radiance Calculation:

Convert DN from band 6 to radiance, similar to the method used for Landsat 8 and 9.

2. Brightness Temperature Calculation:

Convert the radiance to brightness temperature using the same formula as above.

3. Single-Channel Method:

Calculate LST using the single-channel method:

$$LST = BT \times (1 + (0.00115 \times BT)/1 - (0.00115 \times BT \times \epsilon))$$

Where:

ϵ represents surface emissivity, typically estimated based on land cover type.

*Table 3-3: Thermal Band Calibration Constant of Landsat 7 ETM.*

| **Satellite** | **Categories** | **Band 6** |
|---|---|---|
| Landsat 7TM | K1 | 607.76 |
| | K2 | 1260.56 |
| | Radiance Maximum Band | 15.153 |
| | Radiance Minimum Band | 1.238 |
| | Quantize_cal_max | 255 |
| | Quantize_cal_min | 1 |

| | | |
|---|---|---|
| | Map projection | UTM" |
| | Ellipsoid | "WGS84" |
| | UTM Zone | 38 |
| | Grid_cell_size_reflective | 30 |

[Source: Landsat-7 Metadata, Obtained from USGS]

*Table 3-4: Thermal Band Calibration Constant of Landsat 8 OLI/TIRS*

| **Satellite** | **Sensors** | **Categories** | **Band 10** | **Band 11** |
|---|---|---|---|---|
| Landsat 8 OLI/TIRS | | K1 | 777.8853 | 480.8883 |
| | | K2 | 1321.0789 | 1201.1442 |
| | | Radiance_maximum | 22.0018 | 22.0018 |
| | | Radiance_minimum | 0.10033 | 0.10033 |
| | | Quantize_cal_max | 65535 | 65535 |
| | | Quantize_cal_min | 1 | 1 |
| | | Resolution | 100 * (30) | 100 * (30) |

[Source: Landsat-8 Metadata, Obtained from USGS]

4. Surface Emissivity Adjustment

Adjust for surface emissivity based on land cover types, as different surfaces emit thermal radiation differently. Emissivity values typically range from 0.95 for vegetation to about 0.85 for urban areas. This adjustment was necessary because different land cover types emit thermal radiation differently, impacting the accuracy of temperature estimates derived from satellite data.

To begin the adjustment process, emissivity values were assigned based on the specific land cover types present in the study area.

$$E = mPv + n$$

Where

n = 0.986 and m = 0.004
PV is calculated using soil and vegetation NDVI values

$$PV = (NDVI - NDVImin / NDVImax - NDVImin)\ ^\wedge 2$$

Where:

NDVI min is the lowest NDVI value derived from the raster NDVI and
NDVI max is the highest NDVI value.

5. Error Assessment

Evaluate the accuracy of the LST calculations through validation with ground truth data or comparison with other satellite datasets if available. The error assessment of Land Surface Temperature (LST) calculations was a crucial in ensuring the accuracy and reliability of the results obtained from satellite imagery. This evaluation involved several methodologies aimed at validating the LST data against ground truth measurements.

*Ground Truth Validation*

To assess the accuracy of the LST calculations, ground truth data were collected from various sites within the study area. This data comprised in-situ temperature measurements taken during the same periods as the satellite imagery. The ground truth data were essential for establishing a baseline against which the satellite-derived temperatures could be compared. By integrating ground truth data with comparisons to other satellite datasets, we ensured that the findings were reliable and could be confidently used to analyze land surface temperature dynamics.

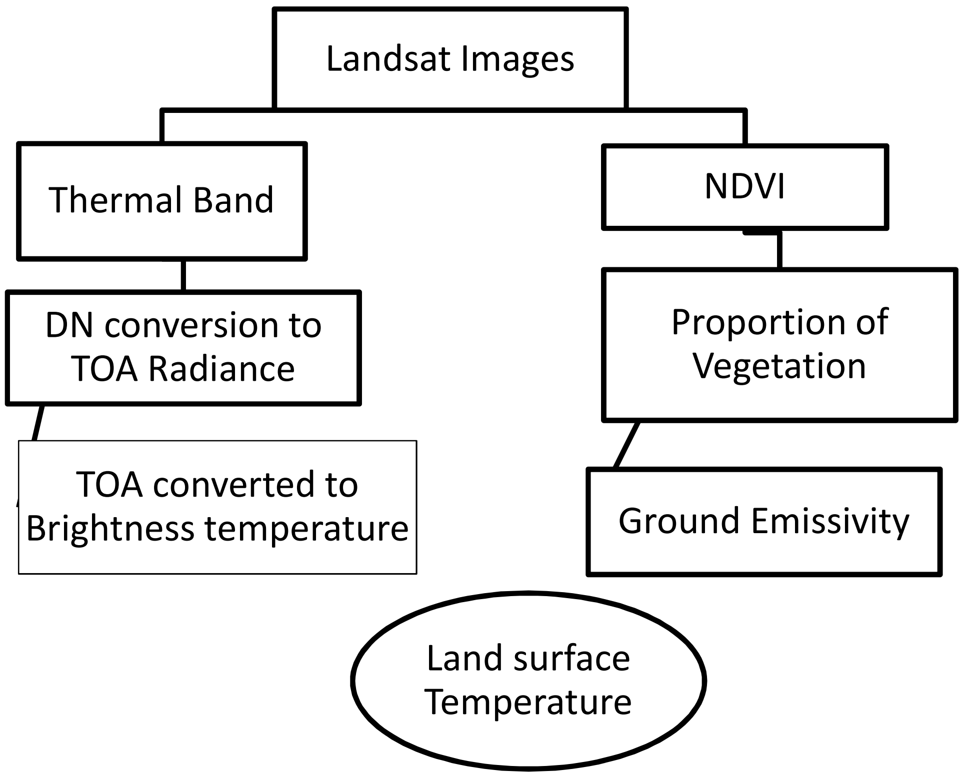


*Figure 3-5: Land Surface Temperature Retrieval Diagram*

### 3.4.6 Analysis and Interpretation

Once the Land Surface Temperature (LST) had been calculated for the specified years the data underwent a comprehensive analysis to identify trends and correlations. This analysis aimed to uncover insights regarding with land cover variations, and the impacts of urbanization on surface temperatures.

*Temporal Trends in LST*

The first step in the analysis involved examining the LST data across the different years to identify any significant trends. This included:

- A time-series: This analysis was conducted to evaluate the LST values over the specified years. Mean LST values for each year were computed and plotted to visualize trends. Statistical tests, such as linear regression, were employed to assess the significance of any observed trends.

- Seasonal Variability: The analysis also considered seasonal variations by comparing LST data from different months within the same years. This helped identify patterns related to seasonal temperature fluctuations.

*Relationships with Land Cover Changes*

The analysis focused on the relationship between LST and land cover changes within Dire Dawa City:

- Comparative Analysis: The mean LST values for each land cover type were compared. For instance, higher LST values were often associated with urban areas, while lower values were found in vegetated regions. The analysis aimed to quantify these differences and determine the degree of correlation between land cover type and LST.

- Change Detection: Changes in land cover over time were analyzed to determine their impact on LST. Areas that transitioned from vegetation to urban land use were particularly scrutinized, as this shift typically leads to increased surface temperatures due to the urban heat island effect.

*Impacts of Urbanization*

The analysis also delved into the specific impacts of urbanization on LST:

- Urban Heat Island Effect: The study assessed the extent of the urban heat island effect within Dire Dawa City. By comparing LST values in urban areas with those in surrounding rural or vegetated regions, we were able to quantify the temperature differences attributable to urbanization.

- Spatial Analysis: Geographic Information System (GIS) tools were employed to visualize LST distributions across the city. Heat maps were generated to highlight areas of high temperature, enabling the identification of hotspots that might require targeted urban planning and environmental management.

- Correlation with Socioeconomic Factors: The analysis also considered socioeconomic factors, such as population density to understand how these elements interacted with urbanization and influenced LST patterns.

### *3.4.7* Statistical Analysis

In the analysis of Land Surface Temperature (LST) data, various statistical methods were employed to uncover relationships and quantify the impacts of environmental factors. The primary techniques used were correlation analysis and regression analysis. The results from both the correlation and regression analyses were interpreted to draw meaningful conclusions about the factors influencing LST. Statistical software (SPSS) was used for conducting correlation analyses and multiple linear regressions, providing a comprehensive understanding of the relationships between LST and its driving factors.

*1. Correlation Analysis*

The Pearson correlation coefficient was calculated to assess the strength and direction of the linear relationship between LST and other variables, such as temperature, precipitation, and humidity. The formula used to compute the Pearson correlation coefficient r is:

$$r = n * (\sum xy) - (\sum x)(\sum y) / [n\sum x2 - (\sum x)2][n\sum y2 - (\sum y)2]2$$

Where:

n = Number of paired observations

$x$ = Variable representing LST
$y$= Variable of interest (e.g., temperature, precipitation, humidity)
$\sum xy$ = Sum of the product of paired scores
$\sum x$ = Sum of LST values
$\sum y$ = Sum of the other variable's values
$\sum x^2$ = Sum of the squares of LST values
$\sum y^2$ = Sum of the squares of the other variable's values

This analysis provided insights into how strongly each variable correlated with LST, helping to identify key factors influencing temperature variations. The Pearson correlation coefficients indicated the strength of the linear relationships between LST and the independent variables. For example, a strong positive correlation with temperature would suggest that higher temperatures are associated with increased LST.

*2. Regression Analysis*

Linear regression is a statistical method used to model the relationship between a dependent variable and one or more independent variables. In the context of analyzing Land Surface Temperature (LST), linear regression helps quantify how different factors, influence LST values over time.

When only one independent variable is used to predict LST, the model is called simple linear regression. The relationship is expressed in the following form:

$$LST = \beta 0 + \beta 1 \cdot X + \epsilon$$

Where:

LST = Dependent variable (Land Surface Temperature)
$\beta 0$ = Intercept of the regression line
$\beta 1$ = Coefficient for the independent variable X (e.g., temperature)
X = Independent variable

$\epsilon$ = Error term (residuals)

Interpretation: The intercept $\beta 0$ represents the expected value of LST when X is zero. The coefficient $\beta 1$ indicates the expected change in LST for a one-unit increase in X. For instance, a positive coefficient for temperature would indicate that an increase in temperature would lead to a corresponding increase in LST, while the coefficients for precipitation and humidity could reveal their mitigating effects on LST.

By employing correlation and regression analyses, the study was able to quantify relationships between LST and environmental factors effectively. This statistical analysis provided robust insights that informed the understanding of temperature dynamics in relation to climatic conditions, ultimately contributing to more informed decision-making in urban planning and environmental management

### 3.4.8 Work flow diagram

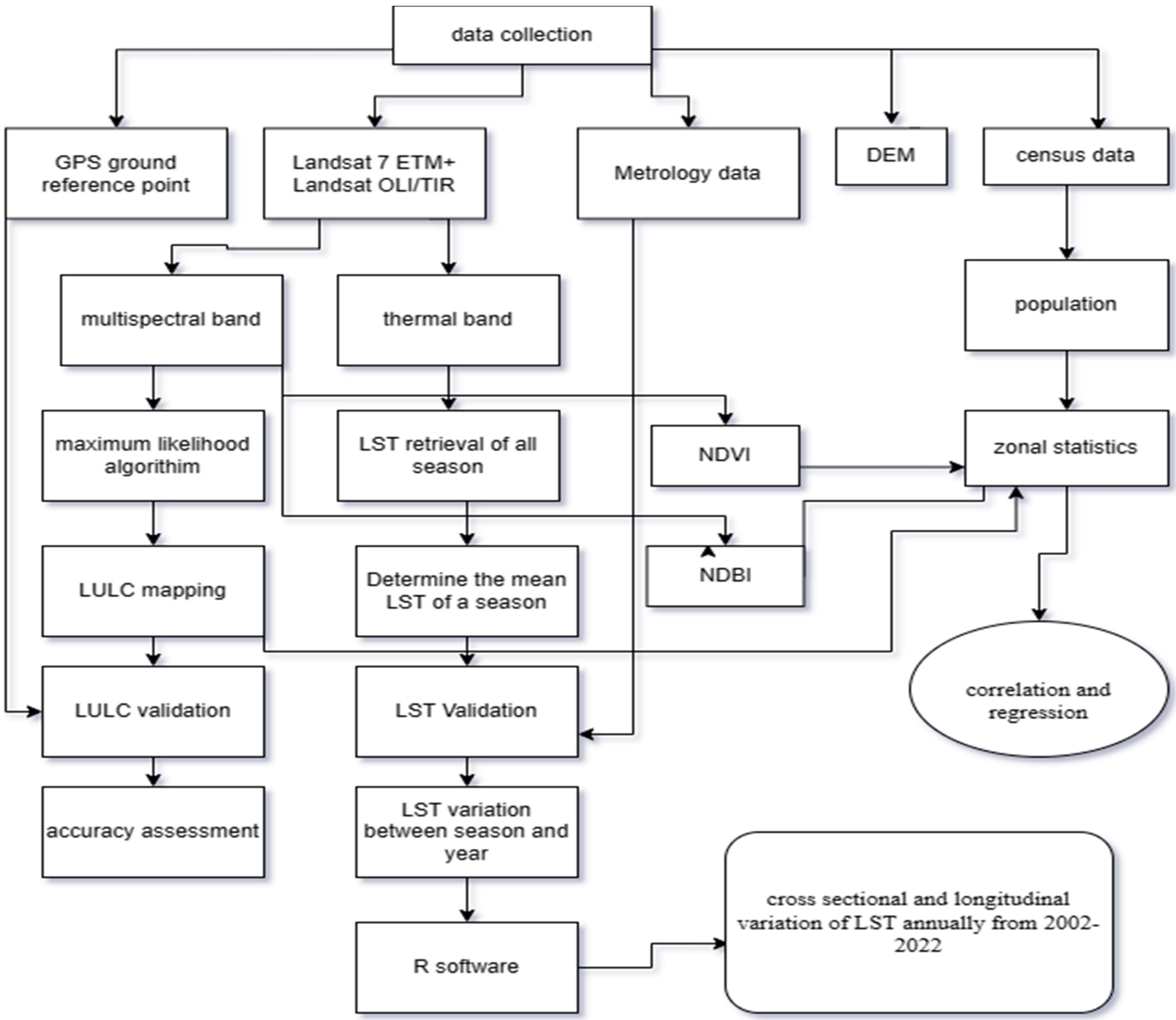


*Figure 3-6: Workflow diagram*

# 4 CHAPTER 4: Results and Discussion

## 4.1 Temporal Trend

Analysis of LST trends from 2002,2012,2017,2024, revealing whether LST is increasing, decreasing, or remaining stable over the study period.

### 4.1.1 Spatiotemporal variation of LST of Kiremt Season

The following analysis explores the variations in land surface temperature (LST) during the Kiremt season across the years 2002, 2012, 2017, and 2024.

The result demonstrated on Figure 4-1 and Table 4-1 shows that the minimum LST recorded during the Kiremt season has experienced notable fluctuations over the selected years. It started at 15.2°C in 2002, rising to 19.2°C in 2012, and then slightly decreased to 18.2°C in 2017. By 2024, the minimum temperature increased again to 20.6°C, indicating variability in the cooler temperatures over time.

Maximum LST values demonstrate significant annual variability as well. The highest temperature recorded was 32.8°C in 2017, which was relatively stable in the surrounding years, peaking at 32°C in 2002 and 33.7°C in 2024, suggesting a range of warmer conditions over the years.

The mean LST during these periods also varied, with an average of 23.6°C in 2002, increasing to 26.1°C in 2012. The mean temperature slightly decreased to 25.5°C in 2017, before rising again to 27.15°C in 2024, indicating an overall warming trend in the most recent years.

*Table 4-1: Min, Max and Mean LST of Dire Dawa 2002 – 2024 Kiremt Season*

| Year | 2002 | 2012 | 2017 | 2024 |
|---|---|---|---|---|
| Min | 15.2 | 19.2 | 18.2 | 20.6 |

| | | | | |
|---|---|---|---|---|
| Max | 32 | 33 | 32.8 | 33.7 |
| Mean | 23.6 | 26.1 | 25.5 | 27.15 |

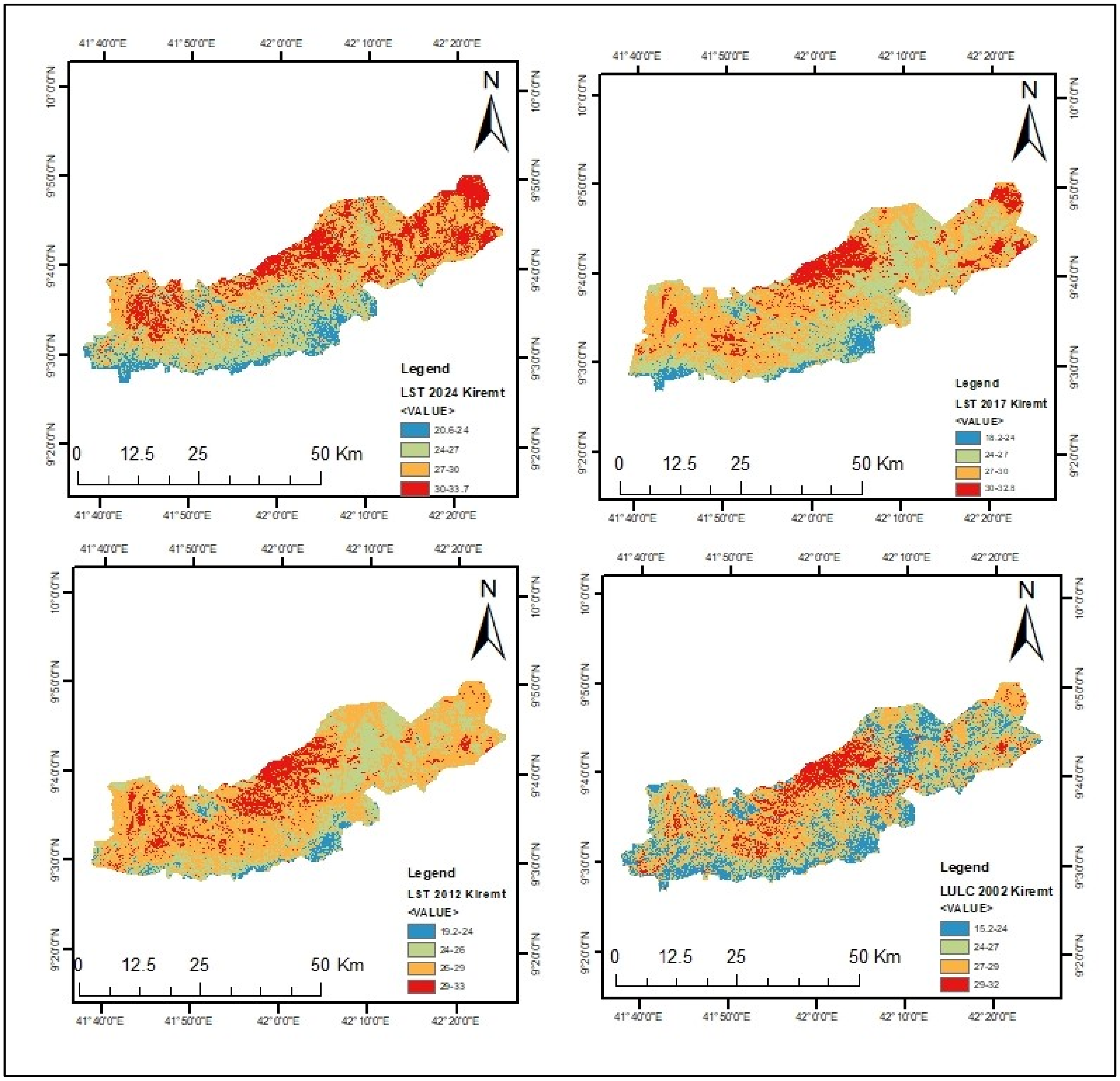


*Figure 4-1: Landsat LST Map of Dire Dawa City 2002 – 2024 Kiremt*

### 4.1.2 Spatiotemporal variation of LST of Belg Season

This analysis explores the variations in land surface temperature (LST) during the Belg season in Dire Dawa City for the years 2002, 2012, 2017, and 2024.

The result demonstrated on Figure 4-2 and Table 4-2 reveals that the minimum LST recorded during the Belg season shows notable fluctuations across the years. It began at 18.2°C in 2002, rising to 19.5°C in 2012, before declining to 17.8°C in 2017. By 2024, the minimum temperature increased to 20°C, indicating variability in cooler temperatures throughout the period.

Maximum LST values reflect a gradual warming trend, starting at 33.2°C in 2002 and slightly increasing to 33.5°C in 2012. This was followed by a small decrease to 32.9°C in 2017, with a notable rise to 34.6°C in 2024, suggesting an upward trajectory in temperature over the years.

Mean LST data also align with this warming trend, beginning at 25.7°C in 2002 and increasing to 26.5°C in 2012. Although there was a dip to 25.35°C in 2017, the average temperature recovered to 27.3°C by 2024, reflecting a general trend toward higher temperatures in the later years. The spatiotemporal variation of LST during the Belg season highlights significant temperature fluctuations over time, with a noticeable warming Trend.

*Table 4-2: Min, Max and Mean LST of Dire Dawa 2002 – 2024 Belg*

| Year | 2002 | 2012 | 2017 | 2024 |
|---|---|---|---|---|
| Min | 18.2 | 19.5 | 17.8 | 20 |
| Max | 33.2 | 33.5 | 32.9 | 34.6 |
| Mean | 25.7 | 26.5 | 25.35 | 27.3 |

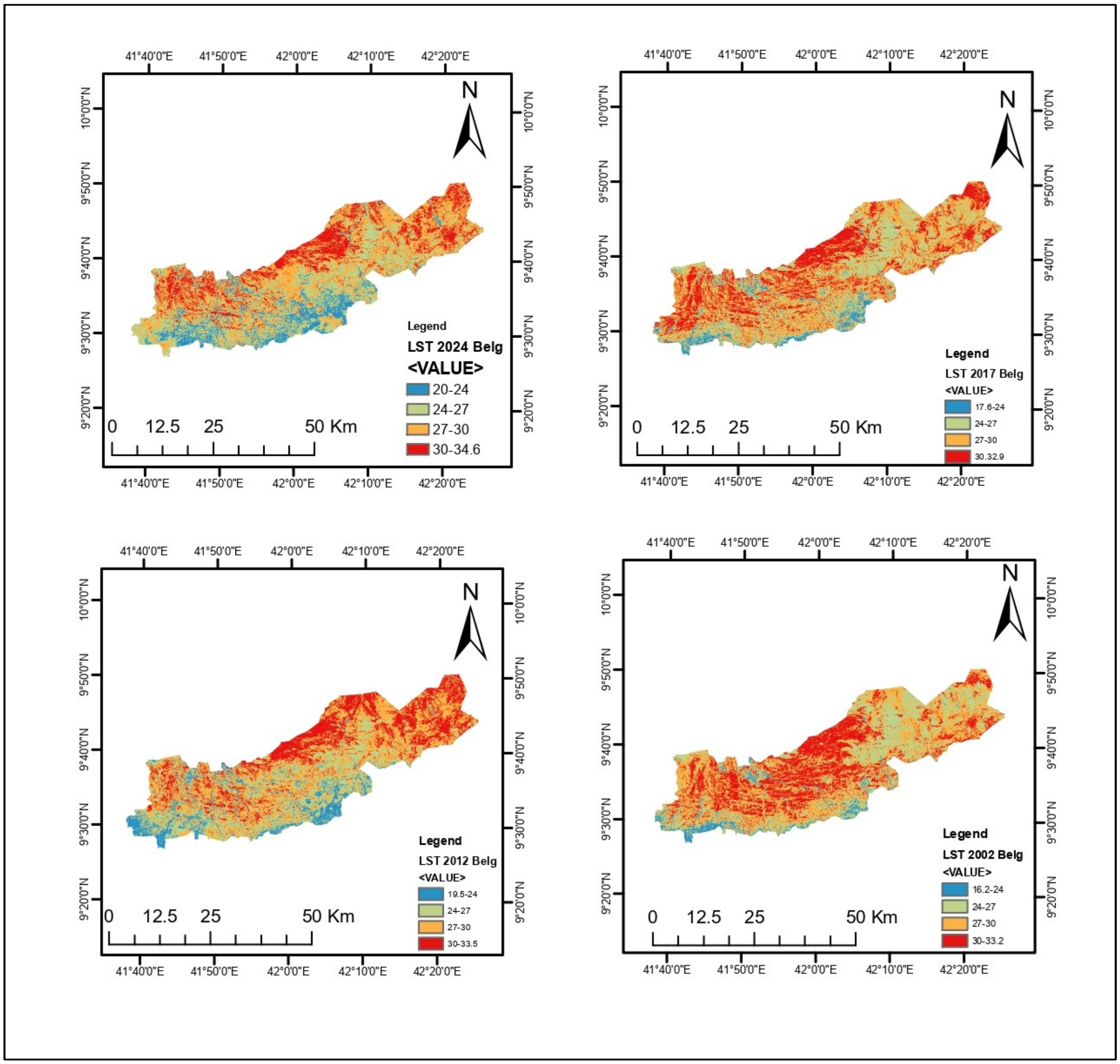


*Figure 4-2: LST Map of Dire Dawa City 2002 – 2024 Belg*

### 4.1.3 Spatiotemporal variation of LST of Bega Season

This analysis examines the variations in land surface temperature (LST) in Dire Dawa City during the Bega season for the years 2002, 2012, 2017, and 2024.

The result obtained on Figure 4-3 and Table 4-3 obtained reveals fluctuations in minimum

LST across the selected years. It started at 18.3°C in 2002, dipped to a lower 17°C in 2012, then increased slightly to 18°C in 2017, and rose again to 19.2°C by 2024.

In terms of maximum LST values, there was a notable peak of 36.92°C in 2024, indicating higher temperatures compared to previous years. Specifically, the maximum temperatures were 33.8°C in 2002, 34.3°C in 2012, and a moderate increase to 35°C in 2017, reflecting a trend of rising temperatures.

The mean LST values exhibited similar variations, beginning at 26.05°C in 2002, slightly declining to 25.65°C in 2012. This figure then increased to 26.5°C in 2017 before reaching a higher average of 28.06°C in 2024. The spatiotemporal variation of LST during the Bega season illustrates a general trend of rising temperatures over the years, with fluctuations in minimum and maximum values

*Table 4-3: Min, Max and Mean LST of Dire Dawa 2002 – 2024 Bega*

| Year | 2002 | 2012 | 2017 | 2024 |
|---|---|---|---|---|
| Min | 18.3 | 17 | 18 | 19.2 |
| Max | 33.8 | 34.3 | 35 | 36.92 |
| Mean | 26.05 | 25.65 | 26.5 | 28.06 |

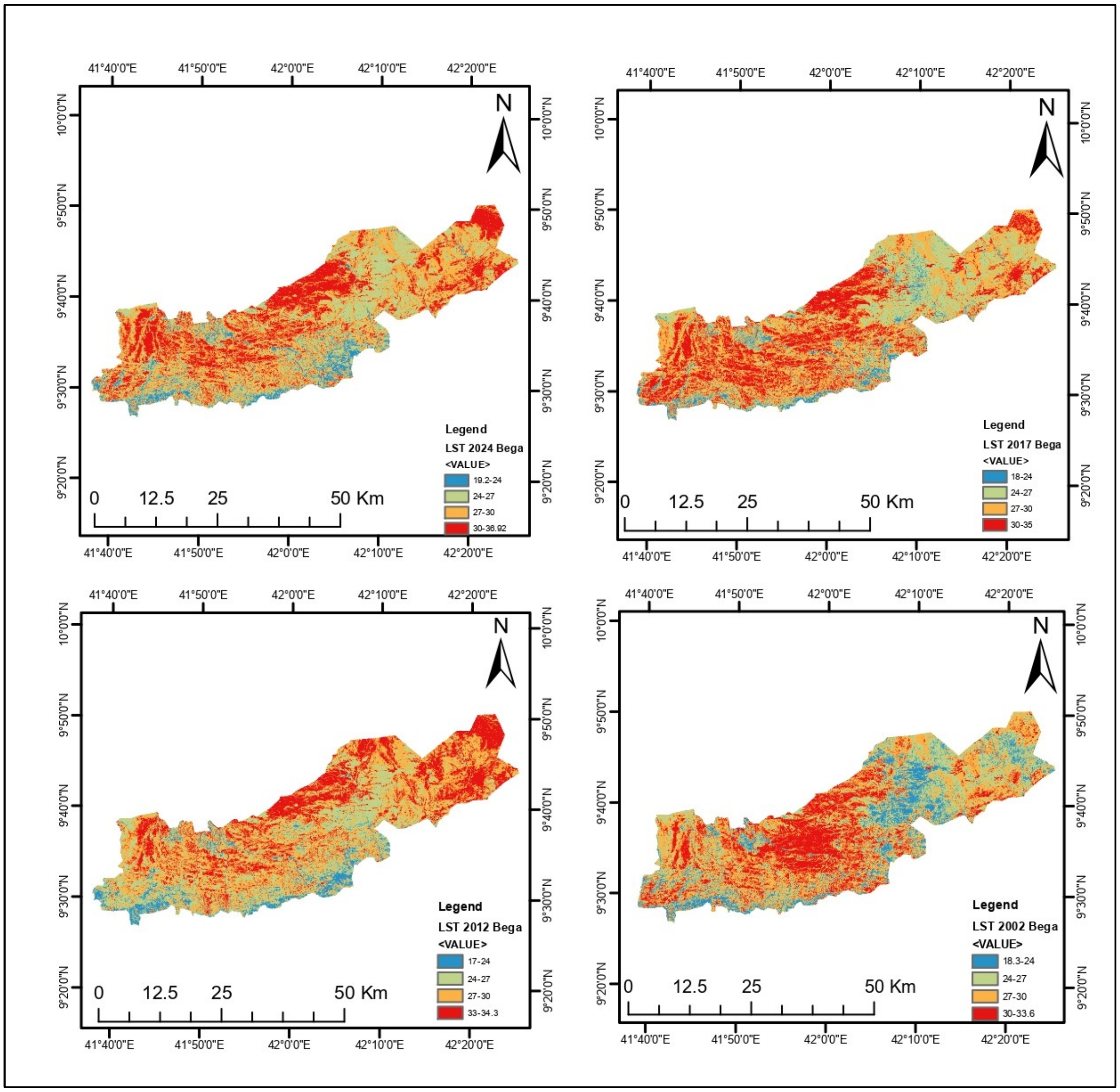


*Figure 4-3: Landsat LST Map of Dire Dawa City 2002 – 2024 Bega*

### 4.1.4 Spatiotemporal variation of LST of Tseday Season

Figure 4-4 and Table 4-4 present an analysis of land surface temperature (LST) variations in Dire Dawa City during the Tseday season for the years 2002, 2012, 2017, and 2024. LST is a crucial environmental indicator that reflects urban heating effects and overall climatic conditions.

The dataset shows notable fluctuations in minimum LST across the years. It started at 15.4°C in 2002, increased to 18.3°C in 2012, further rose to 19.9°C in 2017, and reached 21°C by 2024, indicating a steady upward trend in minimum temperatures.

In terms of maximum LST, the values displayed significant variation, with a peak of 38.4°C in 2024, demonstrating a substantial increase from 32.8°C in 2002 and 33.2°C in 2012, followed by a rise to 34.6°C in 2017. This pattern highlights a progressive warming trend over the years.

The mean LST also experienced fluctuations, beginning at 24.1°C in 2002, increasing to 25.75°C in 2012, and then rising again to 27.25°C in 2017. By 2024, the average LST reached 29.7°C, reflecting an overall warming trend during the Tseday season. the spatiotemporal variation of LST during the Tseday season illustrates a consistent increase in both minimum and maximum temperatures over the years.

*Table 4-4: Min, Max and Mean LST of Dire Dawa 2002 – 2024 Tseday*

| Year | 2002 | 2012 | 2017 | 2024 |
|---|---|---|---|---|
| Min | 15.4 | 18.3 | 19.9 | 21 |
| Max | 32.8 | 33.2 | 34.6 | 38.4 |
| Mean | 24.1 | 25.75 | 27.25 | 29.7 |

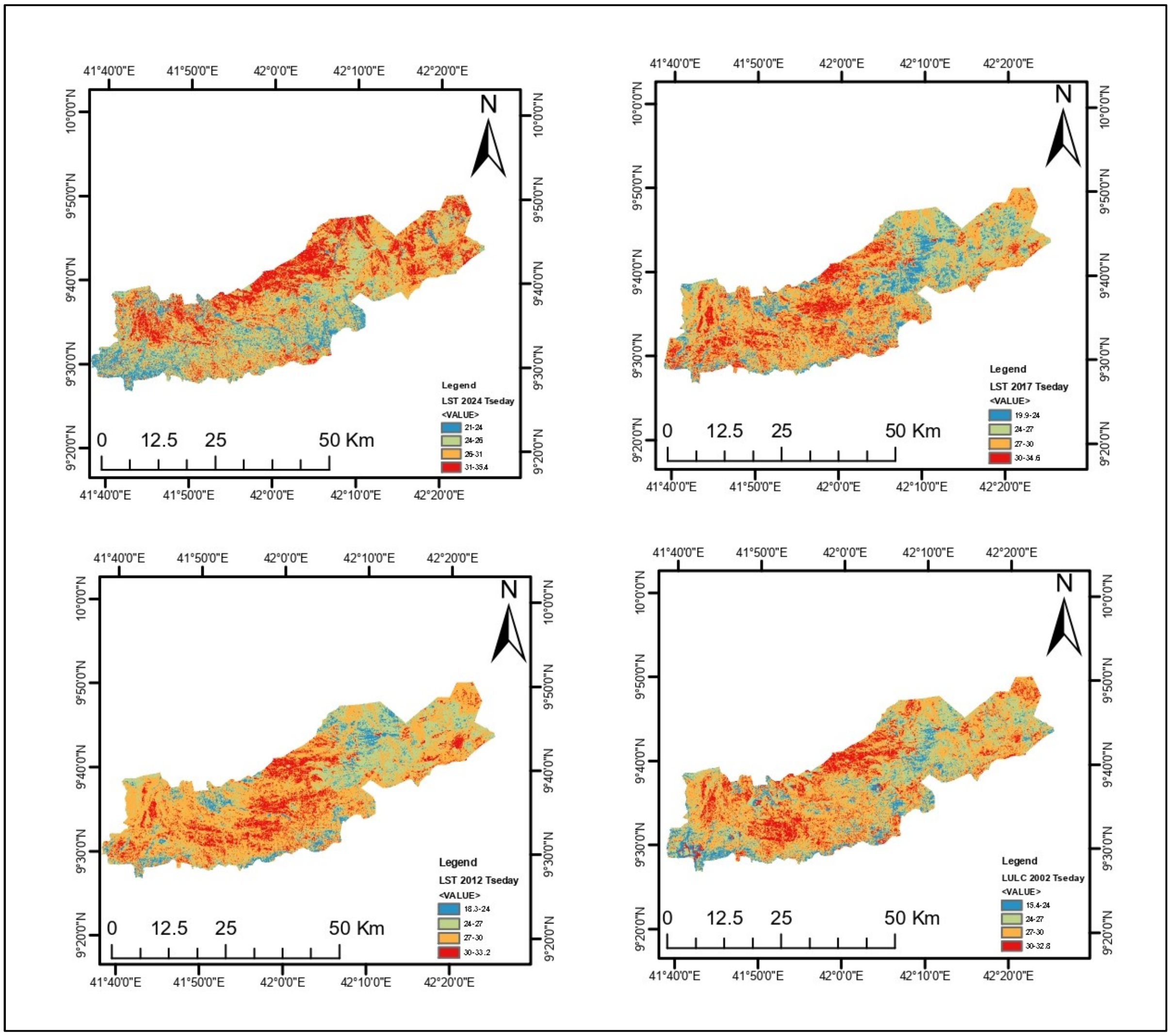


*Figure 4-4: Landsat LST Map of Dire Dawa City 2002 – 2024 Tseday*

## 4.2 Seasonal Trend

In analyzing the seasonal variation of land surface temperature (LST) in Dire Dawa City across the years 2002, 2012, 2017, and 2024, notable patterns emerge regarding temperature fluctuations throughout each season.

In 2002, during the Kiremt season, the minimum LST was recorded at 15.2°C, with a maximum of 32°C and a mean of 23.6°C. This season exhibited moderate temperatures. The

Belg season showed a slight increase, with minimum temperatures at 18.2°C and maximums reaching 33.2°C, resulting in a mean of 25.7°C. The Bega season began to reveal warmer conditions, featuring a minimum LST of 17.51°C and a maximum of 37.44°C, leading to a mean of 29.79°C. Finally, in the Tseday season, the minimum temperature was 15.4°C, the maximum was 32.8°C, and the mean was 24.1°C, making this season warmer than Kiremt but cooler than Bega. Thus, in 2002, Kiremt was the coolest season, while Bega was the warmest.

2012, the Kiremt season recorded a minimum LST of 19.2°C, with a maximum of 33°C and a mean of 26.1°C, reflecting a warming trend. In the Belg season, temperatures rose slightly again, with a minimum of 19.5°C, a maximum of 33.5°C, and a mean of 26.5°C. However, the Bega season experienced a dramatic increase, with a minimum LST of 14.31°C, a peak of 42.31°C, and a mean of 32.76°C, indicating extreme heat. The Tseday season also warmed, with a minimum of 18.3°C, maximum of 33.2°C, and a mean of 25.75°C. In this year, the Belg season was the coolest, while Bega recorded the highest temperatures.

In 2017, the Kiremt season had a minimum LST of 18.2°C, with a maximum of 32.8°C and a mean of 25.5°C, showing stability in temperature. The Belg season recorded a minimum of 17.8°C, maximum of 32.9°C, and mean of 25.35°C, maintaining warm conditions. The Bega season showed significant heat, with a minimum of 16.14°C, a maximum of 38.81°C, and a mean of 31.58°C. The Tseday season continued this trend, with a minimum LST of 19.9°C, a maximum of 34.6°C, and a mean of 27.25°C. Thus, Kiremt was the coolest season in 2017, while Bega remained the warmest.

Finally, in 2024, the Kiremt season recorded a minimum LST of 20.6°C, a maximum of 33.7°C, and a mean of 27.15°C, indicating a continued warming trend. The Belg season showed similar patterns, with minimum temperatures at 20°C, maximums reaching 34.6°C, and a mean of 27.3°C. The Bega season’s minimum LST rose to 17.45°C, with a maximum of 34.57°C and a mean of 29.21°C. The Tseday season registered the highest temperatures, with a minimum of 21°C, maximum of 38.4°C, and a mean of 29.7°C. Therefore, in 2024, the Bega season was the coolest, while Tseday was the warmest.

Overall, throughout these years, Kiremt consistently represented the coolest temperatures, whereas Tseday typically recorded the warmest conditions, highlighting a trend of increasing temperatures across all seasons in Dire Dawa City.

## 4.3 Driving Factors

### 4.3.1 Land use land Cover Dynamics

Image Classification: According to Dire Dawa Administrative Council and Office (2012), the land use/land covertypes have been grouped into four major classes. They are designated as urban built up, physiognomic vegetation types, shrub land, and bare land. Table 4-5 Show the designated land use land cover type with their descriptions.

*Table 4-5: Land-use/land-cover classes and description of the study area*

| No. | **LU/LC Classes** | **Descriptions LU/LC Classes** |
|---|---|---|
| 1 | Shrubs Land | • Areas characterized by shrubs, bushes, and small trees, offering minimal valuable timber, interspersed with grasses and less dense than forests. |
| 2 | Vegetation | • Lands featuring a diverse mix of forests, woody plants, trees, natural vegetation, gardens, parks, vegetated areas, agricultural fields, and crop lands. |
| 3 | Built up | • Areas occupied by residential and commercial buildings, along with infrastructure such as roads, transportation networks, industrial facilities, and mixed urban developments |

| | | |
|---|---|---|
| 4 | Bare Land | • Areas characterized by thin soil and rocky or sandy surfaces, including deserts, dry salt flats, beaches, sand dunes, exposed rock formations, strip mines, quarries, gravel pits, and non-vegetated landscapes dominated by rock outcrops, roads, and eroded or degraded lands. |

The supervised classification image of each year involves pixel categorizations by taking training area for each class of LU/LC. After the training area assigned for each classes, the classification activity was performed. For all the LU/LC classes bare land, Vegetation, shrub land and Built-Up taken 20 training site. Areas in digital images were marked as signature of individual identity and the field truth verification was adapted to represent LU/LC classes.

#### 4.3.1.1 Land use land cover change of 2002

Figure 4-5 Shows, in 2002, the land use and land cover across the four seasons exhibited robust vegetation cover, reflecting a healthy natural environment. Bega showcased a substantial vegetation area of 15,704.32 ha, accompanied by significant shrubland at 11,879.84 ha, while bare land measured 35,871.96 ha. Built-up areas were relatively low at 5,295.40 ha, indicating minimal urban development. In Belg, vegetation covered 11,171.72 ha, with shrubland at 10,583.20 ha, and bare land peaked at 42,922.52 ha. Built-up areas were only 4,395.24 ha. Tseday had 8,986.96 ha of vegetation and 14,734.52 ha of shrubland, with bare land at 41,338.92 ha and built-up areas at 4,033.52 ha. Kiremt boasted the highest vegetation cover at 21,201.32 ha, with shrubland at 18,180.56 ha and bare land lower at 24,014.32 ha, while built-up areas were at 5,496.40 ha.

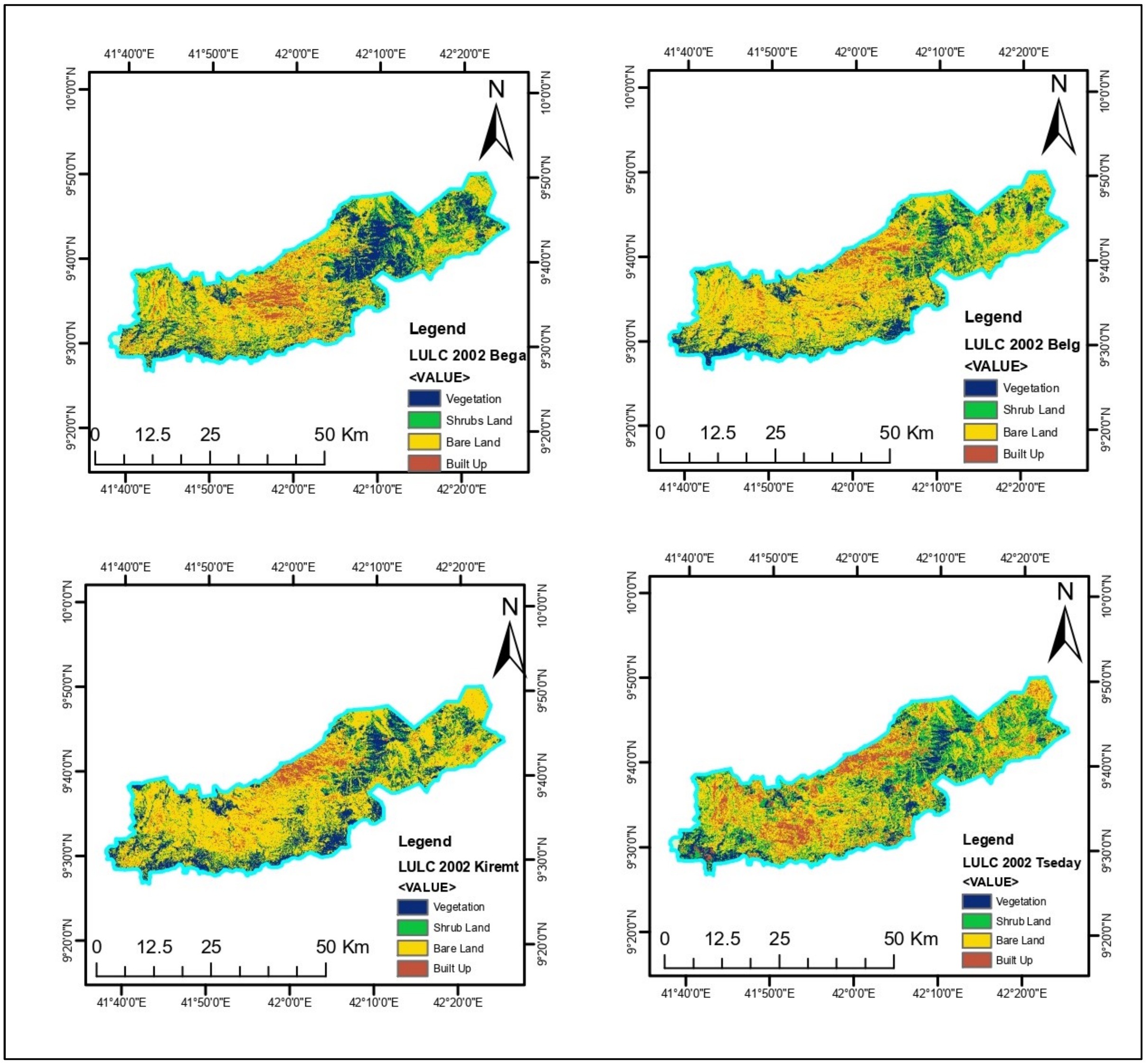


*Figure 4-5: Land use land cover change of 2002*

4.3.1.2 Land use land cover change of 2012

Figure 4-6 Shows by 2012, significant changes occurred, marked by a noticeable decline in vegetation across all seasons. In Bega, vegetation plummeted to 4,242.20 ha, a staggering reduction of approximately 73%. However, shrub land increased to 19,106.64 ha, suggesting a shift towards more resilient land cover. Bare land remained stable at 37,698.88 ha, while built-up areas surged to 8,046.96 ha, indicating substantial urban expansion. Belg saw vegetation drop sharply to 4,039.52 ha, reflecting a 64% decline, while shrubland rose to 20,775.24 ha. Bare land decreased to 33,887.60 ha, and built-up areas increased to 10,392.32 ha. In Tseday, vegetation decreased to 6,586.84 ha, while shrubland saw a slight increase. Bare land measured 39,662.76 ha, and built-up areas increased to 8,378.20 ha. Kiremt experienced a drastic drop in vegetation to 7,277.68 ha, with stable shrubland and increased bare land at 37,142.28 ha. Built-up areas rose to 9,281.76 ha, showcasing ongoing urban pressure.

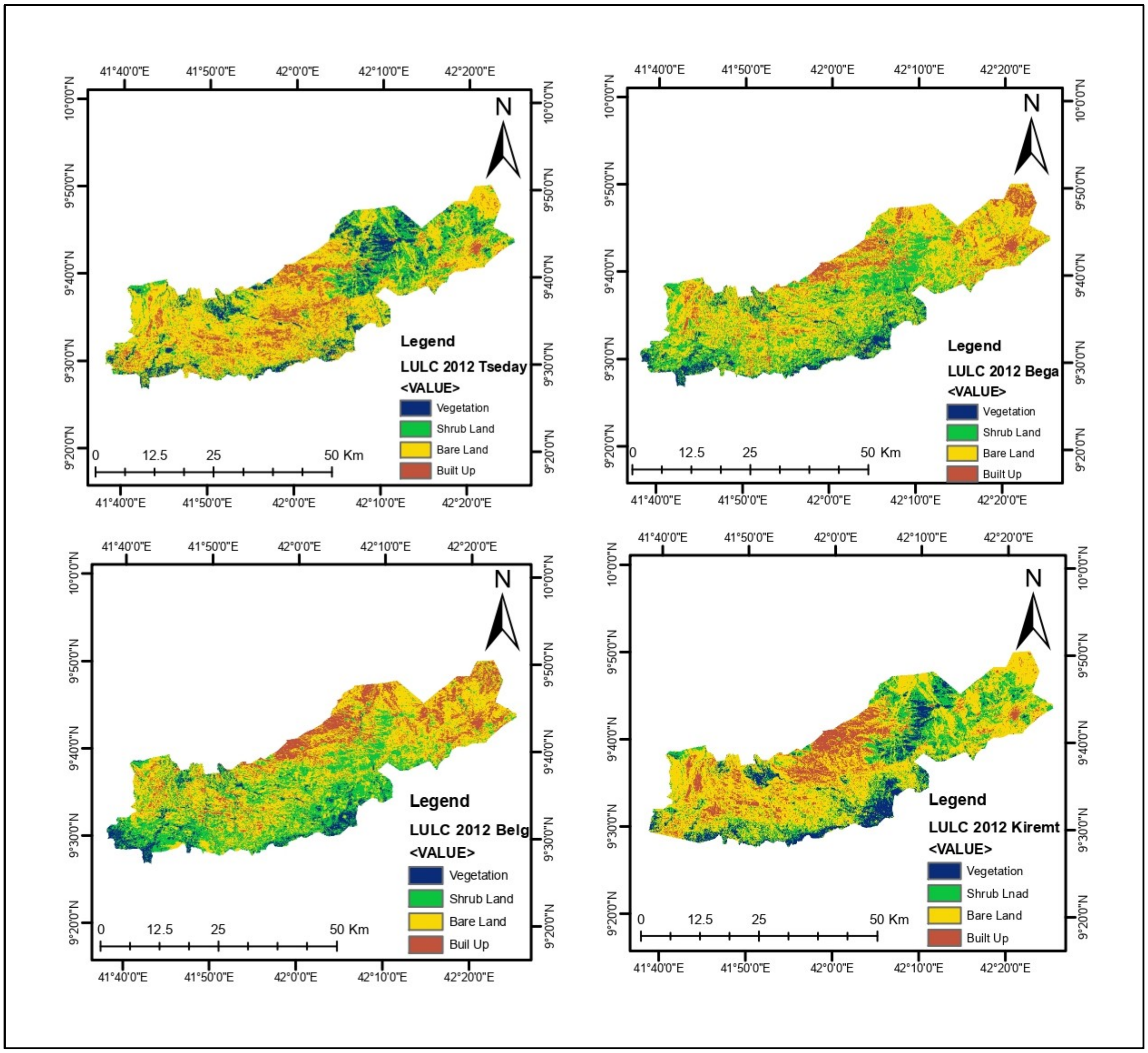


*Figure 4-6: Land use land cover change of 2012*

#### 4.3.1.3 Land use land cover change of 2017

Figure 4-7 Shows in 2017, some regions began to show signs of recovery, although challenges remained. Bega's vegetation saw a slight recovery to 6,750.80 ha, while shrubland increased to 15,265.40 ha, and bare land decreased to 33,268.20 ha. Built-up areas rose significantly to 13,657.60 ha. In Belg, vegetation rebounded slightly to 9,548.60 ha, with shrubland remaining robust at 14,064.48 ha. Bare land saw minor fluctuations, settling at 34,715 ha, and built-up areas grew to 10,709.68 ha. Tseday's vegetation increased to 8,076.12 ha, indicating recovery efforts. Shrubland rose to 17,707.48 ha, while bare land decreased to 27,749.64 ha, and built-up areas surged to 15,243.36 ha. Kiremt continued to experience a decline in vegetation to 3,571.16 ha, though shrubland remained stable at 19,691.20 ha. Bare land measured 26,978.08 ha, while built-up areas increased to 18,205.28 ha, reflecting ongoing urbanization.

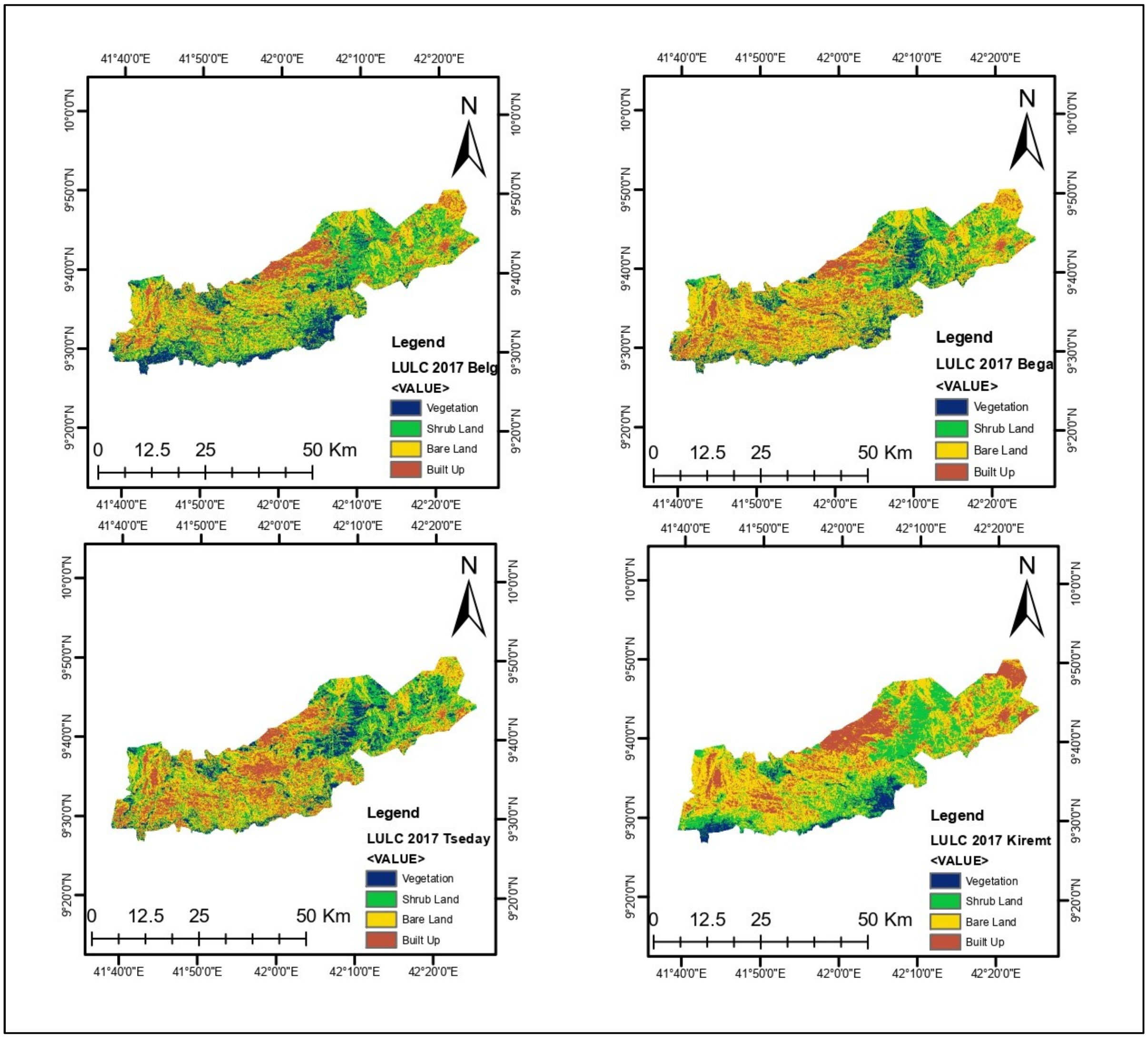


*Figure 4-7: Land use land cover change of 2017*

#### 4.3.1.4 Land use land cover change of 2024

Figure 4-8 Shows by 2024, trends varied, with some areas facing continued challenges while others showed stabilization. In Bega, vegetation declined again to 4,076.40 ha, while shrubland peaked at 18,748.20 ha, and bare land decreased to 26,644.20 ha. Built-up areas expanded to 19,625.88 ha, highlighting rapid urban growth. Belg's vegetation stabilized at 7,876.08 ha, and shrubland reached 14,744 ha. Bare land dropped to 30,015.48 ha, suggesting a potential shift towards more vegetative cover, while built-up areas continued to grow, reaching 16,459.12 ha. Tseday's vegetation saw a slight drop to 7,384.36 ha, with shrubland increasing. Bare land decreased to 26,235.04 ha, and built-up areas rose to 18,411.56 ha. In Kiremt, vegetation increased slightly to 5,986.00 ha, with stable shrubland. Bare land decreased to 24,098 ha, while built-up areas surged to 19,057 ha, underscoring the trend of urban expansion.

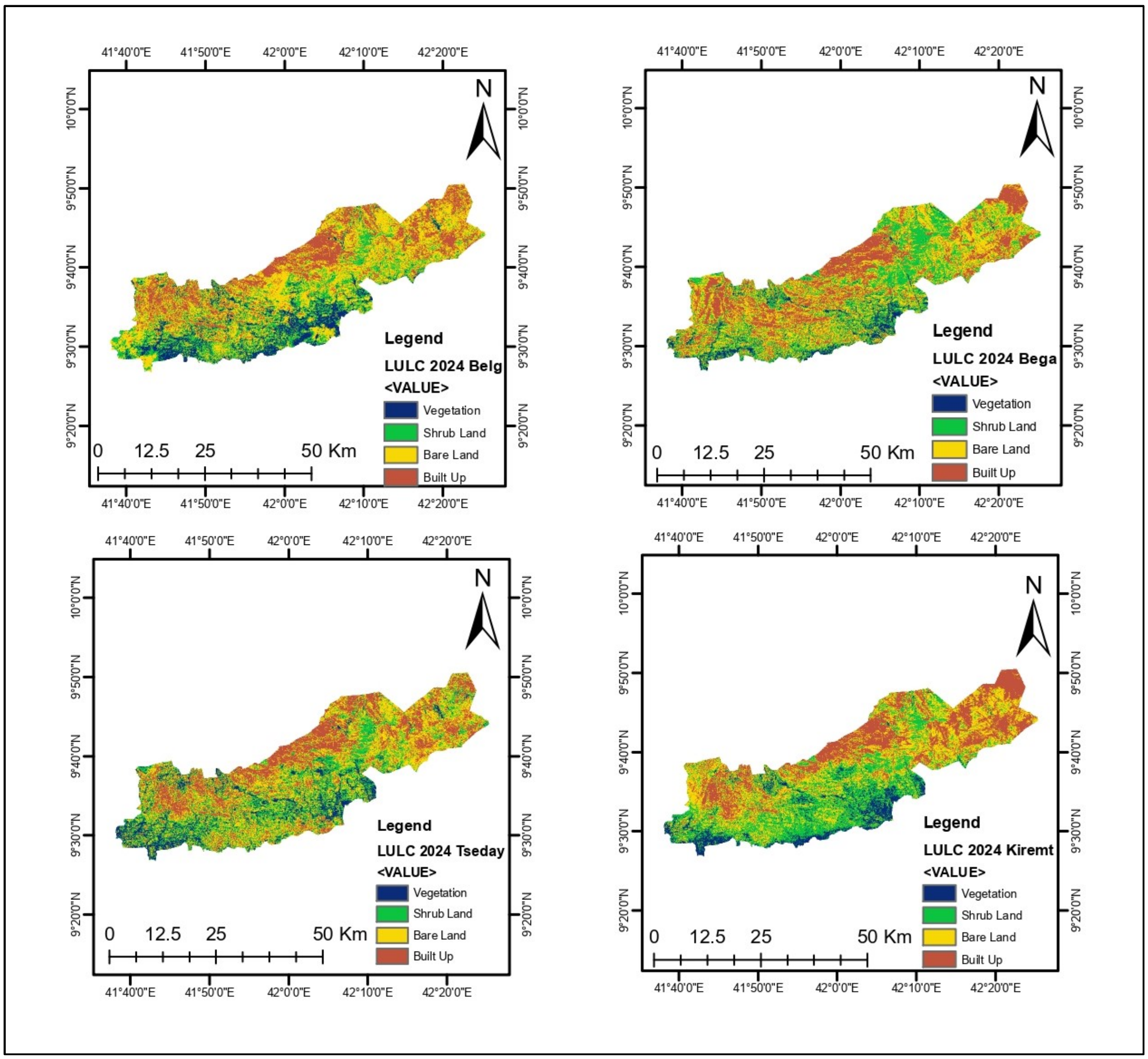


*Figure 4-8: Land use land cover change of 2024*

Overall, the data reveals a clear trend of decreasing vegetation cover and increasing built-up areas across all seasons, indicative of urbanization and land use change. Shrubland has generally increased, reflecting adaptive land management practices, while bare land has shown fluctuations but is trending downward.

### 4.3.2 Temporal Land Use and Land Cover change

#### 4.3.2.1 Spatio-Temporal Variation of Land Use land cover change in bega season

In the Bega season, land use and land cover have shown notable variations over the years. Vegetation decreased dramatically from 15,704.32 ha in 2002 to just 4,076.40 ha in 2024, reflecting significant urban expansion and land conversion pressures. Conversely, shrubland increased from 11,879.84 ha to 18,748.20 ha, indicating a shift towards more resilient landscapes. Bare land exhibited fluctuations, peaking at 35,871.96 ha in 2002 before declining to 26,644.20 ha in 2024, suggesting some recovery of vegetative cover. Built-up areas expanded considerably from 5,295.40 ha in 2002 to 19,625.88 ha in 2024, underscoring the region's rapid urbanization.

#### 4.3.2.2 Spatio-Temporal Variation of Land Use land cover change in belg season

In the Belg season, vegetation decreased from 11,171.72 ha in 2002 to 7,876.08 ha in 2024, reflecting ongoing pressures from urban development. Shrubland increased from 10,583.20 ha to 14,744 ha, indicating a potential shift in land management practices. Bare land fluctuated, peaking at 42,922.52 ha in 2002 before decreasing to 30,015.48 ha, while built-up areas grew significantly from 4,395.24 ha to 16,459.12 ha, highlighting urban sprawl.

#### 4.3.2.3 Spatio-Temporal Variation of Land Use land cover change in Tseday season

For the Tseday season, vegetation started at 8,986.96 ha in 2002 and decreased to 7,384.36 ha in 2024. Shrub land remained relatively stable, rising slightly over the years. Bare land also decreased from 41,338.92 ha to 26,235.04 ha, suggesting a reduction in barren areas. Built-up areas increased from 4,033.52 ha to 18,411.56 ha, indicating increasing urban development pressures

#### 4.3.2.4 Spatio-Temporal Variation of Land Use land cover change in Tseday season

In the Kiremt season, vegetation peaked at 21,201.32 ha in 2002 but fell sharply to 5,986 ha by 2024, demonstrating significant land use changes. Shrub land remained stable, while bare land fluctuated before settling at 24,098 ha. Built-up areas rose significantly from 5,496.40 ha to 19,057 ha, reflecting a trend of urban expansion across the landscape. Overall, the data illustrates a complex interplay between natural land cover types and urban development pressures across all seasons.

Table 4-6 Shows the land use land cover change every class over the study year and seasons.

*Table 4-6: Land Use Land Cover Change of 2002,2012,2017,2024 Over four seasons*

| Season | Year | Vegetation (ha) | Shrubland (ha) | Bare Land (ha) | Built Up (ha) | Total Area (ha) | Vegetation (%) | Shrubland (%) | Bare Land (%) | Built Up (%) |
|---|---|---|---|---|---|---|---|---|---|---|
| Bega | 2002 | 15704.32 | 11879.84 | 35871.96 | 5295.40 | 68751.12 | 22.83 | 17.27 | 52.17 | 7.71 |
| Bega | 2012 | 4242.20 | 19106.64 | 37698.88 | 8046.96 | 39094.68 | 10.84 | 48.91 | 96.51 | 20.62 |
| Bega | 2017 | 6750.80 | 15265.40 | 33268.20 | 13657.60 | 44232.00 | 15.34 | 34.68 | 75.62 | 30.88 |
| Bega | 2024 | 4076.40 | 18748.20 | 26644.20 | 19625.88 | 61194.68 | 6.58 | 30.21 | 43.02 | 31.67 |
| | | | | | | | | | | |
| Belg | 2002 | 11171.72 | 10583.20 | 42922.52 | 4395.24 | 68472.68 | 16.33 | 15.48 | 62.73 | 6.43 |
| Belg | 2012 | 4039.52 | 20775.24 | 33887.60 | 10392.32 | 69394.68 | 5.81 | 29.92 | 48.90 | 14.97 |
| Belg | 2017 | 9548.60 | 14064.48 | 34715.00 | 10709.68 | 68937.76 | 13.85 | 20.39 | 50.37 | 15.47 |
| Belg | 2024 | 7876.08 | 14744.00 | 30015.48 | 16459.12 | 68894.68 | 11.43 | 21.37 | 43.61 | 23.87 |
| | | | | | | | | | | |
| Tseday | 2002 | 8986.96 | 14734.52 | 41338.92 | 4033.52 | 73193.92 | 12.29 | 20.13 | 56.46 | 5.50 |
| Tseday | 2012 | 6586.84 | 14453.76 | 39662.76 | 8378.20 | 70081.56 | 9.39 | 20.60 | 56.63 | 11.98 |
| Tseday | 2017 | 8076.12 | 17707.48 | 27749.64 | 15243.36 | 68876.60 | 11.74 | 25.69 | 40.33 | 22.14 |
| Tseday | 2024 | 7384.36 | 17055.64 | 26235.04 | 18411.56 | 68886.60 | 10.71 | 24.78 | 38.05 | 26.83 |
| | | | | | | | | | | |
| Kiremt | 2002 | 21201.32 | 18180.56 | 24014.32 | 5496.40 | 68192.60 | 31.09 | 26.69 | 35.23 | 8.08 |
| Kiremt | 2012 | 7277.68 | 14633.16 | 37142.28 | 9281.76 | 68834.88 | 10.59 | 21.26 | 54.05 | 13.48 |
| Kiremt | 2017 | 3571.16 | 19691.20 | 26978.08 | 18205.28 | 68845.72 | 5.19 | 28.60 | 39.19 | 26.43 |
| Kiremt | 2024 | 5986.00 | 19953.00 | 24098.00 | 19057.00 | 68894.00 | 8.69 | 28.96 | 34.99 | 27.59 |

### 4.3.3 Spatial distribution of NDVI

#### 4.3.3.1 Spatial distribution of NDVI Kiremt Season

Table 4-7 and Figure 4-9 provide a statistical overview of the Normalized Difference Vegetation Index (NDVI) for Kiremt season across four selected years: 2002, 2012, 2017, and 2024. NDVI values, which range from -1 to 1, are essential for assessing vegetation coverage in the area.

The minimum NDVI values indicate varying levels of vegetation stress over the years. In

2002, the minimum NDVI recorded was -0.002, which slightly worsened to -0.007 in 2012. There was a further decline to -0.008 in 2017, and this deteriorated further to -0.022 in 2024. These fluctuations highlight the changing stress levels experienced by vegetation throughout this period.

Maximum NDVI values show significant variation, with 2024 reaching a peak of 0.4632, suggesting healthier vegetation compared to earlier years. The maximum NDVI values for the preceding years were 0.3648 in 2002, 0.382 in 2012, and 0.305 in 2017. This progression indicates a notable improvement in vegetation cover by 2024.

Mean NDVI values reflect average vegetation health, with 2002 showing a mean of 0.1834, which slightly increased to 0.1875 in 2012. However, the mean dropped to 0.1485 in 2017 before rising again to 0.2206 in 2024. This pattern illustrates fluctuations in overall vegetation, with a notable recovery in the most recent year. Standard deviation values provide insight into the spatial variability of NDVI across the years. The highest standard deviation was observed in 2024 at 0.241, indicating greater variability in vegetation cover, while 2017 had a lower variability at 0.157. This suggests that 2024 experienced a more diverse range of vegetation types and conditions compared to earlier years.

*Table 4-7: Normalized difference vegetation index results from 2002 – 2024 Kiremt*

| Year | 2002 | 2012 | 2017 | 2024 |
|---|---|---|---|---|
| Min | -0.002 | -0.007 | -0.008 | -0.022 |
| Max | 0.3648 | 0.382 | 0.305 | 0.4632 |
| Mean | 0.1834 | 0.1875 | 0.1485 | 0.2206 |
| St_Div | 0.1839 | 0.1947 | 0.157 | 0.241 |

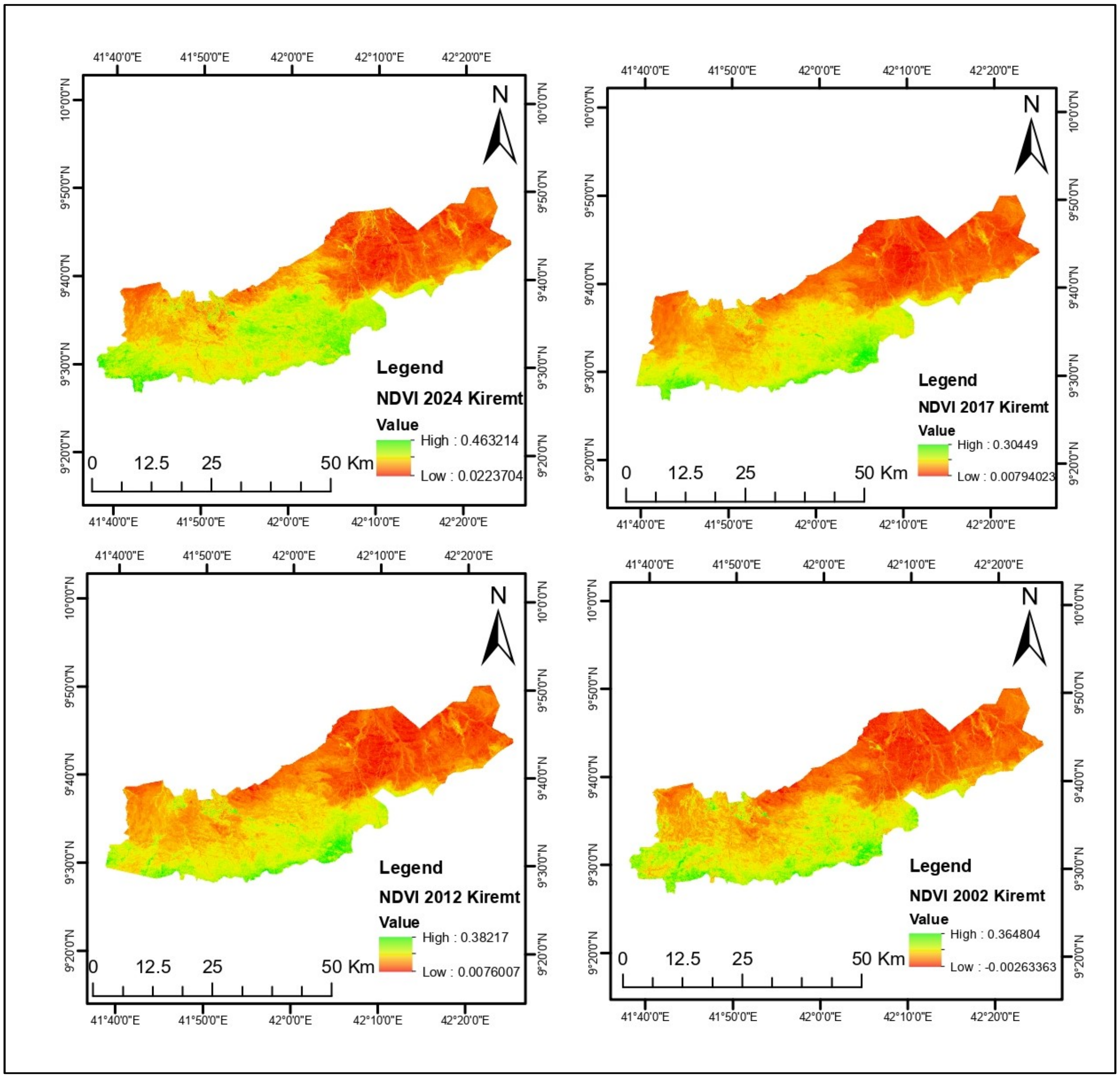


*Figure 4-9: NDVI Map of Dire Dawa City from 2002 – 2024 Kiremt*

4.3.3.2 Spatial distribution of NDVI Belg Season

Table 4-8 and Figure 4-10 provide a statistical analysis of the Normalized Difference Vegetation Index (NDVI) during the Belg season across four distinct years: 2002, 2012, 2017, and 2024. NDVI values, which are essential for assessing the health and density of vegetation, range from -1 to 1.

In 2002, the minimum NDVI was recorded at -0.364, indicating considerable vegetation stress. This situation improved over the following years, with minimum values rising to -0.069 in 2012, -0.043 in 2017, and -0.036 in 2024, suggesting a gradual recovery in vegetation health.

Maximum NDVI values also show significant changes in vegetation quality. The peak value was 0.411 in 2002, which increased to 0.571 in 2012, reflecting healthier vegetation conditions. However, this value declined to 0.473 in 2017, before slightly improving to 0.552 in 2024. These variations indicate fluctuations in vegetation health throughout the years.

The mean NDVI values provide an average measure of vegetation health, starting at a low of 0.0235 in 2002. This value rose significantly to 0.251 in 2012, indicating better vegetation conditions. In 2017, the mean decreased slightly to 0.215, but then improved again to 0.258 in 2024, reflecting an overall positive trend in vegetation health during the Belg season. Standard deviation values highlight the variability of NDVI across the years. In 2002, the standard deviation was quite high at 0.548, suggesting considerable fluctuations in vegetation conditions. This decreased to 0.452 in 2012 and further to 0.365 in 2017, while rising slightly to 0.414 in 2024. This indicates that while there was some variability in vegetation cover, it generally became more consistent over time.

*Table 4-8: Normalized difference vegetation index results from 2002 – 2024 Belg*

| Year | 2002 | 2012 | 2017 | 2024 |
|---|---|---|---|---|
| Min | -0.364 | -0.069 | -0.043 | -0.036 |
| Max | 0.411 | 0.571 | 0.473 | 0.552 |
| Mean | 0.0235 | 0.251 | 0.215 | 0.258 |
| St_Div | 0.548 | 0.452 | 0.365 | 0.414 |

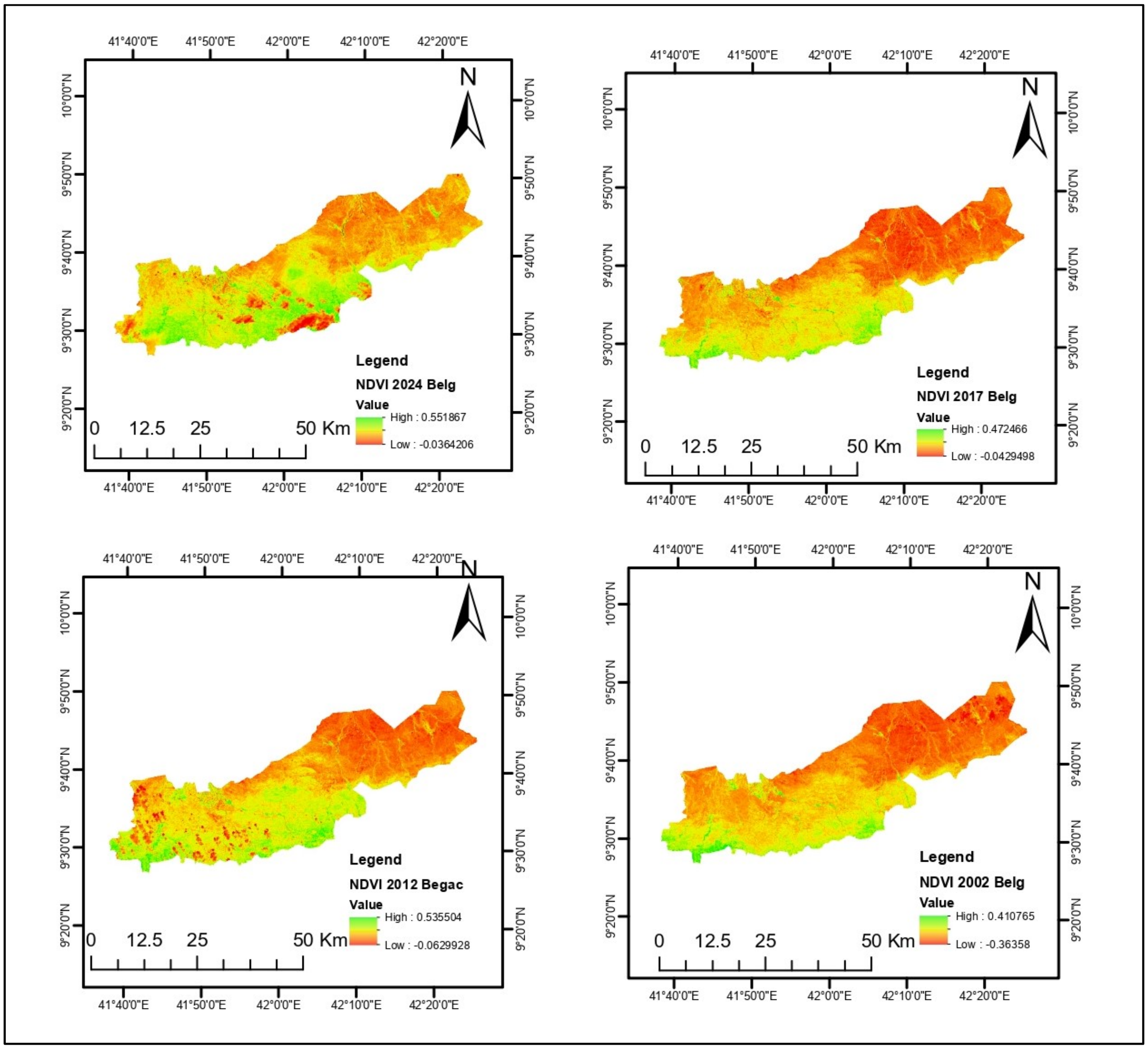


*Figure 4-10: NDVI Map of Dire Dawa City from 2002 – 2024 Belg*

#### 4.3.3.3 Spatial distribution of NDVI Bega Season

Table 4-9 and Figure 4-11 present the NDVI statistics for the Bega season across the years 2002, 2012, 2017, and 2024, highlighting variations in vegetation health and coverage. NDVI values, which measure vegetation greenness on a scale from -1 to 1, exhibited notable differences over the years.

The minimum NDVI values recorded were -0.022 in 2002, -0.063 in 2012, -0.024 in 2017, and -0.021 in 2024, indicating relatively stable but low levels of vegetation health throughout this period. Although these values remained low, the slight fluctuations suggest some variability in the least vegetative conditions.

Maximum NDVI values showed a more positive trend, starting at 0.387 in 2002 and increasing to 0.536 in 2012. This value slightly declined to 0.419 in 2017 but recovered to 0.495 in 2024, demonstrating overall stability and improvements in the healthier vegetation observed over the years.

Mean NDVI values reflect contrasting vegetation conditions, with a modest value of 0.1825 in 2002, rising to 0.2365 in 2012. In 2017, the mean value decreased to 0.1975, but it experienced a notable increase to 0.237 in 2024, suggesting a recovery in average vegetation health by the end of the analyzed period. The standard deviation values, which indicate the spatial variability of NDVI, were lowest in 2002 at 0.289 and peaked in 2012 at 0.423, showing greater variability in vegetation distribution. The values then decreased to 0.316 in 2017 and rose again to 0.365 in 2024, suggesting a fluctuating but gradually stabilizing vegetation cover across the years.

*Table 4-9: Normalized difference vegetation index results from 2002 – 2024 Bega*

| Year | 2002 | 2012 | 2017 | 2024 |
|---|---|---|---|---|
| Min | -0.022 | -0.063 | -0.024 | -0.021 |
| Max | 0.387 | 0.536 | 0.419 | 0.495 |
| Mean | 0.1825 | 0.2365 | 0.1975 | 0.237 |
| St_Div | 0.289 | 0.423 | 0.316 | 0.365 |

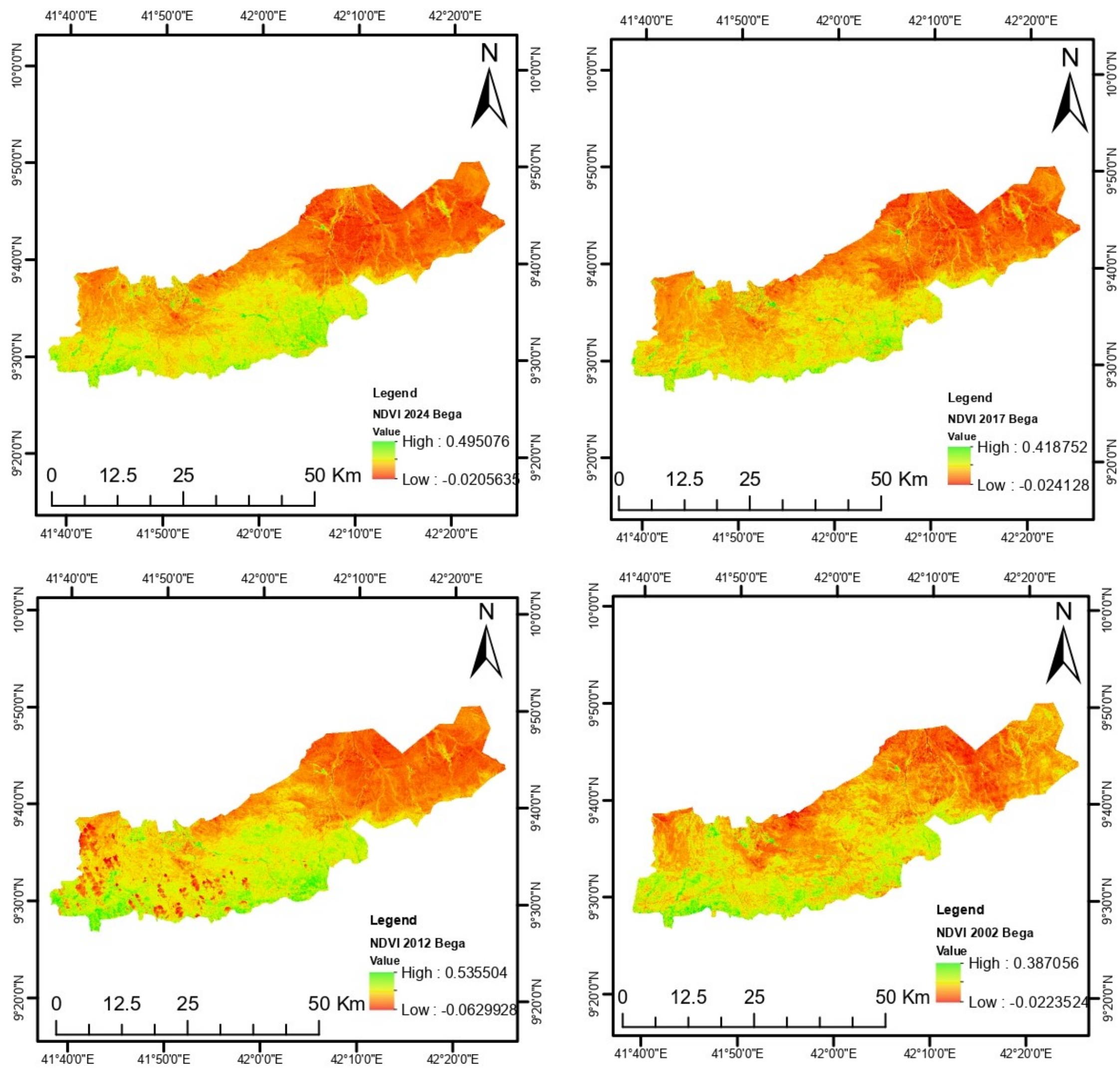


*Figure 4-11: NDVI Map of Dire Dawa City from 2002 – 2024 Bega*

#### 4.3.3.4 Spatial distribution of NDVI Tseday Season

Table 4-10 and Figure 4-12 display the NDVI statistics for the Tseday season across the years 2002, 2012, 2017, and 2024, highlights variations in vegetation health and coverage.

The minimum NDVI values recorded were - 0.069in 2002, -0.014 in 2012, -0.020 in 2017, and -0.036 in 2024. These figures indicate a significant improvement in the least vegetative conditions over time, particularly a marked recovery from the very low value in 2002.

Maximum NDVI values demonstrated a positive trend, starting at 0.571in 2002 and decreasing to 0.502 in 2012. This value saw slight variations, with 0.426 in 2017 and rising to 0.600 in 2024. This increase reflects healthier vegetation over the years and suggests an overall improvement in vegetation coverage.

The mean NDVI values illustrate contrasting conditions throughout the period, beginning with a mean of 0.251in 2002. This value rose significantly to 0.244 in 2012, reflecting better vegetation health. In 2017, the mean decreased slightly to 0.203, but it improved again in 2024 to 0.282, indicating a recovery in average vegetation health over the years. Standard deviation values indicate the spatial variability of NDVI. In 2002, the standard deviation was quite high at 0.571, suggesting considerable variability in vegetation distribution. This value decreased to 0.365 in 2012 and further dropped to 0.3147 in 2017, before rising again to 0.4497 in 2024, indicating fluctuations in vegetation cover consistency across the years.

*Table 4-10: Normalized difference vegetation index results from 2002 – 2024 Tseday*

| Year | 2002 | 2012 | 2017 | 2024 |
|---|---|---|---|---|
| Min | - 0.069 | -0.014 | -0.020 | -0.036 |
| Max | 0.571 | 0.502 | 0.426 | 0.600 |
| Mean | 0.251 | 0.244 | 0.203 | 0.282 |
| St. Div | 0.320 | 0.365 | 0.3147 | 0.4497 |

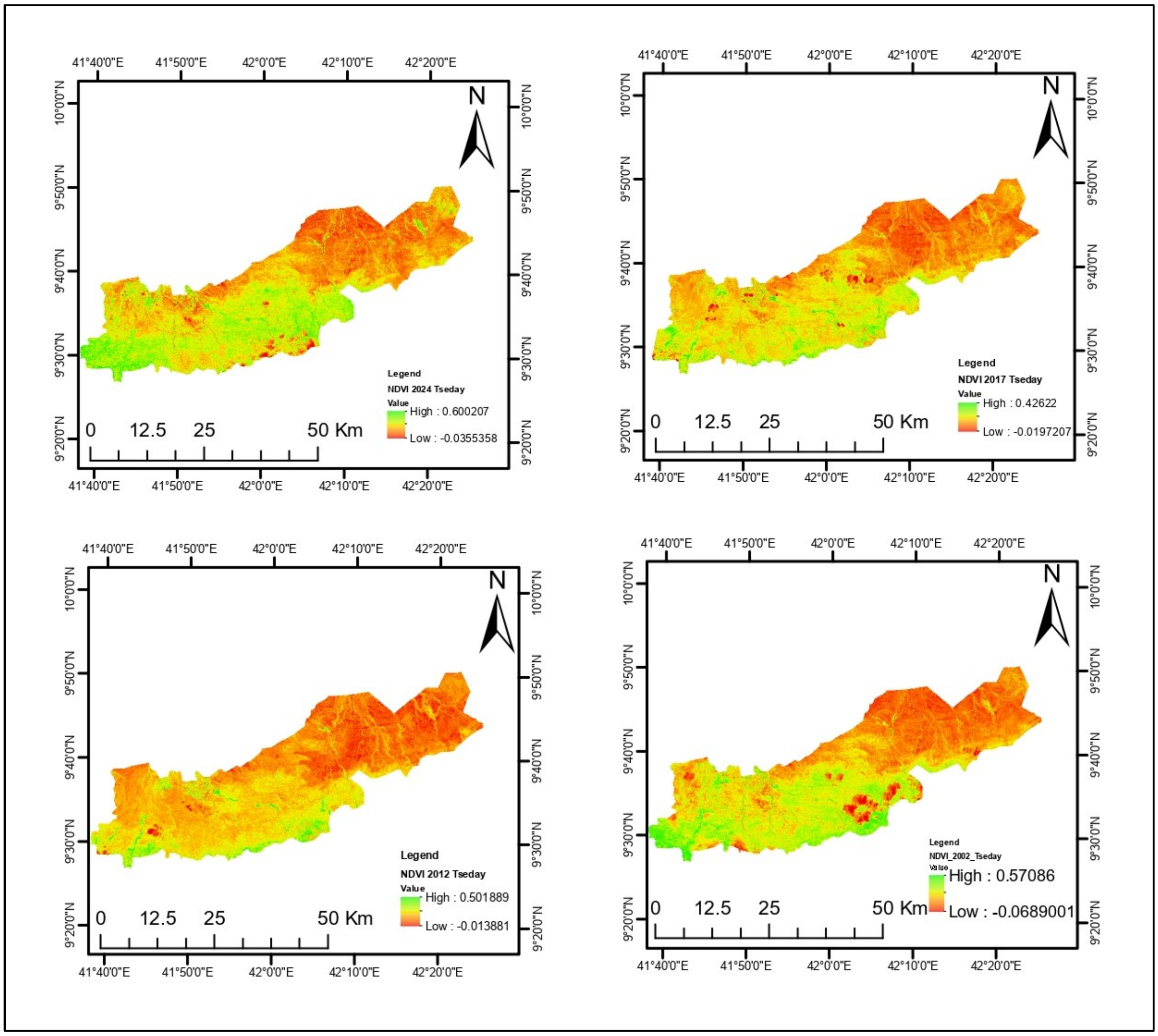


*Figure 4-12: NDVI Map of Dire Dawa City from 2002 – 2024 Tseday*

### 4.3.4 Spatial distribution of NDBI

#### 4.3.4.1 Spatial distribution of NDBI Kiremt Season

Table 4-11 and Figure 4-13 provide an analysis of the NDBI values for the Kiremt season across the years 2002, 2012, 2017, and 2024, offering insights into changes in built-up areas. The NDBI, an indicator used to assess urbanization, spans values from -1 to 1, where positive values suggest greater built-up density.

The minimum NDBI values have demonstrated significant variability over the years, starting from -0.231 in 2002 and fluctuating slightly to -0.238 in 2012 and -0.162 in 2017, before decreasing further to -0.292 in 2024. This pattern indicates some instability in the least built-up areas over the analyzed period.

Maximum NDBI values indicate a consistent presence of built-up areas, peaking at 0.434 in 2002. This value decreased in subsequent years, reaching 0.244 in 2012 and 0.247 in 2017, before experiencing a notable recovery to 0.660 in 2024. This suggests an overall increase in built-up density in the later years.

Mean NDBI values reflect predominantly low averages, indicating a general scarcity of built-up areas throughout the years. The least negative mean was observed in 2002 at 0.1015, while 2012 saw a drop to nearly neutral at 0.003. The mean improved slightly to 0.0425 in 2017 and rose to 0.184 in 2024, showing a trend toward increased built-up density over time.

Standard deviation values, which indicate the variability of NDBI, were highest in 2024 at 0.672, suggesting greater fluctuations in built-up area distribution compared to previous years. In contrast, the standard deviation was lower in 2012 at 0.341 and decreased further to 0.289 in 2017, indicating a more stable spatial distribution of built-up areas in those years.

*Table 4-11: Normalized difference Built Up index results from 2002 – 2024 Kiremt*

| Year | 2002 | 2012 | 2017 | 2024 |
|---|---|---|---|---|
| Min | -0.231 | -0.238 | -0.162 | -0.292 |
| Max | 0.434 | 0.244 | 0.247 | 0.660 |
| Mean | 0.1015 | 0.003 | 0.0425 | 0.184 |
| St_Div | 0.4705 | 0.341 | 0.289 | 0.672 |

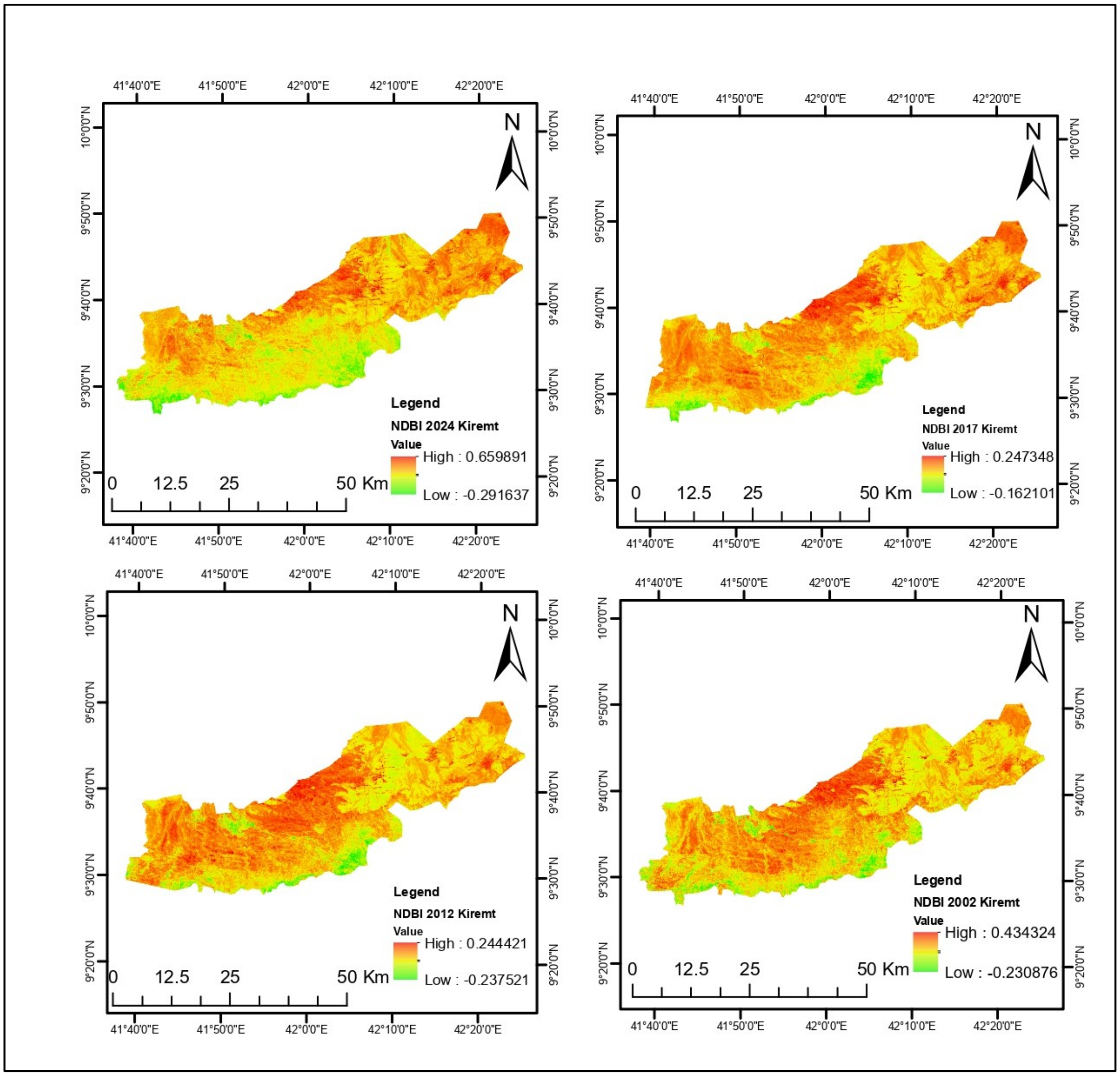


*Figure 4-13: NDBI Map of Dire Dawa City from 2002 – 2024 Kiremt*

4.3.4.2 Spatial distribution of Normalized differential built up index Belg Season

Table 4-12 and Figure 4-14 present the NDBI values for the Belg season across the years 2002, 2012, 2017, and 2024, providing insights into urban expansion and dynamics of built-up areas.

The minimum NDBI values showed a decline from -0.289 in 2002 to -0.370 in 2012, indicating increasing sparsity of built-up areas. This trend improved slightly in 2017 to -0.283, but then deteriorated again to -0.413 in 2024, suggesting fluctuations in the least developed areas over time.

Maximum NDBI values reflected the peak extent of built-up areas, reaching 0.229 in 2002, increasing to 0.293 in 2012, and slightly rising to 0.236 in 2017. By 2024, this value improved further to 0.350, indicating notable urban development in the most recent year compared to earlier periods.

Mean NDBI values varied throughout the years, starting with a near-neutral average of -0.030 in 2002. This average dropped to -0.0385 in 2012, remaining low in subsequent years with -0.0235 in 2017 and -0.0315 in 2024. These figures indicate a persistent scarcity of built-up areas across the analyzed years. Standard deviation values, which indicate the variability of NDBI, remained relatively consistent, with the lowest variability observed in 2024 at 0.539. This suggests a more homogeneous distribution of built-up areas in that year, while values were slightly higher in previous years, indicating greater variability in built-up area distribution.

*Table 4-12: Normalized difference Built Up index results from 2002 – 2024 Belg*

| Year | 2002 | 2012 | 2017 | 2024 |
|---|---|---|---|---|
| Min | -0.289 | -0.370 | -0.283 | -0.413 |
| Max | 0.229 | 0.293 | 0.236 | 0.350 |
| Mean | −0.030 | −0.0385 | −0.0235 | −0.0315 |
| St_Div | 0.366 | 0.469 | 0.368 | 0.539 |

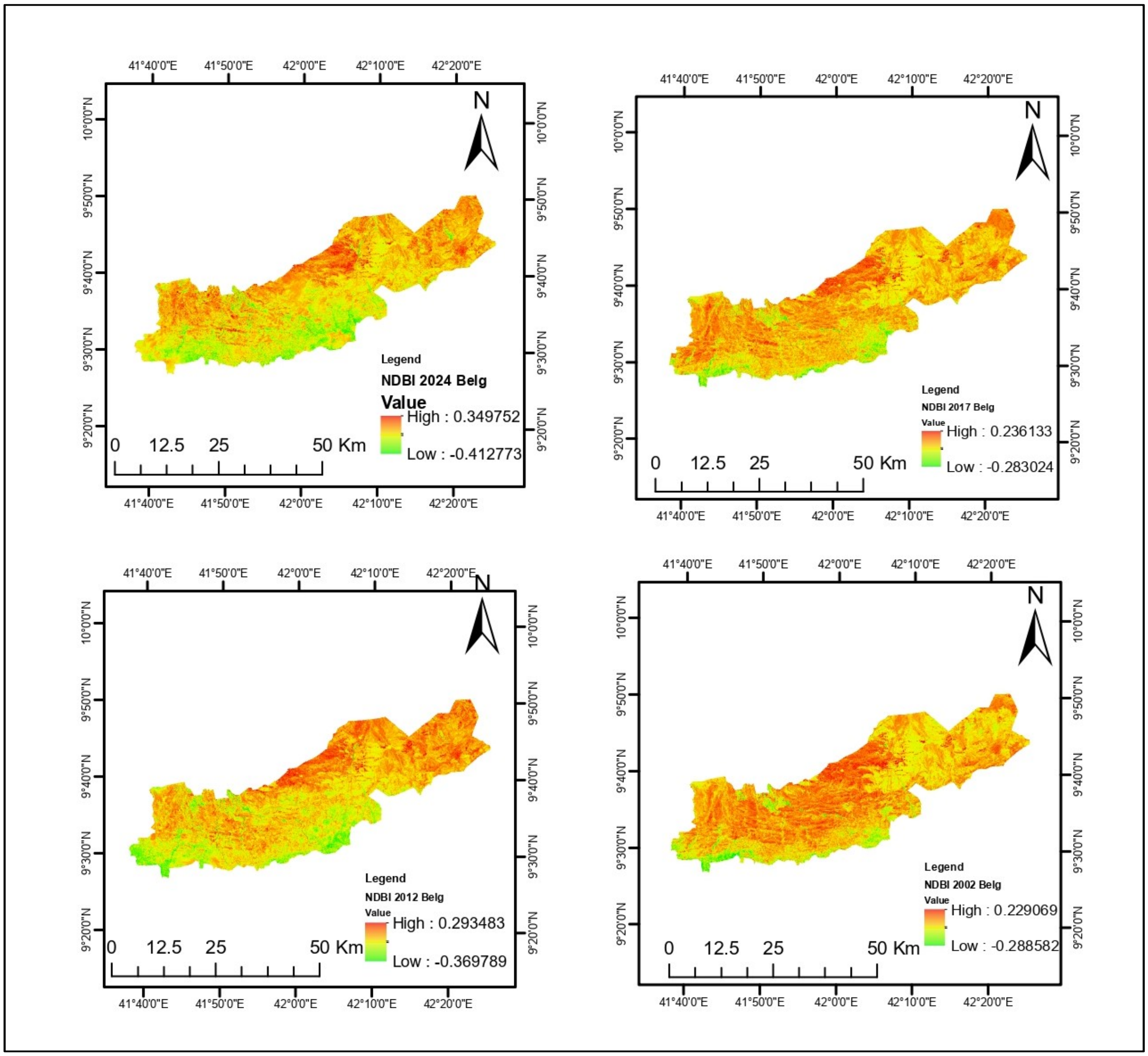


*Figure 4-14: NDBI Map of Dire Dawa City from 2002 – 2024 Belg*

#### 4.3.4.3 Spatial distribution of Normalized differential built up index Bega Season

Table 4-13 and Figure 4-15 analyze the NDBI values for the Bega season across the years 2002, 2012, 2017, and 2024, providing insights into urbanization dynamics over time. The NDBI is essential for assessing the extent of built-up areas, with values ranging from -1 to 1, where higher positive values signify increased urban density.

The minimum NDBI values show an improvement in the least developed areas, starting at -0.273 in 2002 and improving to -0.343 in 2024. The lowest recorded value occurred in 2012 at -0.368, indicating a temporary setback in built-up area development during that year.

Maximum NDBI values reflect the extent of built-up presence, with a peak of 0.474 in 2002, followed by a decrease to 0.392 in 2012. This downward trend continued, reaching 0.228 in 2017 and further declining to 0.294 by 2024, suggesting a reduction in urban expansion over these years.

Mean NDBI values exhibit varying trends, peaking at 0.1005 in 2002, then dropping to 0.012 in 2012. The mean further declined to -0.0125 in 2017 and continued to decrease to -0.0245 in 2024. These changes indicate fluctuations in average urban density across the years. Standard deviation values, which reflect the variability of NDBI, were highest in 2012 at 0.537, suggesting considerable variation in built-up area distribution during that time. By 2024, the standard deviation decreased to 0.450, indicating a more uniform distribution of built-up areas.

*Table 4-13: Normalized difference Built Up index results from 2002 – 2024 Bega*

| Year | 2002 | 2012 | 2017 | 2024 |
|---|---|---|---|---|
| Min | -0.273 | -0.368 | -0.253 | -0.343 |
| Max | 0.474 | 0.392 | 0.228 | 0.294 |
| Mean | 0.1005 | 0.012 | −0.0125 | −0.0245 |
| St_Div | 0.528 | 0.537 | 0.338 | 0.450 |

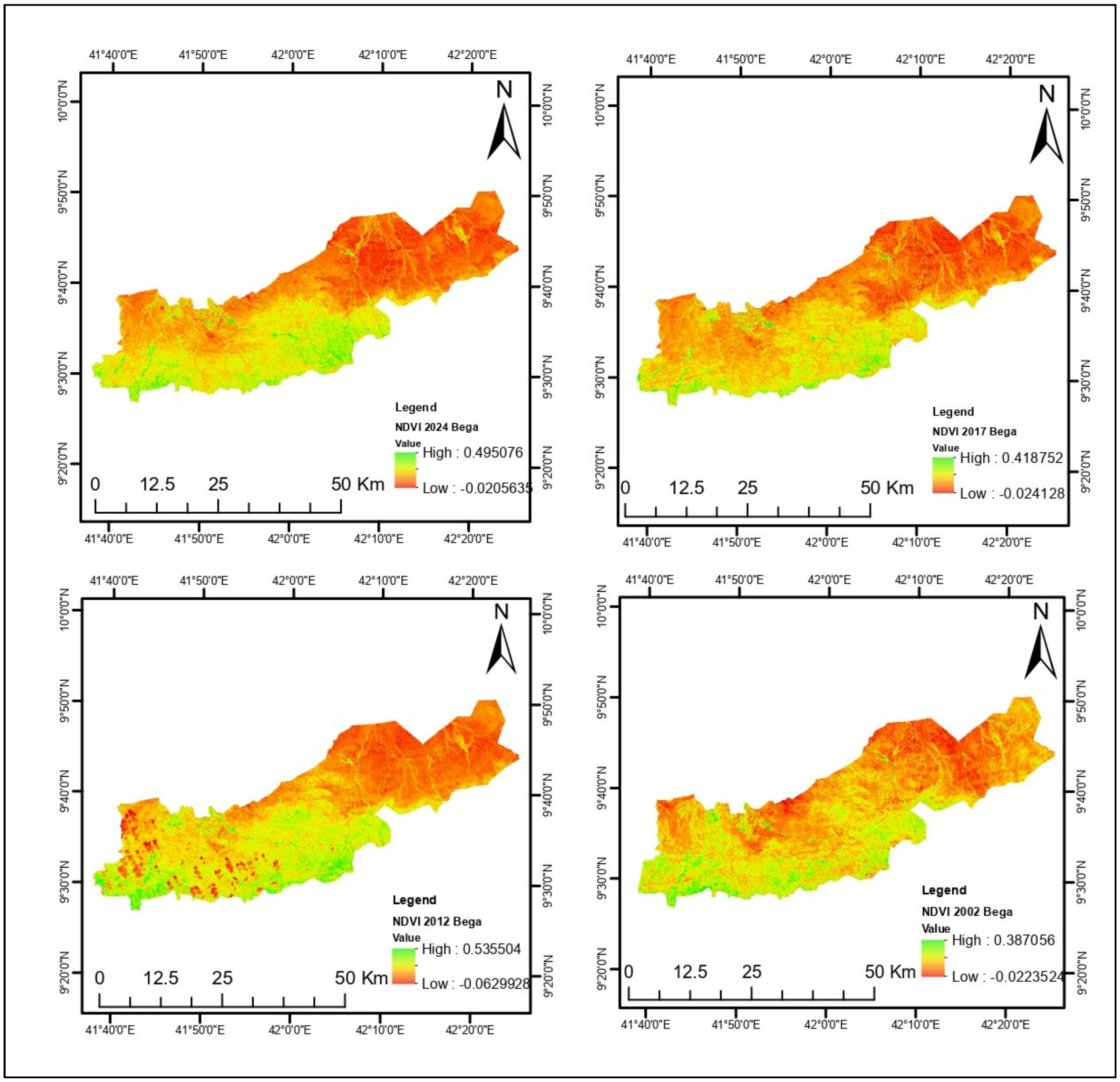


*Figure 4-15: NDBI Map of Dire Dawa City from 2002 – 2024 Bega*

#### 4.3.4.4 Spatial distribution of Normalized differential built up index Tseday Season

Table 4-14 and Figure 4-16 analyze the NDBI values for the Tseday season across the years 2002, 2012, 2017, and 2024, providing insights into urbanization dynamics over time. The NDBI is essential for assessing the extent of built-up areas, with values ranging from -1 to 1, where higher positive values indicate increased urban density.

The minimum NDBI values reflect an improvement in the least developed areas, beginning at -0.283 in 2002 and decreasing to -0.350 in 2024. The lowest recorded value occurred in 2012 at -0.298, highlighting a temporary reduction in built-up area development during that year.

Maximum NDBI values indicate the extent of built-up presence, peaking at 0.236 in 2002. This value declined significantly to 0.255 in 2012 and further decreased to 0.246 in 2017. By 2024, the maximum NDBI value showed a slight recovery to 0.369, suggesting some improvement in urban expansion in the latest year.

Mean NDBI values displayed varied trends, starting at a neutral average of 0.0234in 2002, followed by a decline into negative territory in 2012 (-0.298). The mean remained close to zero in 2017 at 0.001 and improved slightly to 0.0095 by 2024, indicating overall fluctuations in average urban density throughout the period.

Standard deviation values, which indicate the variability of NDBI, were highest in 2002 at 0.260, suggesting significant variation in built-up area distribution. In 2012, this value decreased to 0.390, and then further declined to 0.346 in 2017, before rising again to 0.5085 in 2024, indicating a more uniform distribution of built-up areas in the most recent year compared to earlier periods.

*Table 4-14: Normalized difference Built Up index results from 2002 – 2024 Tseday*

| Year | 2002 | 2012 | 2017 | 2024 |
|---|---|---|---|---|
| Min | -0.283 | -0.298 | -0.244 | -0.350 |
| Max | 0.236 | 0.255 | 0.246 | 0.369 |
| Mean | 0.0234 | -0.298 | 0.001 | 0.0095 |
| St_Div | 0.260 | 0.39 | 0.346 | 0.5085 |

.

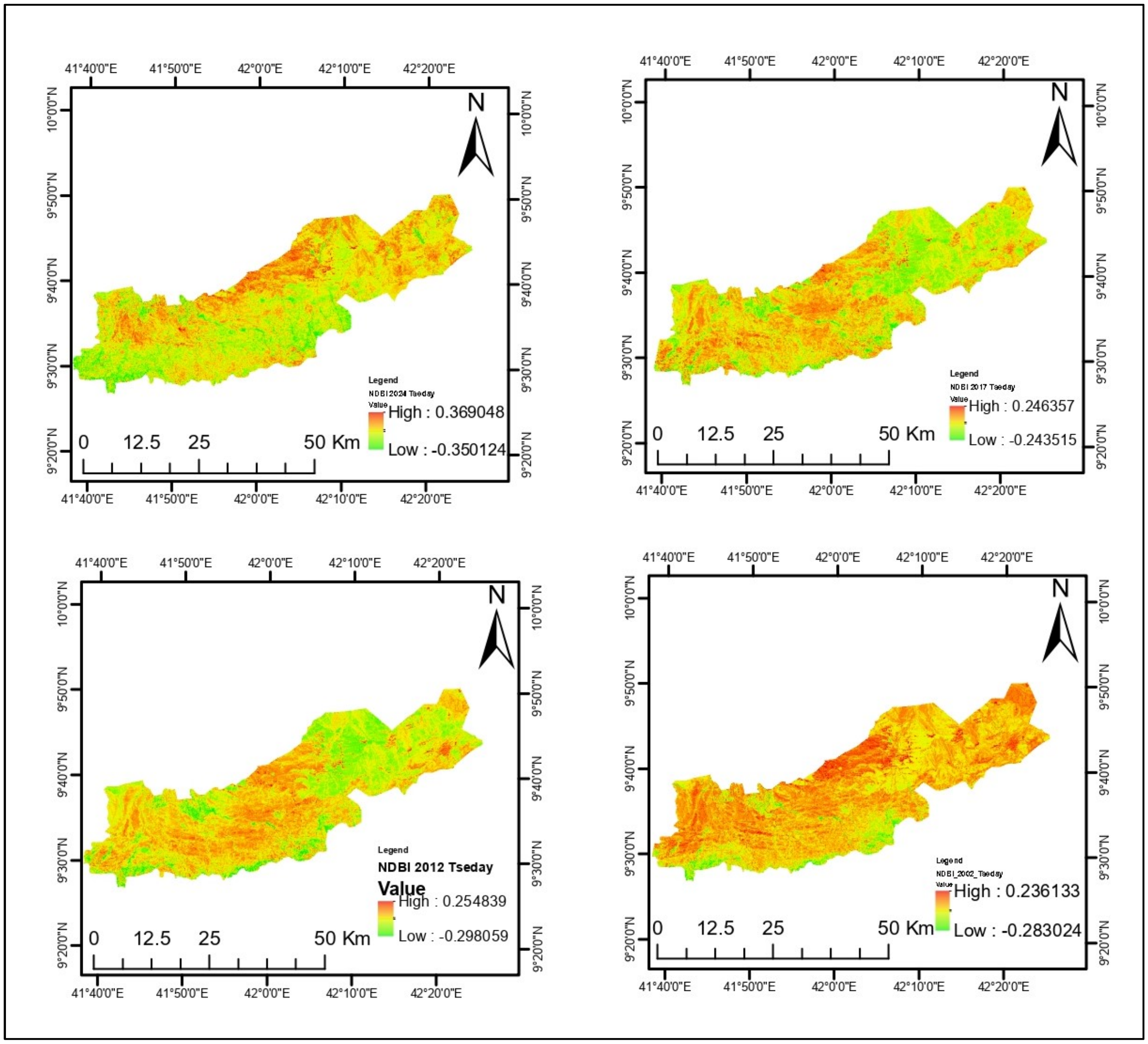


*Figure 4-16: NDBI Map of Dire Dawa City from 2002 – 2024 Bega*

## 4.4 Comparative Analysis

### 4.4.1 Impact of land use land cover on land surface temperature in each season for 2002

In 2002, the relationship between land use and land cover (LU/LC) types—specifically vegetation, shrub land, bare land, and built-up areas—played a crucial role in influencing land surface temperatures (LST) during the various seasons of Dire Dawa City.

Kiremt Season

During the Kiremt season, which recorded a minimum LST of 15.2°C and a maximum of 32°C (mean: 23.6°C), vegetation cover contributed significantly to maintaining moderate temperatures. Areas dominated by vegetation typically exhibited lower surface temperatures due to the cooling effects of evapotranspiration. In contrast, shrub lands, while slightly warmer than fully vegetated areas, still provided some cooling benefits. The presence of bare land, characterized by its exposed surfaces, likely contributed to higher temperature extremes within this season. Built-up areas, with their impervious surfaces, would also have elevated the LST, particularly near urban centers, thereby contrasting with the cooler temperatures found in more vegetated regions.

Belg Season

In the Belg season, which experienced a slight warming with minimum temperatures rising to 18.2°C and maximums reaching 33.2°C (mean: 25.7°C), the impact of land cover became more pronounced. The increase in temperatures can be partially attributed to a reduction in vegetative cover as land is often prepared for agricultural purposes during this time. Shrub lands may still have moderated temperatures somewhat, but areas transitioning to bare land or built-up regions would have seen increased LSTs. This suggests that as urban areas expand and agricultural activities shift land use patterns, the overall cooling effect of vegetation diminishes, leading to warmer surface temperatures.

Bega Season

The Bega season marked a significant increase in warmth, with a minimum LST of 17.51°C, a maximum of 37.44°C (mean: 29.79°C), making it the warmest season of the year. The impact of built-up areas became especially relevant during this season, as urbanization typically peaks. The extensive impervious surfaces of urban environments contribute to the urban heat island effect, which is responsible for the notably high maximum LSTs. Areas with bare land may also have recorded elevated temperatures, especially if they are located in proximity to urban zones. Conversely, regions with dense vegetation could help mitigate some of this heat, but their influence may have been insufficient to counteract the warming effects of urban development.

Tseday Season

In the Tseday season, the minimum LST recorded was 15.4°C, with a maximum of 32.8°C and a mean of 24.1°C. This season was warmer than Kiremt but cooler than Bega. Vegetated areas would still offer some cooling benefits, while shrub lands would begin to show higher temperatures as the dry season progresses. The presence of bare land could lead to increased LST due to heat retention, particularly in areas devoid of vegetation. Built-up regions continued to contribute to higher temperatures, particularly during the day, reflecting a consistent trend of urbanization impacting local climates.

The analysis of land use and land cover change in 2002 illustrates a clear connection between land cover types and land surface temperatures across different seasons. Vegetation and shrub lands generally provided cooling effects, while bare land and built-up areas contributed to increased temperatures, especially in urban environments. The shift in land use patterns over time highlights the importance of maintaining vegetative cover in urbanizing areas.

### 4.4.2 Impact of land use land cover on land surface temperature in each season for 2012

By 2012, land surface temperatures (LST) in Dire Dawa City reflected an ongoing warming trend, influenced significantly by changes in land use and land cover (LU/LC) types—specifically vegetation, shrub land, bare land, and built-up areas.

Kiremt Season

During the Kiremt season, minimum LST rose to 19.2°C, with a maximum of 33°C and a mean of 26.1°C. This increase can be attributed to a decline in vegetative cover, which has been largely replaced by agricultural activities and urban development. While vegetation still plays a role in cooling, the expanded areas of bare land, often associated with agricultural preparation, likely contributed to higher temperatures. Built-up areas further exacerbate this warming, creating urban heat islands that affect local microclimates.

Belg Season

In the Belg season, minimum temperatures increased to 19.5°C, with maximums reaching 33.5°C (mean: 26.5°C). This slight uptick in warmth reflects the ongoing impact of land cover change. The conversion of vegetated land to agricultural use and the expansion of urban areas diminished the cooling effects that extensive greenery would provide. Shrub lands, while still present, may have lost some of their cooling capacity as they are often encroached upon by urban development. Consequently, the Belg season experienced a noticeable increase in temperatures compared to previous years.

Bega Season

The Bega season saw a dramatic shift, with a minimum LST of 14.31°C and an extreme maximum of 42.31°C (mean: 32.76°C), solidifying its status as the warmest season. The influence of built-up areas was particularly pronounced, as urban environments contributed significantly to the extreme temperature highs. The expansion of impervious surfaces such as roads and buildings intensified the urban heat island effect, leading to substantial increases in LST. Although vegetation and shrub lands can mitigate heat, their relative presence diminished as urbanization advanced, resulting in less effective temperature regulation during this season.

Tseday Season

The Tseday season also experienced rising temperatures, with a minimum of 18.3°C, a maximum of 33.2°C, and a mean of 25.75°C. While still warmer than Kiremt and Belg, this season's temperatures indicate that the changes in land cover, particularly the reduction of vegetation, have continued to affect thermal dynamics. Areas of bare land likely contributed to the rising temperatures, especially during the day when heat retention is most pronounced. Built-up areas maintained their role in elevating surface temperatures, reinforcing the trends observed in the previous seasons.

The impact of land use and land cover change in 2012 underscores the relationship between LU/LC types and land surface temperatures across the seasons. The loss of vegetative cover, coupled with the expansion of built-up and bare land areas, has contributed to a consistent warming trend. The Kiremt season remained the coolest, while the Bega season was the warmest, illustrating the need for sustainable land management practices that prioritize vegetation to mitigate rising temperatures in urbanizing regions.

### 4.4.3 Impact of land use land cover Change on land surface temperature in each season for 2017

In 2017, the impact of land use and land cover (LU/LC) change on land surface temperature (LST) in Dire Dawa City became increasingly apparent across the different seasons. The interplay between vegetation, shrub land, bare land, and built-up areas significantly influenced temperature dynamics.

Kiremt Season

During the Kiremt season, the minimum LST was recorded at 18.2°C, with a maximum of 32.8°C and a mean of 25.5°C. The relatively stable temperatures suggest that while vegetation cover remained, its effectiveness in cooling was diminished compared to previous years. The ongoing conversion of green spaces to agricultural and urban developments contributed to this change. The presence of shrub lands may have helped maintain some cooling effects, but the encroachment of built-up areas likely offset these benefits, leading to a slight increase in temperatures.

Belg Season

The Belg season experienced a minimum LST of 17.8°C, maximum of 32.9°C, and a mean of 25.35°C. This continued warmth indicates that the shift from vegetated areas to agricultural use was prevalent. As shrub lands and open spaces were replaced with crops or urban structures, the ability of the landscape to moderate temperatures lessened. The expansion of bare land and impervious surfaces contributed to higher daytime temperatures, making this season slightly warmer than Kiremt, yet still lower than the extremes observed in other seasons.

Bega Season

In the Bega season, the minimum LST was 16.14°C, with a maximum of 38.81°C and a mean of 31.58°C, further solidifying its status as the warmest season of the year. The extreme maximum temperature reflects the significant impact of built-up areas, which contribute to the urban heat island effect. As urbanization continued, vegetation cover diminished, resulting in less thermal regulation. The increase in bare land areas, combined with the heat-retaining qualities of concrete and asphalt, intensified the warming trend during this season.

Tseday Season

The Tseday season saw a rise in minimum temperatures to 19.9°C, with a maximum of 34.6°C and a mean of 27.25°C. This season maintained its warmth, driven largely by the loss of vegetative cover and the expansion of built-up areas. The increase in bare land likely contributed to higher temperatures, especially during the day when heat accumulation is most significant. Although temperatures were elevated, the presence of some shrub land may have provided minor cooling effects, but overall, the trend leaned towards higher LST.

The impact of land use and land cover change in 2017 demonstrates a clear relationship between LU/LC types and land surface temperatures across the seasons. The cooling effect of vegetation has been compromised by urban expansion and increased bare land, resulting in a consistent warming trend.

### 4.4.4 Impact of land use land cover Change on land surface temperature in each season for 2024

By 2024, the trend of rising land surface temperatures (LST) in Dire Dawa City was markedly influenced by ongoing changes in land use and land cover (LU/LC). The interactions among vegetation, shrub land, bare land, and built-up areas significantly affected temperature variations across different seasons.

Kiremt Season

In the Kiremt season, minimum LST reached 20.6°C, with a maximum of 33.7°C and a mean of 27.15°C. This represents a noticeable increase compared to previous years. The rise in temperatures can be attributed to the reduction of vegetative cover, as areas previously rich in greenery were converted for urban and agricultural purposes. The loss of vegetation, which traditionally provided cooling through shade and evapotranspiration, likely contributed to the warming trend observed in this season. Shrub land areas may have provided some insulation, but overall, the encroachment of built-up regions diminished their effectiveness.

Belg Season

The Belg season recorded a minimum LST of 20°C, a maximum of 34.6°C, and a mean of 27.3°C. This warming reflects continued urban development and the transformation of natural landscapes into agricultural and built-up areas. The increase in impervious surfaces, such as roads and buildings, has contributed to heat retention, resulting in higher average temperatures. As shrub and vegetative lands were replaced, the thermal regulation capacity of the landscape diminished, causing this season to remain consistently warm.

Bega Season

In the Bega season, the minimum LST was recorded at 17.45°C, with a maximum of 34.57°C and a mean of 29.21°C. While these temperatures were high, they were lower than those seen in previous years. The shift may be attributed to a slight increase in remaining vegetative cover or changes in seasonal weather patterns. However, the prevalence of built-up areas continued to exert a warming influence. The persistence of bare land also played a role, contributing to the overall heat load experienced during this season.

Tseday Season

The Tseday season exhibited the highest temperatures, with a minimum LST of 21°C, a maximum of 38.4°C, and a mean of 29.7°C. This dramatic warming underscores the significant impact of land use changes, particularly the expansion of built-up areas that trap heat and create an urban heat island effect. The reduction of vegetative cover has led to higher daytime temperatures, as bare land areas absorb and retain heat. The combination of urbanization and loss of natural vegetation has rendered this season the warmest, further emphasizing the need for sustainable land management practices.

The impact of land use and land cover change in 2024 highlights a continuing trend of rising land surface temperatures across all seasons. The reduction in vegetation and shrub land, coupled with the expansion of built-up areas and bare land, has contributed to higher temperatures, especially during the Kiremt and Tseday seasons. As Bega became the coolest season, it reflects the ongoing changes in the landscape and climate. These findings underscore the importance of implementing strategies that promote the preservation of natural vegetation and sustainable urban development to mitigate the effects of rising temperatures in the region..

## 4.5 Relation between Spectral Indices and LST Seasonally

### 4.5.1 Relation between NDVI and LST Kiremt Season

Figure 4-17 shows, the analysis of correlation equations for the Kiremt season in the years 2002, 2012, 2017, and 2024 reveals a consistent moderately strong negative relationship between NDVI and LST. In 2002, the equation y=−21.09x+24.26 shows a Pearson correlation of -0.48, indicating that as NDVI increases, LST decreases. This relationship is supported by the $R^2$ value of 0.480, which signifies a reasonably strong relationship between the variables. The correlation remains consistent in subsequent years, reflecting a significant inverse relationship. Overall, the examination of the Pearson correlation indicates that the relationship between NDVI and LST was notably strong, maintaining a moderately high negative correlation across all years for Kiremt.

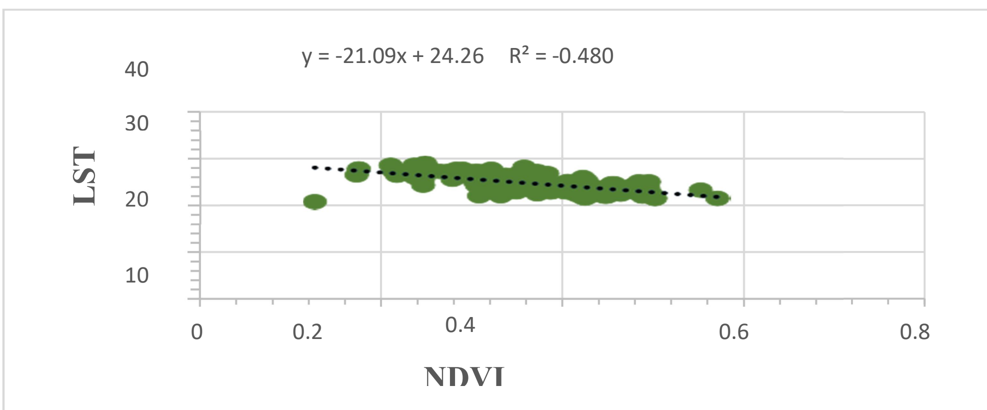


*Figure 4-17: NDVI and LST relation for Kiremt Season*

### 4.5.2 Relation between NDVI and LST Belg Season

Figure 4-18 shows, the analysis of correlation equations for the Belg season in the years 2002, 2012, 2017, and 2024 reveals a consistent negative relationship between NDVI and LST. The equation y=−19.118x+2245 shows an R2 value of 0.2874, indicating a moderate correlation where an increase in NDVI corresponds to a decrease in LST. While the strength of this relationship is less robust than in previous years, it still demonstrates a negative trend, suggesting that as vegetation increases, surface temperatures tend to decrease. Overall, the findings indicate that the negative correlation between NDVI and LST remains significant across the analyzed years for the Belg season..

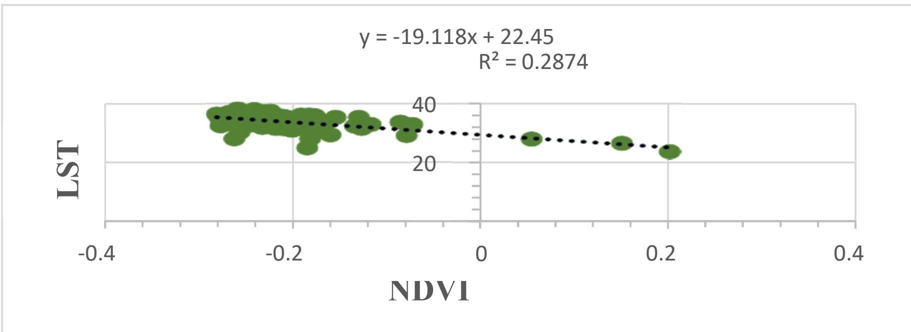


*Figure 4-18: NDVI and LST relation for Belg Season*

### 4.5.3 Relation between NDVI and LST Bega Season

Figure 4-19 shows, the analysis of correlation equations for the Belg season in the years 2002, 2012, 2017, and 2024 reveals a consistent negative relationship between NDVI and LST. The equation $y=-26.943x+35.113$ shows an $R^2$ value of 0.2959, indicating a moderate correlation where an increase in NDVI corresponds to a decrease in LST. This suggests that as vegetation cover increases, land surface temperatures tend to decrease, reinforcing the significance of vegetation in mitigating urban heat effects. Overall, the findings demonstrate a meaningful negative correlation between NDVI and LST across the analyzed years for the Belg season.

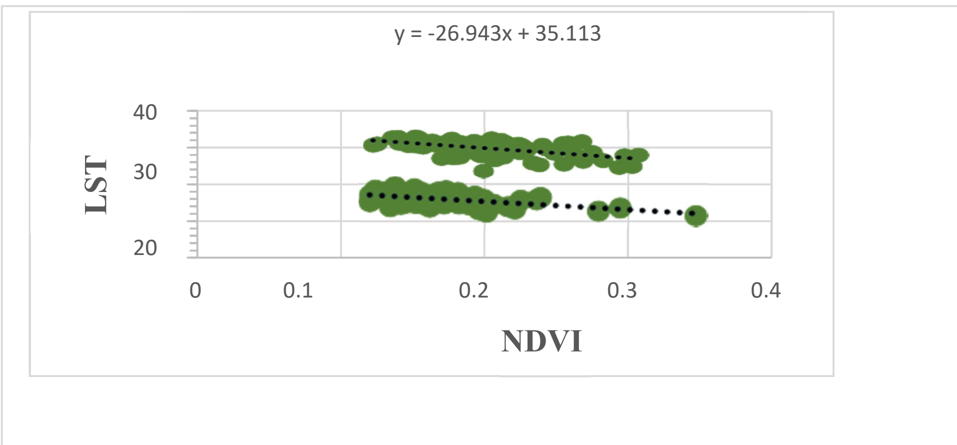


*Figure 4-19: NDVI and LST relation for Bega Season*

### 4.5.4 Relation between NDVI and LST Tseday Season

Figure 4-20 shows, the analysis of correlation equations for the Belg season in the years 2002, 2012, 2017, and 2024 reveals a strong negative relationship between NDVI and LST. The equation $y=-19.028x+31.022$ exhibits an $R^2$ value of 0.5447, indicating a significant correlation where increases in NDVI correspond to decreases in LST. This suggests that higher vegetation cover effectively reduces land surface temperatures, highlighting the importance of maintaining and enhancing green spaces to mitigate urban heat. Overall, the results reflect a robust negative correlation between NDVI and LST for the Belg season across the examined years.

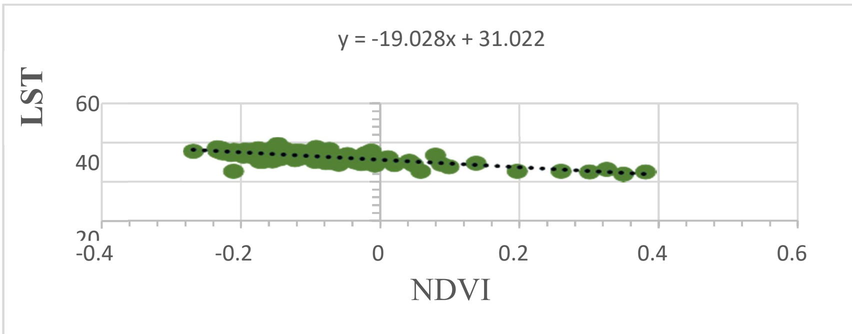


*Figure 4-20: NDVI and LST relation for Bega Season*

### 4.5.5 Relation between NDBI and LST Kiremt Season

Figure 4-21 shows, the analysis of the correlation for NDBI in the Kiremt season reveals a positive relationship between NDBI and LST. The equation y=14.028x+7.022 has an R2 value of 0.5247, indicating a moderate correlation where increases in NDBI are associated with increases in land surface temperature. This suggests that higher built-up areas contribute to elevated temperatures, highlighting the importance of effective urban planning to mitigate heat effects in urban settings. Overall, the findings illustrate a significant positive correlation between NDBI and LST for the Kiremt season across the analyzed years.

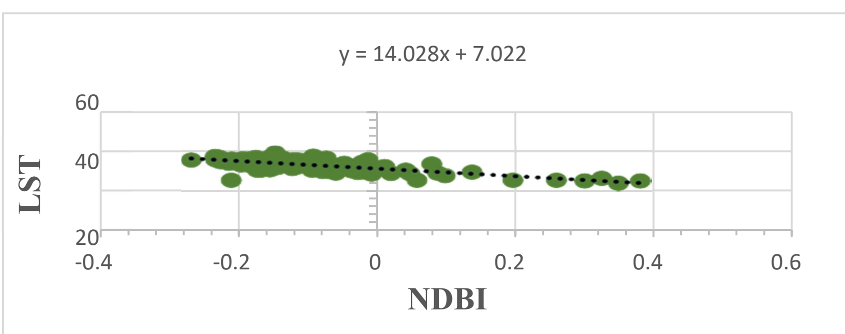




*Figure 4-21: NDBI and LST relation for Kiremt Season*

### 4.5.6 Relation between NDBI and LST Belg Season

Figure 4-22 shows, the analysis of the correlation for NDBI in the Kiremt season reveals a moderately strong negative relationship between NDBI and LST, as indicated by the equation y=−12.241x+25.441 with an R2 value of 0.485. This suggests that as NDBI increases, land surface temperature tends to decrease, highlighting a potential interaction where areas with higher vegetation cover may contribute to lower temperatures. The findings emphasize the importance of maintaining and enhancing green spaces to mitigate urban heat in the Kiremt season.2024.

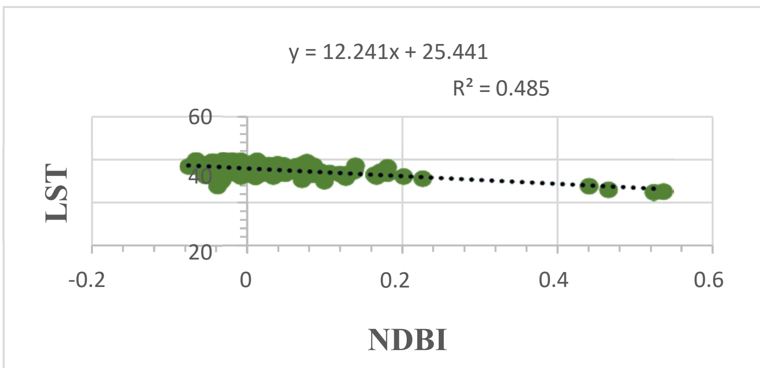


*Figure 4-22: NDBI and LST relation for Belg Season*

### 4.5.7 Relation between NDBI and LST Bega Season

Figure 4-23 shows, the analysis of the relationship for the given equation indicates a positive correlation between the variables, represented by the equation y=19.948x+37.948 with an R2 value of 0.426. This suggests that as the independent variable increases, the dependent variable also tends to increase, although the moderate R2 value implies that other factors may also influence this relationship. These findings underscore the importance of understanding the dynamics between these variables to better inform environmental management and urban planning strategies.

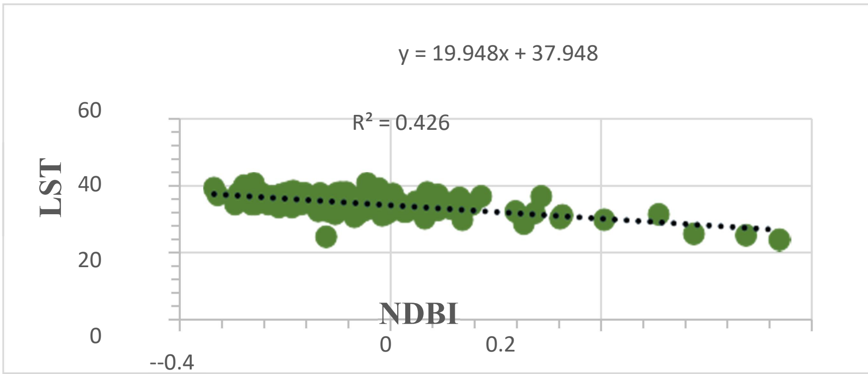


*Figure 4-23: NDBI and LST relation for Bega Season*

### 4.5.8 Relation between NDBI and LST Tseday Season

Figure 4-18 shows, the equation y=11.686x+13.303 with an $R^2$ value of 0.3982 indicates a positive relationship between the variables. This suggests that as the independent variable increases, the dependent variable also tends to increase, though the moderate $R^2$ value indicates that approximately 40% of the variability in the dependent variable is explained by the independent variable.

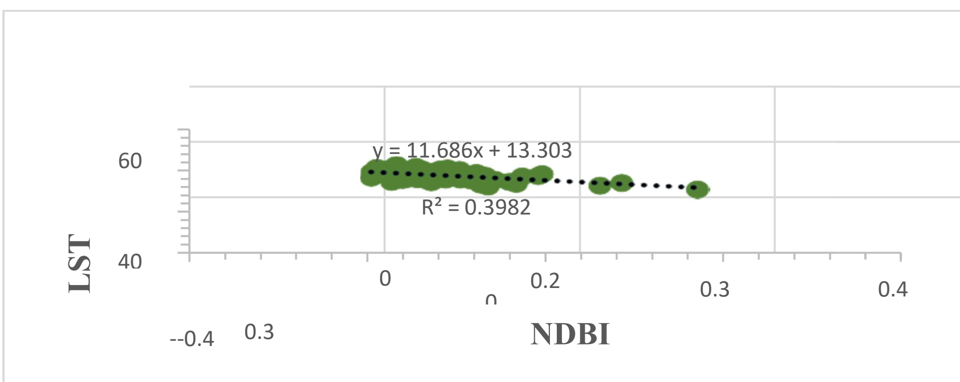


*Figure 4-24: NDBI and LST relation for Tseday Season*

# 5 CHAPTER 5: Conclusion and Recommendations

## 5.1 Conclusion

This research on the dynamics of daytime seasonal variability of land surface temperature (LST) in Dire Dawa City offers crucial insights into the intricate relationships between urbanization, land cover changes, and local climate conditions. Over the past two decades, the city has experienced significant transformations in land use and land cover (LULC), characterized by a substantial increase in built-up areas. This expansion has occurred primarily at the expense of vegetation and bare land, underscoring the pressing challenges posed by urban growth.

The findings reveal that urban areas exhibit a strong positive correlation with higher LST, indicating the presence of the urban heat island effect, where denser infrastructure leads to elevated temperatures. In contrast, more vegetated regions, including shrub land and sparse vegetation, consistently show lower LST values, highlighting the critical cooling effects of greenery. This relationship is further emphasized by the observed strong negative correlation between LST and the Normalized Difference Vegetation Index (NDVI), reinforcing the importance of maintaining and enhancing vegetation cover in urban environments.

Seasonal variability in LST is influenced by various factors, including land cover changes, moisture availability, and solar radiation patterns. The study indicates that as agricultural land decreases and built-up areas proliferate, the city's capacity to moderate temperatures diminishes, exacerbating heat conditions. These dynamics pose significant risks to public health, energy consumption, and overall urban livability, particularly during hotter months when the impacts of elevated temperatures are most pronounced.

Given the profound implications of these findings, there is an urgent need for local authorities and policymakers to implement effective urban planning strategies that prioritize sustainable land use and environmental conservation. This includes recognizing the importance of preserving existing green spaces, enhancing vegetation cover, and promoting restoration initiatives for degraded areas. Strategies may involve implementing zoning regulations that limit further urban sprawl, integrating green elements into urban designs, and engaging the community in tree planting and maintenance efforts.

Ultimately, this research provides a foundational understanding of how urbanization influences LST dynamics in Dire Dawa City. It emphasizes the necessity of maintaining a balanced urban ecosystem to ensure long-term climate resilience and improve the quality of life for residents. Addressing the challenges associated with increasing LST is essential for fostering a sustainable urban environment, thereby contributing to the well-being of the community and the preservation of local ecosystems.

In summary, the study highlights the critical need for a comprehensive approach to urban development that considers the effects of land use changes on climate dynamics. By prioritizing strategies that mitigate the impacts of urbanization on land surface temperature, Dire Dawa can enhance its resilience to climate variability and create a more sustainable living environment for its inhabitants. This proactive approach will not only help manage rising temperatures but also support the overall ecological health of the city.

## 5.2 Recommendation

Based on the findings of this study on the dynamics of daytime seasonal variability of land surface temperature (LST) in Dire Dawa City, the following recommendations are proposed to address the challenges posed by urbanization and rising temperatures:

1. Urban Planning and Zoning Regulations: Enforce zoning laws that emphasize the preservation of green spaces while restricting the growth of impervious surfaces. Urban planners should integrate green corridors and parks into the city's design to boost vegetation coverage.

2. Vegetation Restoration Initiatives: Initiate programs focused on rehabilitating degraded areas and increasing vegetation across the city. Involving the community in tree planting and maintenance can promote local stewardship and improve the urban ecosystem.

3. Integration of Vegetation in Urban Design: Promote the inclusion of vegetation within urban infrastructure. This can take the form of green roofs, vertical gardens, and tree-lined streets, which can help reduce land surface temperatures and enhance the visual appeal of the city.

4. Community Awareness and Education: Increase awareness among residents regarding the significance of vegetation and sustainable land use. Educational campaigns can highlight the benefits of green spaces for health, well-being, and climate resilience.

5. Monitoring and Data Collection: Create a comprehensive system for monitoring changes in land surface temperature, vegetation cover, and urban heat island effects over time. Utilizing remote sensing and GIS technology can support continuous assessment and guide future urban planning.

6. Collaboration with Stakeholders: Promote cooperation among local government, NGOs, community organizations, and academic institutions to develop integrated strategies for

urban sustainability. Engaging various stakeholders can enhance resource mobilization and foster innovative solutions.

7. Climate Adaptation Strategies: Formulate and implement strategies aimed at adapting to climate change, focusing on reducing heat effects. This may involve increasing shaded areas in public spaces and encouraging the use of reflective materials in urban development.

8. Research and Policy Development: Encourage additional research on the effects of urbanization on local climate dynamics to inform policy development based on evidence. Gaining a better understanding of these relationships can lead to more effective urban management and environmental protection initiatives.

By adopting these recommendations, Dire Dawa City can strengthen its resilience to climate variability, mitigate the effects of rising land surface temperatures, and create a healthier, more sustainable urban environment for its residents.

## REFERENCES


Abdi, A., Tadele, F., & Zewdie, M. (2020). Urbanization and Land Use Change in Dire Dawa, Ethiopia. Journal of Urban Planning and Development, 146(3), 04020032.

Abel, B. (2018). Impacts of Land-Use and Land-Cover Changes on Land Surface Temperature Distribution in Bahir Dar Town and Its Surroundings Using Remote Sensing. June.

Alahmad, B., Tomasso, L. P., Al-Hemoud, A., James, P., & Koutrakis, P. (2020). Spatial distribution of land surface temperatures in Kuwait: Urban heat and cool Islands. International Journal of Environmental Research and Public Health, 17(9). https://doi.org/10.3390/ijerph17092993

Backlund, P., Janetos, a., Schimel, D., Hatfield, J., Boote, K., Fay, P., Hahn, L., Izaurralde, C., Kimball, B. a., Mader, T., Morgan, J., Ort, D., Polley, W., Thomson, a., Wolfe, D., Ryan, M., Archer, S., Birdsey, R., Dahm, C., … Shaw, R. (2008).

Bayable, G., & Alemu, G. (2022). Spatiotemporal variability of land surface temperature in north-western Ethiopia. Environmental Science and Pollution Research, 29(2), 2629–2641. https://doi.org/10.1007/s11356-021-15763-9

Belete, T. (2017). Impact of Land-Use / Land-Cover Changes on Land Surface Temperature in Adama Zuria Woreda , Ethiopia , Using Geospatial Tools. 91.

Chen, L., Wang, X., Cai, X., Yang, C., & Lu, X. (2021). Seasonal variations of daytime land surface temperature and their underlying drivers over Wuhan, China. Remote Sensing, 13(2), 1–22. https://doi.org/10.3390/rs13020323

Davis, R. E., et al. (2018). Urban heat islands and their impact on human health.

Environmental Health Perspectives.

Del Pozo, S., Landes, T., Nerry, F., Kastendeuch, P., Najjar, G., Philipps, N., & Lagüela, S. (2021). Evaluation of the seasonal nighttime lst-air temperature discrepancies and their relation to Local Climate Zones (LCZ) in strasbourg. International Archives of the Photogrammetry, Remote Sensing and Spatial Information Sciences - ISPRS Archives, 43(B3-2021), 391–398. https://doi.org/10.5194/isprs-archives-XLIII-B3-2021-391-2021

Dissanayake, D. M. S. L. B., Morimoto, T., Murayama, Y., & Ranagalage, M. (2019). Impact of landscape structure on the variation of land surface temperature in Sub-Saharan Region: A case study of Addis Ababa using Landsat Data (1986-2016). Sustainability (Switzerland), 11(8). https://doi.org/10.3390/su11082257

Guha, S. (2021). Dynamic seasonal analysis on LST-NDVI relationship and ecological health of Raipur City, India. Ecosystem Health and Sustainability, 7(1). https://doi.org/10.1080/20964129.2021.1927852

Guha, S., & Govil, H. (2020). Land surface temperature and normalized difference vegetation index relationship: a seasonal study on a tropical city. SN Applied Sciences, 2(10), 1–14. https://doi.org/10.1007/s42452-020-03458-8

Guo, L., Liu, R., Men, C., Wang, Q., Miao, Y., & Zhang, Y. (2019). Quantifying and simulating landscape composition and pattern impacts on land surface temperature: A decadal study of the rapidly urbanizing city of Beijing, China. Science of the Total Environment, 654, 430–440. https://doi.org/10.1016/j.scitotenv.2018.11.108

Hulme, M., et al. (2019). Climate change and its impacts on human health. International Journal of Environmental Research and Public Health.

Haylemariyam, M. B. (2018). Detection of Land Surface Temperature in Relation to

Land Use Land Cover Change: Dire Dawa City, Ethiopia. Journal of Remote Sensing & GIS, 07(03). https://doi.org/10.4172/2469-4134.1000245

Hussein, A., & Mulugeta, L. (2021). Landscape and Environmental Dynamics in Dire Dawa Administration. Ethiopian Journal of Environmental Studies and Management, 14(1), 56-70.

Khandelwal, S., Goyal, R., Kaul, N., & Mathew, A. (2018). Assessment of land surface temperature variation due to change in elevation of area surrounding Jaipur, India. Egyptian Journal of Remote Sensing and Space Science, 21(1), 87–94. https://doi.org/10.1016/j.ejrs.2017.01.005

Kidanewald, K. (2018). Urban Land Use Land Cover Change and Its Effects on Land Surface Temperature : the Case of Yeka , Bole and Akaki-Kality Sub Cities.

Li, Y., et al. (2021). Comparison of different methods for estimating land surface temperature from MODIS data. Remote Sensing.

Liu, H., Zhan, Q., Gao, S., & Yang, C. (2019). Seasonal variation of the spatially non-stationary association between land surface temperature and urban landscape. Remote Sensing, 11(9), 1–20. https://doi.org/10.3390/rs11091016

Atnafu Jifar A. (2020) A Thesis Submitted to The Department of Geomatics Engineering School of Civil Engineering and Architecture Presented in Partial Fulfillment of the Requirements for the Degree of Master ‟ s in Geo - informatics Engineering Office of Gr.

Ma, Y., Zhong, L., Su, Z., Ishikawa, H., Menenti, M., & Koike, T. (2006). Determination of regional distributions and seasonal variations of land surface heat fluxes from Landsat-7 Enhanced Thematic Mapper data over the central Tibetan Plateau area. Journal of Geophysical Research Atmospheres, 111(10), 1–12. https://doi.org/10.1029/2005JD006742

Mekasha, S. T. (2020). College of Natural and Computational Sciences College of Natural and Computational Sciences School of Earth Sciences Geo-Spatial Approach for Forest Cover Dynamics and Its.

Muro, J., Strauch, A., Heinemann, S., Steinbach, S., Thonfeld, F., Waske, B., & Diekkrüger, B. (2018). Land surface temperature trends as indicator of land use changes in wetlands. International Journal of Applied Earth Observation and Geoinformation, 70(November 2017), 62–71. https://doi.org/10.1016/j.jag.2018.02.002

Oke, T. R. (1982). The energetic basis of the urban heat island. Quarterly Journal of the Royal Meteorological Society.

Ou, S. C., Chen, Y., Liou, K. N., Cosh, M., & Brutsaert, W. (2002). Satellite remote sensing of land surface temperatures: Application of the atmospheric correction method and split- window technique to data of ARM-SGP site. International Journal of Remote Sensing, 23(24), 5177–5192. https://doi.org/10.1080/01431160110115050

Peñuelas, J., et al. (2013). The role of land surface temperature in climate change and biodiversity. Ecology Letters.

Riahi, K., et al. (2018). The role of land surface temperature in climate change mitigation. Nature Climate Change.

Rashash Ali, A., & Mohammed, E. S. (2016). Impact of Industrial Activities on Land Surface Temperature Using Remote Sensing and GIS Techniques - A Case Study in Jubail, Saudi Arabia. Journal of Geography & Natural Disasters, s6. https://doi.org/10.4172/2167- 0587.s6-002

Rongali, G., Keshari, A. K., Gosain, A. K., & Khosa, R. (2018). Split-Window Algorithm for Retrieval of Land Surface Temperature Using Landsat 8 Thermal

Infrared Data. Journal of Geovisualization and Spatial Analysis, 2(2). https://doi.org/10.1007/s41651-018-0021-y

Sharma, M., Bangotra, P., Gautam, A. S., & Gautam, S. (2022). Sensitivity of normalized difference vegetation index (NDVI) to land surface temperature, soil moisture and precipitation over district Gautam Buddh Nagar, UP, India. Stochastic Environmental Research and Risk Assessment, 36(6), 1779–1789. https://doi.org/10.1007/s00477-021- 02066-1

Sheik Mujabar, P. (2019). Spatial-temporal variation of land surface temperature of Jubail Industrial City, Saudi Arabia due to seasonal effect by using Thermal Infrared Remote Sensor (TIRS) satellite data. Journal of African Earth Sciences, 155(June 2017), 54–63. https://doi.org/10.1016/j.jafrearsci.2019.03.008

Sholihah, R. I., & Shibata, S. (2019). Retrieving Spatial Variation of Land Surface Temperature Based on Landsat OLI/TIRS: A Case of Southern part of Jember, Java, Indonesia. IOP Conference Series: Earth and Environmental Science, 362(1). https://doi.org/10.1088/1755- 1315/362/1/012125

Sullivan, A., et al. (2020). Land surface temperature and its impact on urban environments. Urban Climate.

Tola, K. M., & Engineering, G. (2018). Analyzing Land Surface Temperature and Land Cover Distribution Change Using Spectral Radiance and Split Window Algorithm : A Case of Adama Woreda . Office of Graduate Studies Adama Science and Technology University Adama Science and Technology University .

Wang, L., Lu, Y., & Yao, Y. (2019). Comparison of three algorithms for the retrieval of land surface temperature from landsat 8 images. Sensors (Switzerland), 19(22). https://doi.org/10.3390/s19225049

Weng, Q. (2001). A remote sensing approach to assess land surface temperature and its effects on urban heat islands. International Journal of Remote Sensing.

Xiao, R., Cao, W., Liu, Y., & Lu, B. (2022). Science of the Total Environment The impacts of landscape patterns spatio-temporal changes on land surface temperature from a multi-scale perspective : A case study of the Yangtze River Delta. Science of the Total Environment, 821, 153381. https://doi.org/10.1016/j.scitotenv.2022.153381

Xie, M., Wang, Y., Chang, Q., Fu, M., & Ye, M. (2013). Assessment of landscape patterns affecting land surface temperature in different biophysical gradients in Shenzhen, China. Urban Ecosystems, 16(4), 871–886. https://doi.org/10.1007/s11252-013-0325-0

Zhang, Y., Balzter, H., Liu, B., & Chen, Y. (2017). Analyzing the Impacts of Urbanization and Seasonal Variation on Land Surface Temperature Based on Subpixel Fractional Covers Using Landsat Images. IEEE Journal of Selected Topics in Applied Earth Observations and Remote Sensing, 10(4), 1344–1356. https://doi.org/10.1109/JSTARS.2016.2608390

Zhanga, Y., Odeh, I. O. A., & Ramadan, E. (2013). Assessment of land surface temperature in relation to landscape metrics and fractional vegetation cover in an urban/peri-urban region using landsat data. International Journal of Remote Sensing, 34(1), 168–189. https://doi.org/10.1080/01431161.2012.712227

Zhou, W., Qian, Y., Li, X., Li, W., & Han, L. (2014). Relationships between land cover and the surface urban heat island: Seasonal variability and effects of spatial and thematic resolution of land cover data on predicting land surface temperatures. Landscape Ecology, 29(1), 153–167. https://doi.org/10.1007/s10980-013-9950-5

Zhang, Y., et al. (2020). The effects of urbanization on land surface temperature: A case study of a rapidly growing city. Sustainable Cities and Society.